

EUROPEAN ORGANISATION FOR NUCLEAR RESEARCH (CERN)



Submitted to: Phys. Lett. B.

CERN-EP-2020-165
22nd December 2024

Observation of photon-induced W^+W^- production in $p p$ collisions at $\sqrt{s} = 13$ TeV using the ATLAS detector

The ATLAS Collaboration

This letter reports the observation of photon-induced production of W -boson pairs, $\gamma\gamma \rightarrow WW$. The analysis uses 139 fb^{-1} of LHC proton–proton collision data taken at $\sqrt{s} = 13$ TeV recorded by the ATLAS experiment during the years 2015–2018. The measurement is performed selecting one electron and one muon, corresponding to the decay of the diboson system as $WW \rightarrow e^\pm\nu\mu^\mp\nu$ final state. The background-only hypothesis is rejected with a significance of 8.4 standard deviations which is consistent within uncertainty with the expectation from Monte Carlo simulation. A cross section for the $\gamma\gamma \rightarrow WW$ process of $3.13 \pm 0.31(\text{stat.}) \pm 0.28(\text{syst.})\text{ fb}$ is measured in a fiducial volume close to the acceptance of the detector, by requiring an electron and a muon of opposite signs with large dilepton transverse momentum and exactly zero additional charged particles.

Contents

1	Introduction	2
2	ATLAS detector	3
3	Data and simulated event samples	4
4	Event reconstruction and selection	5
5	Modelling of signal and backgrounds	7
5.1	Modelling of additional pp interactions	7
5.2	Modelling of the underlying event	9
5.3	Signal modelling	10
6	Event categories and background estimation	12
7	Systematic uncertainties	13
8	Results	14
9	Conclusion	18

1 Introduction

The study of W -boson pair production from the interaction of incoming photons ($\gamma\gamma \rightarrow WW$) in proton–proton (pp) collisions offers a unique window to a wide range of physical phenomena. In the Standard Model (SM), the $\gamma\gamma \rightarrow WW$ process proceeds through trilinear and quartic gauge-boson interactions. This process is unique in that, at leading order, it only involves diagrams with self-couplings of the electroweak gauge bosons, as shown in Figure 1. Hence, a cross-section measurement directly tests the $SU(2) \times U(1)$ gauge structure of the SM. At the same time, as a process driven only by electroweak boson self-interactions, it is sensitive to anomalous gauge-boson interactions [1] as parameterised in effective field theory (EFT) with additional dimension-6 and dimension-8 operators [2, 3]. Thus, cross-section measurements of $\gamma\gamma \rightarrow WW$ can provide valuable input into the global EFT fits.

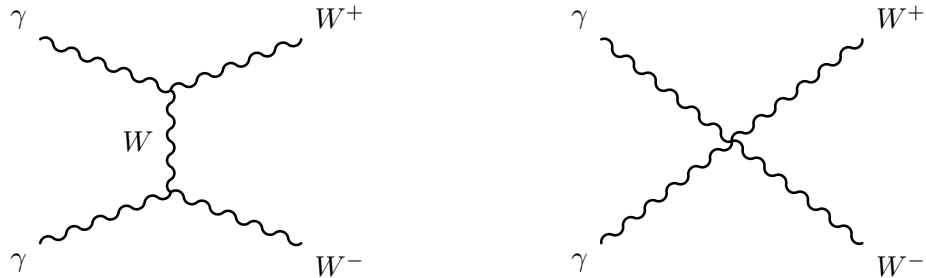


Figure 1: The leading-order Feynman diagrams contributing to the $\gamma\gamma \rightarrow WW$ process are the t-channel diagram (left) proceeding via the exchange of a W boson between two γWW vertices and a diagram with a quartic $\gamma\gamma WW$ coupling (right). In addition, a u-channel diagram exists (not shown) which also proceeds via two γWW vertices.

This letter presents a measurement in the $W^+W^- \rightarrow e^\pm\nu\mu^\mp\nu$ channel to establish the observation of photon-induced WW production. Previously, the ATLAS and CMS Collaborations found only evidence for $\gamma\gamma \rightarrow WW$ production with the Run-1 data, ATLAS by using 8 TeV pp collisions [4] and CMS by combining their 7 TeV and 8 TeV pp collision data [5, 6].

The signal process proceeds through the $pp(\gamma\gamma) \rightarrow p^{(*)}W^+W^-p^{(*)}$ reaction, where $p^{(*)}$ indicates that the final-state proton either stays intact or fragments after emitting a photon. Whilst the former occurs through a coherent photon radiation off the whole proton without disintegration, for the latter at least one of the photons can be considered as being radiated off a parton in the proton. These contributions are classified as elastic, single-dissociative and double-dissociative WW production. Elastic $\gamma\gamma \rightarrow WW$ production with leptonic decays of the W bosons results in a final state containing two charged leptons and no additional charged-particle activity. Even in the case of dissociative photon-induced production, the charged particles from the proton remnants often fall outside the acceptance of the tracking detector.

The suppressed activity in the central region of the detector in the $\gamma\gamma \rightarrow WW$ signal gives the means to control and significantly reduce background from quark- and gluon-induced WW production or top-quark production where the leptonic final state is typically produced in association with a substantial amount of hadronic activity. The analysis therefore selects events that have no additional charged-particle tracks reconstructed in the vicinity of the selected interaction vertex. The modelling of the hadronic activity in quark- and gluon-induced processes, as well as uncorrelated activity from additional pp interactions, is constrained using same-flavour ee and $\mu\mu$ Drell–Yan, DY($\rightarrow ee/\mu\mu$), events in data, reducing the associated uncertainties by a significant amount. Background from other photon-induced processes, mainly dilepton production $\gamma\gamma \rightarrow \ell\ell$, is reduced by selecting only different-flavour lepton pairs, $e\mu$, leaving a smaller contribution from $\gamma\gamma \rightarrow \tau\tau$ production with leptonic τ decays. Since the contribution from the $\gamma\gamma \rightarrow \tau\tau$ process falls off rapidly with increasing transverse momentum of the dilepton system, $p_T^{e\mu}$, it can be further suppressed by placing requirements on $p_T^{e\mu}$. A cross section for the $pp(\gamma\gamma) \rightarrow p^{(*)}W^+W^-p^{(*)}$ process through the decay channel $W^+W^- \rightarrow e^\pm\nu\mu^\mp\nu$ is measured in a fit to the number of events in several kinematic regions with different signal and background contributions.

2 ATLAS detector

The ATLAS detector [7] at the Large Hadron Collider (LHC) is a multipurpose detector with a forward–backward symmetric cylindrical geometry and nearly 4π coverage in solid angle.¹ It consists of an inner tracking detector surrounded by a thin superconducting solenoid providing a 2 T axial magnetic field, electromagnetic and hadron calorimeters, and a muon spectrometer.

The inner tracking detector (ID) covers the pseudorapidity range $|\eta| < 2.5$ and is composed of three subdetectors. The high-granularity silicon pixel detector covers the vertex region and typically provides four measurements per track, the first hit normally being in the insertable B-layer [8, 9]. It is followed by the silicon microstrip tracker (SCT), which usually provides eight measurements per charged-particle track. These silicon detectors are complemented by the transition radiation tracker, which enables radially extended track reconstruction up to $|\eta| = 2.0$ and provides electron identification information. The resolution of the z -coordinate of tracks at the point of closest approach to the beam line is about 0.170 mm for tracks

¹ ATLAS uses a right-handed coordinate system with its origin at the nominal interaction point in the centre of the detector and the z -axis coinciding with the axis of the beam pipe. The x -axis points from the interaction point to the centre of the LHC ring, and the y -axis points upward. The pseudorapidity is defined in terms of the polar angle θ as $\eta = -\ln \tan(\theta/2)$, and ϕ is the azimuthal angle around the beam pipe relative to the x -axis. The angular distance is defined as $\Delta R = \sqrt{(\Delta\eta)^2 + (\Delta\phi)^2}$.

with $p_T = 500$ MeV and improves with higher track momentum [10]. For tracks with $p_T < 1$ GeV, the dominant contribution to the z -resolution is due to multiple scattering.

Lead/liquid-argon (LAr) sampling calorimeters provide electromagnetic (EM) energy measurements with high granularity. A steel/scintillator-tile hadron calorimeter covers the central pseudorapidity range ($|\eta| < 1.7$). The endcap and forward regions are instrumented with LAr calorimeters for EM and hadronic energy measurements up to $|\eta| = 4.9$. The muon spectrometer (MS) surrounds the calorimeters and is based on three large air-core toroidal superconducting magnets with eight coils each. The muon spectrometer includes a system of precision tracking chambers ($|\eta| < 2.7$) and fast detectors for triggering ($|\eta| < 2.4$). A two-level trigger system [11] selects the events used in the analysis.

3 Data and simulated event samples

The analysis uses proton–proton collision data recorded with the ATLAS detector during the Run-2 data-taking period (2015–2018) at $\sqrt{s} = 13$ TeV with an average number of interactions, μ_{int} , per bunch crossing (also referred to as pile-up) of 33.7 [12]. The size of the region where the collisions occur, the so-called beam spot, is a result of the operating parameters of the LHC. Of specific importance for this analysis is its width along the z -direction, which determines the density of pp interactions. The width is determined by fitting the distribution of the z positions of the reconstructed vertices to Gaussian functions using an unbinned likelihood fit [13]. The data correspond to an integrated luminosity of $\mathcal{L} = 139.0 \pm 2.4 \text{ fb}^{-1}$ after data quality requirements [14] have been applied. This value is derived from the calibration of the luminosity scale with the method explained in Ref. [12], using the LUCID-2 detector [15] for the primary luminosity measurement.

Signal and background processes were modelled using Monte Carlo (MC) event generators to study kinematic distributions, to evaluate background contamination in the signal region and to interpret the results. To simulate the detector response, the generated events were passed through a detailed simulation of the ATLAS detector [16] based on GEANT4 [17] or on a combination of GEANT4 and a parameterised calorimeter simulation [18]. Multiple pp interactions occurring in the same or adjacent bunch crossings are included in the simulation by overlaying several inelastic pp collisions matching the average number of interactions per bunch crossing. The inelastic pp collisions were generated with PYTHIA 8.186 [19] using a set of tuned parameters called the A3 tune [20] and the NNPDF2.3LO [21] set of parton distribution functions (PDF). All MC samples are corrected to the beam conditions of the data as described in Section 5.1. In all samples using PYTHIA8 or HERWIG7 to simulate the parton showering, underlying event and hadronisation, the decays of bottom and charm hadrons were performed with EvtGen 1.2.0 [22].

The elastic component of the $\gamma\gamma \rightarrow WW$ signal process was modelled at leading order (LO) using HERWIG 7.1.5 [23, 24] interfaced with the BudnevQED photon flux [25] through THEPEG software [26]. This sample is used to model the photon-induced processes in the fiducial region of the measurement. It is corrected to match the cross section, including the dissociative components, using a data-driven method described in Section 5.3. This approach is validated using elastic and dissociative $\gamma\gamma \rightarrow WW$ samples produced using MG5_AMC@NLO [27] interfaced to PYTHIA 8.243. The default photon flux in MG5_AMC@NLO and the CT14QED [28] PDF were used to model the photon radiation from protons and quarks, respectively. These samples are used whenever regions with reconstructed track multiplicities larger than zero are studied.

The production of $\gamma\gamma \rightarrow \ell\ell$, with $\ell = e, \mu, \tau$, was modelled in the same way as for the $\gamma\gamma \rightarrow WW$ signal process. Additional generators were used to validate the modelling of the $\gamma\gamma \rightarrow \ell\ell$ dissociative events. The

single-dissociative processes were modelled using LPAIR [29]. Alternative $\gamma\gamma \rightarrow \ell\ell$ double-dissociative samples were produced with PYTHIA 8.240 using the NNPDF3.1NLOluxQED PDF set [30]. Diffractive QCD-processes and $\gamma\gamma \rightarrow 4\ell$ production were produced using PYTHIA 8.244 and MG5_AMC@NLO interfaced to PYTHIA 8.243 and studied using particle-level information only. The contribution of these processes was found to be negligible in the signal region of the measurement.

The dominant background from quark-induced WW production, also referred to as $qq \rightarrow WW$, was modelled at next-to-leading-order (NLO) accuracy using the Powheg-Box [31–35] generator interfaced to PYTHIA8 and alternatively to HERWIG7. The Powheg-Box v2 sample employs the CT10 [36] PDF for the matrix element calculation and is interfaced to PYTHIA 8.212 for parton showering and hadronisation employing the parameter values of the AZNLO tune [37] and the CTEQ6L1 [38] PDF. Samples using a set of variations in the tune parameters (eigentune variations) sensitive to initial- and final-state radiation, as well as further variations related to multiple parton interactions and colour reconnection, were produced to study the description of the parton showers and hadronisation. HERWIG 7.1.6 was used as an alternative parton shower, using the H7UE tune [24] and the MMHT2014LO PDF set [39] for events generated with the Powheg-Box v2 generator. An alternative sample for quark-induced WW production was generated using the SHERPA [40, 41] event generator. The SHERPA 2.2.2 sample uses matrix elements at NLO accuracy in QCD for up to one additional parton and at LO accuracy for up to three additional parton emissions. The matrix element calculations were matched and merged with the SHERPA parton shower based on Catani–Seymour dipole factorisation [42, 43] using the MEPS@NLO prescription [40, 44–46]. The virtual QCD corrections were provided by the OPENLOOPS 1 library [47–49]. The sample was generated using the NNPDF3.0NNLO set [50], along with the dedicated set of tuned parton-shower parameters developed by the SHERPA authors.

DY production, $pp \rightarrow Z/\gamma^* \rightarrow \ell\ell$ with $\ell = e, \mu, \tau$, was modelled using the same settings for SHERPA, Powheg+PYTHIA8 and Powheg+HERWIG7 as for the quark-induced WW event generation described above. DY($\rightarrow \tau\tau$) was modelled with Powheg interfaced to PYTHIA 8.186 using the NNPDF3.0NLO PDF set [50] and the AZNLO tune together with the CTEQ6L1 PDF set for parton showering and hadronisation.

The WZ and ZZ background processes were modelled at NLO using SHERPA as well as Powheg-Box v2 interfaced to PYTHIA 8.212 with the same settings as employed for the WW event generation. $W\gamma$ production, gluon-induced WW production including resonant and non-resonant contributions and $WWjj$ production in vector-boson scattering were simulated using the SHERPA 2.2.2 generator with the NNPDF3.0NNLO PDF set. These samples use matrix elements at NLO QCD accuracy for up to one additional parton and LO accuracy for up to three additional parton emissions for $W\gamma$ and gluon-induced WW production and LO-accurate matrix elements for $WWjj$ production in vector-boson scattering.

The $t\bar{t}$ and Wt processes were simulated with the Powheg-Box [31–33, 51, 52] v2 generator at NLO with the NNPDF3.0NLO PDF interfaced to PYTHIA 8.230 using the A14 tune [53] and the NNPDF2.3LO set of PDFs. For the Wt process, the diagram removal scheme [54] was applied to remove interference and overlap with $t\bar{t}$ production.

4 Event reconstruction and selection

Candidate events from $\gamma\gamma \rightarrow WW$ production are identified by the presence of an electron and a muon with high transverse momentum and the absence of additional reconstructed charged-particle tracks associated with the interaction vertex.

Tracks are reconstructed from position measurements (hits) in the ID caused by the passage of charged particles [55, 56]. The track reconstruction consists of an iterative track-finding algorithm seeded by combinations of at least three silicon-detector hits followed by a combinatorial Kalman filter [57] to build track candidates based on hits compatible with the extrapolated trajectory. Ambiguities between the track candidates are then resolved and quality criteria are applied to suppress combinations of hits unlikely to originate from a single charged particle. At least one hit in the two innermost layers is required if the extrapolated track crosses the sensitive region of an active sensor module. The number of silicon hits in the pixel and SCT detectors must be larger than 9 for $|\eta| \leq 1.65$ or larger than 11 for $|\eta| > 1.65$, with no more than two missing SCT hits on a track if the respective SCT modules are operational. Additionally, a selection is imposed on the transverse impact parameter, $|d_0| < 1$ mm, to reject tracks from secondary interactions. Tracks are required to have $p_T > 500$ MeV and be within $|\eta| < 2.5$. These selection criteria result in an efficiency of 75–80% depending on the track p_T . The largest source of inefficiency is hadronic interactions with the detector material. In simulated events, reconstructed tracks can be classified as originating from the hard scatter or from additional pp collisions by matching the hits that contributed to the track fit to the energy deposited by the charged particle in the GEANT4 simulation. The respective tracks are counted as $n_{\text{trk}}^{\text{HS}}$ and $n_{\text{trk}}^{\text{PU}}$.

Electrons are reconstructed from energy clusters in the electromagnetic calorimeter that are matched to tracks reconstructed in the ID [58, 59]. The best-matching track is selected using as criteria track–cluster spatial distance and the number of hits in the silicon detectors [59]. Further tracks may be assigned to the electron candidate if they are likely to originate from interactions with detector material. The pseudorapidity of electrons is required to be within the range of $|\eta| < 2.47$, excluding the transition region between the barrel and endcaps in the LAr calorimeter ($1.37 < |\eta| < 1.52$). Electron candidates are required to have transverse momenta $p_T > 20$ GeV.

Muons are built from tracks reconstructed using MS hits matched to ID tracks. A global fit using the hits from both subdetectors is performed [60]. Each muon candidate is matched uniquely to exactly one ID track and is required to satisfy $|\eta| < 2.4$ and $p_T > 20$ GeV.

Identification and isolation criteria are applied to electron and muon candidates to suppress non-prompt leptons from hadron decays. Identification criteria are based on shower shapes and track parameters for the electrons, and on track parameters for the muons. The isolation criteria use information about ID tracks and calorimeter energy deposits in a fixed cone of $\Delta R = 0.2$ around each lepton. Electrons must satisfy the ‘medium’ identification criteria as well as the loose isolation criteria described in Ref. [59]. Muon candidates are required to satisfy the ‘medium’ identification and loose isolation criteria introduced in Ref. [60]. The significance of the transverse impact parameter, defined as the absolute value of d_0 , divided by its uncertainty, σ_{d_0} , must satisfy $|d_0|/\sigma_{d_0} < 3$ for muons and $|d_0|/\sigma_{d_0} < 5$ for electrons.

The decision on whether or not to record the event was made by single-electron or single-muon triggers with requirements on lepton identification and isolation similar to those applied offline. The transverse momentum thresholds for these triggers were 24 GeV for electrons [61] and 20 GeV for muons [62] in 2015, whilst during the 2016–2018 data-taking period the thresholds were both raised to 26 GeV and requirements on lepton identification and isolation were tightened. Complementary triggers with higher p_T thresholds and no isolation or looser identification criteria were used to increase the trigger efficiency.

Events are required to contain exactly two leptons of opposite electric charge that satisfy the above criteria. One of the leptons must have transverse momentum exceeding 27 GeV and be matched to an object that provided one of the triggers used for the read-out and storage of the event. The invariant mass of the two

selected leptons must exceed $m_{\ell\ell} = 20$ GeV. Both same-flavour ($ee/\mu\mu$) and different-flavour ($e\mu$) events are accepted either for auxiliary measurements or for the signal extraction, respectively.

The interaction vertex is reconstructed from the two leptons in the event, ℓ_1 and ℓ_2 , as the weighted average z -position of the tracks extrapolated to the beam line:

$$z_{\text{vtx}}^{\ell\ell} = \frac{z_{\ell_1} \sin^2 \theta_{\ell_1} + z_{\ell_2} \sin^2 \theta_{\ell_2}}{\sin^2 \theta_{\ell_1} + \sin^2 \theta_{\ell_2}},$$

where $\sin^2 \theta_\ell$ approximately parameterises the resolution of the z -position [10]. This definition of the interaction vertex is not biased by the presence of additional tracks from hadronic activity in association with the dilepton pair production or by additional tracks from nearby pile-up interactions. It results in better resolution and higher efficiency than a primary vertex selection based on the sum of squared track transverse momenta [63]. Requirements are placed on each lepton to fulfil $|(z_\ell - z_{\text{vtx}}^{\ell\ell}) \sin \theta| < 0.5$ mm.

A window of $\Delta z = \pm 1$ mm around $z_{\text{vtx}}^{\ell\ell}$ defines the region in which ID tracks are matched to the interaction vertex. The number of tracks in this window, excluding those used in the reconstruction of leptons, is counted as n_{trk} . Signal $\gamma\gamma \rightarrow WW$ event candidates are selected using the exclusivity requirement that $n_{\text{trk}} = 0$. Events with low track multiplicities, $1 \leq n_{\text{trk}} \leq 4$, are used to evaluate backgrounds. The modelling of n_{trk} is therefore vital to the extraction of the $\gamma\gamma \rightarrow WW$ signal, and this is discussed further in the following section.

5 Modelling of signal and backgrounds

Corrections are applied to the simulated signal and background event samples to adjust the lepton trigger, reconstruction, identification and isolation efficiencies, as well as the energy and momentum resolutions, to those observed in data. The muon momentum scale is corrected in the MC simulation, whilst the electron energy scale is corrected in data [59–62]. Accurate modelling of the transverse momenta of the bosons is important because of its correlation with the expected charged-particle multiplicity from hadronic activity. The p_T^{WW} distribution in the MC samples for quark-induced WW production is reweighted to the theoretical calculation at next-to-next-to-leading-order (NNLO) accuracy in perturbative quantum chromodynamics with resummation of soft gluon emissions up to next-to-next-to-next-to-leading-logarithm ($N^3\text{LL}$) accuracy using MATRIX+RadISH [48, 49, 64–72]. A correction for the transverse momentum distribution of dilepton pairs from the DY process is derived from data using ee and $\mu\mu$ final states with an invariant mass within 15 GeV of the nominal Z boson mass corrected for background, and is applied to all DY samples as a function of the generator-level p_T^Z . Additional data-driven corrections are needed for this analysis to account for (i) mismodelling of the additional pp interactions produced in the same bunch crossing, (ii) mismodelling of the charged-particle multiplicity in the $qq \rightarrow WW$ background process, and (iii) the dissociative contribution to the $\gamma\gamma \rightarrow WW$ signal process.

5.1 Modelling of additional pp interactions

Tracks from nearby additional pp interactions can be matched to the interaction vertex and, thus, lower the efficiency of the exclusivity requirement. Their number depends on the density of additional pp interactions and the number of tracks originating from these interactions. Data-driven techniques are used

to derive corrections to the simulated events to further improve their description of the data, targeting the density of pp interactions and the number of tracks per interaction separately.

The simulated events are reweighted such that the distribution of the average number of pp interactions per bunch crossing reproduces the one measured in the data. The longitudinal width of the beam spot, σ^{BS} , determines the average density, along z , of additional pp interactions near the interaction vertex. The average longitudinal width of the beam spot varied throughout the data-collection period due to changes in the LHC beam optics. It was about 44 mm in 2015 and between 34 and 38 mm in 2016–2018 compared to 42 mm in MC simulation. The photon-induced MC samples were also produced with a beam spot width of 35 mm and these were used in the final analysis. To account for the different densities of additional pp interactions in data and simulation, the beam spot width is effectively corrected by modifying the matching of tracks to the interaction vertex in simulation: tracks classified as originating from a pile-up interaction are counted in n_{trk} if they have a longitudinal impact parameter z within $1 \text{ mm} \times \sigma_{\text{MC}}^{\text{BS}}/\sigma_{\text{Data}}^{\text{BS}}$ of $z_{\text{vtx}}^{\ell\ell}$. The values for $\sigma_{\text{Data}}^{\text{BS}}$ are sampled from the LHC run conditions during Run 2 according to the luminosity taken at a given value of $\sigma_{\text{Data}}^{\text{BS}}$.

An ancillary data measurement is used to determine the correction for the number of tracks from additional pp interactions randomly matched to the interaction vertex, $n_{\text{trk}}^{\text{PU}}$. In same-flavour $Z \rightarrow \ell\ell$ events, this correction is obtained by counting the number of tracks satisfying the nominal selection criteria relative to a random position in z that is well separated from the interaction vertex, $|z_{\text{vtx}}^{\ell\ell} - z| > 10 \text{ mm}$. Each event is sampled multiple times using non-overlapping regions in z . This procedure optimises the statistical power, but does not consider the actual distribution of $z_{\text{vtx}}^{\ell\ell}$ along z . To correct for the resulting bias, $n_{\text{trk}}^{\text{PU}}$ is extracted as a function of the z -coordinate and weighted with the normalised beam spot distribution.

This method is tested using simulated events and found to reproduce the $n_{\text{trk}}^{\text{PU}}$ distribution in data within 0.1–3.5% for low track multiplicities, with larger disagreement for larger n_{trk} . Figure 2 shows the probability distribution of $n_{\text{trk}}^{\text{PU}}$ associated with $z_{\text{vtx}}^{\ell\ell}$, extracted in data and simulation before and after the corrections for the beam spot width. The bottom panel shows the ratio to data. The inverse ratio of the beam-spot-corrected simulation to data corresponds to the correction applied as a function of $n_{\text{trk}}^{\text{PU}}$ in the simulation. The distributions of the number of $n_{\text{trk}}^{\text{PU}}$ in $\gamma\gamma \rightarrow \ell\ell$ and $\gamma\gamma \rightarrow WW$ MC events are shown after the beam spot and the pile-up corrections. Before any corrections, the disagreement can be up to 15% depending on the beam spot conditions in the simulation. After the σ^{BS} correction, for low track multiplicities disagreements of about 10% persists and are corrected using the $n_{\text{trk}}^{\text{PU}}$ correction. The full set of corrections is applied to all MC samples used in the analysis.

The presence of the additional tracks from pile-up will randomly lead to the rejection of signal events and therefore the distribution of $n_{\text{trk}}^{\text{PU}}$ can be used to extract the signal efficiency of the exclusivity requirement ($n_{\text{trk}} = 0$). This exclusive efficiency depends strongly on the number of interactions per bunch crossing and the general beam conditions. The average efficiency for the 2015–2018 dataset with an average μ_{int} of 33.7 is 52.6%. It drops from 60% at $\mu_{\text{int}} = 20$ to about 30% at $\mu_{\text{int}} = 60$. When comparing the data-driven efficiency with that obtained directly from signal MC samples, the results agree to better than 0.2%.

The full effect of the data-driven correction for tracks from additional pp interactions is assigned as a systematic uncertainty, resulting in 1% and 3% uncertainty in the efficiency to select events without any additional associated tracks ($n_{\text{trk}} = 0$) for signal and background, respectively. The uncertainty of having a low number of tracks associated with the vertex ($1 \leq n_{\text{trk}} \leq 4$) is 2% for photon-induced processes and 10% for quark- and gluon-induced processes.

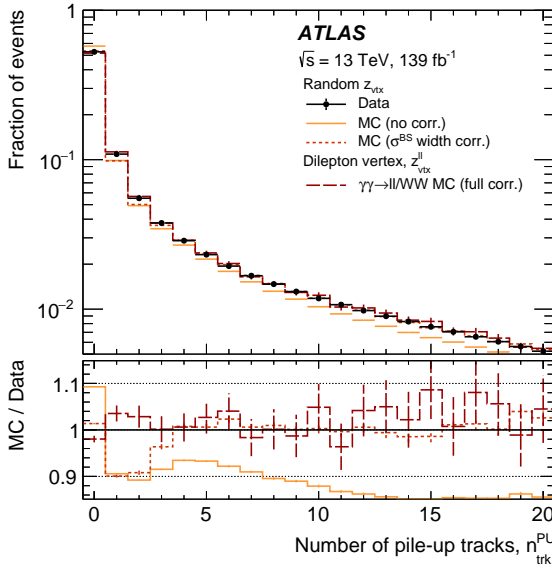


Figure 2: The normalised distribution of tracks from additional pp interactions, $n_{\text{trk}}^{\text{PU}}$, associated with the interaction vertex, in data and signal simulated with a beam spot width of $\sigma_{\text{MC}}^{\text{BS}} = 42$ mm. For data, $n_{\text{trk}}^{\text{PU}}$ is determined using a random z -position along the beam axis away from the interaction vertex. The same quantity is shown for simulated $\gamma\gamma \rightarrow WW$ events before and after correcting the beam spot width to the one observed in data. The inverse ratio of the beam-spot-corrected simulation to data corresponds to the correction applied to $n_{\text{trk}}^{\text{PU}}$ in the simulation using the GEANT4-based classification. To demonstrate the closure of the correction, the number of tracks reconstructed in elastic $\gamma\gamma \rightarrow WW$ signal MC samples is shown after applying the full set of corrections, namely the σ^{BS} correction and the $n_{\text{trk}}^{\text{PU}}$ correction. The shown uncertainties are statistical only.

5.2 Modelling of the underlying event

For quark-induced diboson production, additional charged particles can be produced from initial-state radiation or secondary partonic scatters in the same pp collision, also called the underlying event. However, for low values of the number of charged particles, the n_{ch} distribution was found to be not well modelled by many of the phenomenological models implemented in the generators [73–76]. The underlying event can be assumed to be similar for quark-induced production of different colourless final states if the transverse momenta of these final states are comparable [76]. Therefore, the charged-particle multiplicity in $qq \rightarrow WW$ events can be constrained using data measurements of DY production of $\ell\ell$ pairs in pp collisions. Specifically, the charged-particle multiplicity is measured for $Z \rightarrow \ell\ell$ produced in slices of p_{T} . This two-dimensional measurement is then used to correct the DY and diboson simulation. The general validity of this approach has been tested using DY and diboson samples generated with PowHEG+PYTHIA8, SHERPA and PowHEG+HERWIG7. The multiplicity spectra of charged particles are found to be very different in the different MC samples, yet relatively similar between the respective DY and diboson processes at a constant value of the boson or diboson p_{T} with the agreement being of the order to 10–20%.

The $Z \rightarrow \ell\ell$ events are selected using the criteria described in Section 4 with an additional requirement on the dilepton mass ($70 \text{ GeV} < m_{\ell\ell} < 105 \text{ GeV}$) to suppress contributions from background processes. The contribution of pile-up tracks is estimated from data by sampling random z -positions well separated from the dilepton vertex as discussed in Section 5.1. The background at low track multiplicities is dominated by $\gamma\gamma \rightarrow \ell\ell$ events, which have a different $p_{\text{T}}^{\ell\ell}$ dependence than DY events and amount to about 5% of the total events selected with $70 \text{ GeV} < m_{\ell\ell} < 105 \text{ GeV}$ and $n_{\text{trk}} = 0$ while their contribution is 0.5%

or smaller for higher track multiplicities. The relative normalisations for the elastic, single-dissociative and double-dissociative $\gamma\gamma \rightarrow \ell\ell$ as well as the DY process are determined in a fit to the measured $p_T^{\ell\ell}$ distribution in a $m_{\ell\ell} > 105$ GeV sideband, requiring $n_{\text{trk}} = 0$ and using the shapes from MC simulation. In this sideband, the $\gamma\gamma \rightarrow \ell\ell$ process contributes about 60% to the total event sample. The contribution from the $\gamma\gamma \rightarrow WW$ process with a same-flavour final state amounts to less than 1% of the $\gamma\gamma \rightarrow \ell\ell$ processes in this kinematic region and is neglected. The overall normalisations of the different $\gamma\gamma \rightarrow \ell\ell$ contributions relative to the prediction are compatible within the statistical uncertainty with those from earlier ATLAS studies [77].

After the $\gamma\gamma \rightarrow \ell\ell$ and pile-up contributions are subtracted as backgrounds, iterative Bayesian unfolding [78, 79] is used to unfold the distribution of the reconstructed track multiplicity, n_{trk} , to that of the number of charged particles, n_{ch} , using four iterations.² The charged-particle multiplicity is extracted as a function of the p_T of the dilepton system, which corresponds to the transverse momentum of the recoil, using 5-GeV-wide intervals of p_T . The largest sources of uncertainty are the contributions from pile-up tracks and uncertainties in the distribution used as the prior, assessed by comparing Powheg+Pythia8 and Sherpa. Other uncertainties originate from the event selection and the $\gamma\gamma \rightarrow \ell\ell$ background subtraction, assessed by varying the kinematic selection and the normalisation of the photon-induced background within the uncertainties of the fit in the $m_{\ell\ell}$ sideband. Figure 3 (left) compares the unfolded charged-particle multiplicity distribution for different MC models and data. For low values of n_{ch} , the charged-particle multiplicity distribution is mismodelled by a factor of 2.5 in Powheg+Pythia8 and by a factor of 4 in Sherpa, whilst good agreement with the Powheg+Herwig7 model is found.

The charged-particle multiplicity in simulated DY events is corrected using per-event weights determined as the ratio of the unfolded data to the unfolded MC simulation as a function of the charged-particle multiplicity, and of the particle-level p_T of the decay products of the Z boson. The impact of the charged-particle multiplicity correction is shown in Figure 3 (right) for DY events. The simulation is shown both before and after the correction for pile-up modelling and underlying-event modelling in $Z \rightarrow \ell\ell$ events satisfying $70 \text{ GeV} < m_{\ell\ell} < 105 \text{ GeV}$. The corrections bring the MC simulation into agreement with data within the systematic uncertainty of the charged-particle measurement. The correction for the underlying-event modelling is applied to WW, WZ and ZZ processes as a function of the charged-particle multiplicity, and of the particle-level p_T of the decay products of the diboson system.

5.3 Signal modelling

After the initial $\gamma\gamma \rightarrow WW$ process, the protons can undergo a second inelastic interaction. In most cases, these additional rescatterings do not change the kinematics of the $\gamma\gamma \rightarrow WW$ process but lead to the production of particles such that the cross section of $\gamma\gamma \rightarrow WW$ production without associated tracks is reduced. This effect is not included in the modelling of the signal. The probability that no such additional particles are produced is commonly referred to as the survival factor. In addition, the $\gamma\gamma \rightarrow WW$ signal when applying the exclusivity requirement is modelled by Herwig7 which includes only the elastic component. To obtain a better estimate of the expected signal yield including the dissociative components and to correct for effects from the rescattering of protons, a correction factor is obtained from a $\gamma\gamma \rightarrow \ell\ell$ control sample in data, following a procedure similar to that applied in Refs. [4, 6] using same-flavour lepton final states. To enhance the purity in $\gamma\gamma \rightarrow \ell\ell$ production and to mimic the kinematic threshold

² Similarly to Ref. [80], charged particles are defined to be stable if they have a mean lifetime $\tau > 30$ ps and satisfy $p_T > 500$ MeV and $|\eta| < 2.5$.

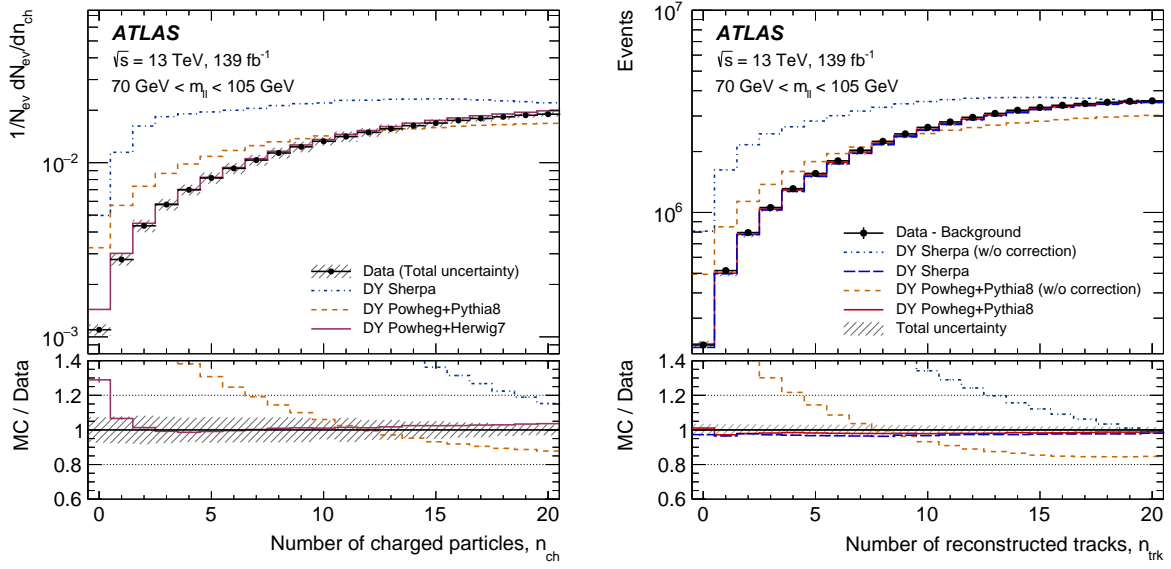


Figure 3: On the left, the normalised number of events with a given number of charged particles, $1/N_{\text{ev}} dN_{\text{ev}}/dn_{\text{ch}}$, predicted by SHERPA POWHEG+PYTHIA8 and POWHEG+HERWIG7 is compared with the unfolded data. The ratio on the bottom is the inverse of the weights that are applied at particle level as a function of the number of charged particles. The effect of the correction for the underlying event is illustrated for the number of reconstructed tracks on the right. SHERPA and POWHEG+PYTHIA8 are shown before and after the correction and compared with data. The total uncertainty of the correction is shown for POWHEG+PYTHIA8 in the upper panel, and as a band around unity for the lower panel. The total uncertainties for SHERPA and POWHEG+PYTHIA8 are very similar.

of $\gamma\gamma \rightarrow WW$ production, the dilepton mass is required to be larger than 160 GeV. The exclusivity requirement of $n_{\text{trk}} = 0$ is applied. In the region, where the correction factor is extracted, the predicted event yield from the $\gamma\gamma \rightarrow WW$ process with same-flavour final states is approximately 1.5% of the $\gamma\gamma \rightarrow \ell\ell$ yield so that the derived correction factor is essentially independent of the $\gamma\gamma \rightarrow WW$ signal process.

The dominant background from DY production is estimated using a data-driven technique. The shape of the $m_{\ell\ell}$ distribution for background events is estimated using events with $n_{\text{trk}} = 5$. This template is normalised to the $n_{\text{trk}} = 0$ selection using a narrow window around the nominal Z boson mass ($83.5 \text{ GeV} < m_{\ell\ell} < 98.5 \text{ GeV}$) where the contribution from photon-induced processes is small. The $m_{\ell\ell}$ lineshape in simulated DY events is found to be independent of n_{trk} for low multiplicities.

When applying the exclusivity requirement of $n_{\text{trk}} = 0$, the ratio of the yield from photon-induced processes in data to the MC prediction for the elastic processes is found to be 3.59 ± 0.15 (tot.). This agrees with the expectation from MC simulation. Figure 4 illustrates the extraction of the signal modelling correction from data. The signal modelling correction is only applicable to events with $n_{\text{trk}} = 0$. The simulated HERWIG7 events are used in conjunction with the signal modelling correction for predictions of photon-induced processes in events where the $n_{\text{trk}} = 0$ requirement is applied, while the event samples from MG5_AMC@NLO+PYTHIA8 are used for predictions in regions with larger track multiplicities.

Uncertainties are evaluated by increasing the mass window of the DY background normalisation region to $73.5 \text{ GeV} < m_{\ell\ell} < 108.5 \text{ GeV}$ and by changing the number of tracks used in the selection of the template, using $n_{\text{trk}} = 2$ instead of the nominal value. The total uncertainty of the signal modelling correction amounts to 4.2%. When the signal modelling correction is applied to $\gamma\gamma \rightarrow WW$, an additional transfer uncertainty is included to account for potential differences between $\gamma\gamma \rightarrow \ell\ell$ and $\gamma\gamma \rightarrow WW$ events due to

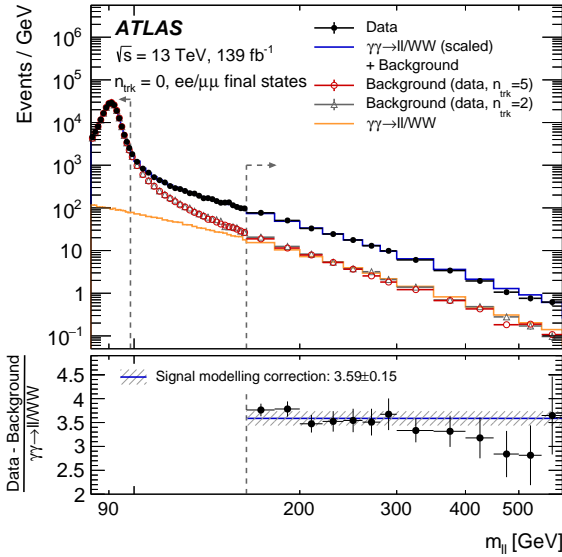


Figure 4: The distribution of $m_{\ell\ell}$ in the region where the signal modelling correction is extracted as the ratio of the yield of $\gamma\gamma \rightarrow \ell\ell$ and $\gamma\gamma \rightarrow WW$ processes passing the exclusivity requirement of $n_{\text{trk}} = 0$ to the yield of the simulated elastic process only. Shown are the data, where a requirement of $n_{\text{trk}} = 0$ has been applied, and the background templates selected from data using $n_{\text{trk}} = 2$ and $n_{\text{trk}} = 5$. In addition, the $\gamma\gamma \rightarrow \ell\ell$ and $\gamma\gamma \rightarrow WW$ MC predictions are depicted, as well as the sum of the nominal background template ($n_{\text{trk}} = 5$) and the $\gamma\gamma \rightarrow \ell\ell$ and $\gamma\gamma \rightarrow WW$ MC predictions scaled by the signal modelling correction. The normalisation region around the nominal Z boson mass is indicated with a vertical line, as is the region where the signal modelling correction is extracted ($m_{\ell\ell} > 160$ GeV). The excess in data relative to the elastic $\gamma\gamma \rightarrow \ell\ell$ and $\gamma\gamma \rightarrow WW$ prediction is attributed to the dissociative photon-induced processes and used to extract the signal modelling correction which is shown in the lower panel of the plot. The uncertainties shown are statistical only.

the fact that rescattering effects are mass-dependent. It is calculated as the largest variation that arises from placing different lower bounds on the evaluation region; the lower bound on $m_{\ell\ell}$ was varied from $m_{\ell\ell} = 110$ GeV to 400 GeV in intervals of 10 GeV. The resulting uncertainty amounts to 11%. This uncertainty affects only the scaling of the $\gamma\gamma \rightarrow WW$ process and thus the measured signal strength and any cross section prediction derived using the signal correction factor but cancels out in the measurement of the fiducial cross section.

6 Event categories and background estimation

One signal region and three control regions, enriched in signal and background events respectively, are defined using the dilepton transverse momentum, $p_T^{e\mu}$, and the number of additional tracks associated with the interaction vertex, n_{trk} . The signal region is defined by selecting $p_T^{e\mu} > 30$ GeV and $n_{\text{trk}} = 0$. It has an expected purity of 57% and an expected background contamination from $qq \rightarrow WW$ production of 33%.

Additional kinematic regions with alternative requirements on $p_T^{e\mu}$ and n_{trk} are used to control the modelling of background processes. The first control region is defined by $p_T^{e\mu} < 30$ GeV and $1 \leq n_{\text{trk}} \leq 4$ and helps to constrain the DY($\rightarrow \tau\tau$) normalisation, as this process contributes 75% of the selected events in this region. It also has non-negligible contributions from $qq \rightarrow WW$ events and non-prompt leptons. The second control region is defined by $p_T^{e\mu} > 30$ GeV and $1 \leq n_{\text{trk}} \leq 4$ and is designed to be enriched in

$qq \rightarrow WW$ events, with an expected contribution of 70% from that process and minor contributions from the DY process and non-prompt lepton events. An additional control region is selected with $p_T^{e\mu} < 30$ GeV and $n_{\text{trk}} = 0$. It brings some additional control for the modelling of backgrounds specific to events with no tracks, however has a signal contamination of the order of 10%. The boundaries between these regions are chosen such that good signal–background separation is achieved. In addition, the regions used to control the normalisation of the backgrounds are defined to be topologically very similar to the signal region, which helps to minimise uncertainties in extrapolating the normalisation from the control regions to the signal region.

Background events from non-prompt leptons contribute about 6% of the selected signal candidates in the signal region. The primary source of non-prompt leptons in dilepton events is $W+\text{jets}$ production where one of the leptons is prompt and the other stems from light-hadron or heavy-flavour decays. Background events from non-prompt leptons are estimated from a control region where exactly one of the leptons must fail to satisfy some of the lepton identification criteria of the nominal event selection. All other kinematic selection criteria are the same as for the signal selection. The contribution from non-prompt leptons is then estimated by scaling the number of events in the control region by the ratio of the number of non-prompt leptons passing all identification requirements to those failing some of these requirements. This ratio is measured in data selected with one electron and one muon with the same electric charge, and requiring $1 \leq n_{\text{trk}} \leq 4$. Contributions from prompt leptons are subtracted using MC simulation. For the extrapolation to the event samples selected with $n_{\text{trk}} = 0$ a dedicated uncertainty is assigned.

7 Systematic uncertainties

Uncertainties including their correlations are evaluated in each of the signal and control regions. The uncertainties in the measurement of tracks originate from uncertainties in the inner detector alignment, the reconstruction efficiency, and the probability to incorrectly reconstruct tracks by including hits from noise or from several tracks. The combined uncertainty amounts to 5–7% of the event yields for DY and $qq \rightarrow WW$ production, whilst for photon-induced processes these uncertainties are < 1% in the regions where these processes contribute significantly.

Systematic uncertainties in the event yields due to electron and muon reconstruction, including effects from the trigger and reconstruction efficiencies, energy/momentum scale and resolution, and pile-up modelling are 0.5% and up to 2% depending on the process, in the signal and control regions, respectively [59–62].

The uncertainty in the background from non-prompt leptons is dominated by the uncertainty in the measurement of the ratio of non-prompt leptons passing all identification requirements to those failing some, in particular the subtraction of contributions from genuine leptons in the numerator of that ratio. The resulting uncertainty ranges between 50% and 100% depending on the region. The statistical uncertainty in the control region for the estimation of background from misidentified leptons is also a significant source of uncertainty.

The uncertainties in the correction of pile-up modelling and the underlying event as well as the uncertainty in the signal modelling correction are described in Section 5. The correction for the underlying-event modelling in the WW , WZ and ZZ processes is derived in bins of $p_T^{\ell\ell}$, but applied as a function of diboson p_T , utilising the fact that there are only relatively small differences in charged-particle multiplicity between the DY and diboson processes. Residual differences are evaluated at the particle level and considered as systematic uncertainties. For the largest source of background, the quark-induced WW process, further

studies are made. The predicted event yields are compared for PowHEG+PYTHIA8 and variations of the PYTHIA8 parton-shower tunes, and for PowHEG+HERWIG7 and SHERPA, with each prediction using its dedicated underlying-event correction. The event yields agree well for $1 \leq n_{\text{trk}} \leq 4$ but disagree in the signal region, $n_{\text{trk}} = 0$. The background yield from the quark-induced WW process is estimated as the average of the highest and lowest value of the various predictions. The envelope of all predictions is taken as the upper and lower one-standard-deviation boundary, amounting to $\pm 7\%$ for events selected with $n_{\text{trk}} = 0$, and amounting to less than 1% for events selected with $1 \leq n_{\text{trk}} \leq 4$. The uncertainties in the total quark-induced WW cross section and the shape of the p_T^{WW} distribution are taken from the MATRIX+RadISH prediction used to reweight the WW samples, amounting to 5–6%.

Because of the specific event selection of the analysis, large uncertainties are applied to minor backgrounds, where the n_{trk} modelling cannot be easily studied in data: the uncertainty in the $W\gamma$ normalisation is taken to be $\pm 100\%$, whereas uncertainties of $\pm 30\%$ are used for the normalisation of top-quark production and $WWjj$ production through vector-boson scattering (VBS) as well as gluon-induced resonant and non-resonant WW production. The numbers are informed by the size of the underlying-event correction in DY and WW events and studies on events with forward jets outside the acceptance of the ID. For the smaller background contributions from WZ and ZZ production the uncertainty is assessed by comparing the event yields predicted by PowHEG+PYTHIA8 with those predicted in SHERPA after applying the underlying-event correction described in Section 5.2.

The systematic uncertainty in the measured cross section also includes a contribution due to differences in reconstruction efficiency between elastic and dissociative photon-induced processes as well as an uncertainty due to missing spin correlations in HERWIG7. These uncertainties are evaluated separately by comparing the reconstruction efficiency of the elastic-only prediction with that including all production mechanisms and by comparing the reconstruction efficiency between HERWIG7 and MG5_AMC@NLO+PYTHIA8. Their combined effect is $\pm 2\%$.

8 Results

The $\gamma\gamma \rightarrow WW$ signal in proton–proton collisions is extracted using a profile likelihood fit of the estimated signal and background event yields to data. The fit uses the integrated event yields in the four kinematic regions introduced in Section 6, and the $ee + \mu\mu$ events selected as described in Section 5.3. It maximises the product of Poisson probabilities to produce the observed number of data events, N_{obs} , in each of these regions [81].

The normalisation of the backgrounds from DY and $qq \rightarrow WW$ processes are free parameters in the fit. The expected elastic $\gamma\gamma \rightarrow \ell\ell$ and $\gamma\gamma \rightarrow WW$ event yields for $n_{\text{trk}} = 0$ are multiplied by the signal modelling correction discussed in Section 5.3, which is obtained as described within the fit to preserve the experimental correlations correctly. The event yield for the $\gamma\gamma \rightarrow WW$ signal process is also multiplied by a signal strength that is a free parameter in the fit. Systematic uncertainties are included in the fit as nuisance parameters constrained by Gaussian functions. The fit can only constrain the sum of the backgrounds, since the background composition is similar in events selected with $n_{\text{trk}} = 0$ and those selected with $1 \leq n_{\text{trk}} \leq 4$. Overall, the uncertainty in the sum of their yields is dominated by the systematic uncertainties assigned to events selected with $n_{\text{trk}} = 0$. In this fit, the background-only hypothesis is expected to be rejected with a significance of 6.7 standard deviations.

Table 1: Summary of the data event yields, and the predicted signal and background event yields in the signal region and control regions as obtained after the fit. The uncertainties shown include statistical and systematic components. Because the fit introduces correlations between systematic uncertainties, the uncertainty in the total expected yield is smaller than its components. The leftmost column of values corresponds to the signal region used to measure $\gamma\gamma \rightarrow WW$ in proton–proton collisions. The numbers for $qq \rightarrow WW$ also contain a small contribution from gluon-induced WW and electroweak $WWjj$ production. The event yields for other backgrounds include contributions from WZ and ZZ diboson production, top-quark production and other gluon-induced processes.

n_{trk} $p_T^{e\mu}$	Signal region		Control regions		
	$n_{\text{trk}} = 0$		$1 \leq n_{\text{trk}} \leq 4$		
	$> 30 \text{ GeV}$	$< 30 \text{ GeV}$	$> 30 \text{ GeV}$	$< 30 \text{ GeV}$	
$\gamma\gamma \rightarrow WW$	174 \pm 20	45 \pm 6	95 \pm 19	24 \pm 5	
$\gamma\gamma \rightarrow \ell\ell$	5.5 \pm 0.3	39.6 \pm 1.9	5.6 \pm 1.2	32 \pm 7	
Drell–Yan	4.5 \pm 0.9	280 \pm 40	106 \pm 19	4700 \pm 400	
$qq \rightarrow WW$ (incl. gg and VBS)	101 \pm 17	55 \pm 10	1700 \pm 270	970 \pm 150	
Non-prompt	14 \pm 14	36 \pm 35	220 \pm 220	500 \pm 400	
Other backgrounds	7.1 \pm 1.7	1.9 \pm 0.4	311 \pm 76	81 \pm 15	
Total	305 \pm 18	459 \pm 19	2460 \pm 60	6320 \pm 130	
Data	307	449	2458	6332	

Table 1 gives an overview of the number of data events compared to background and signal event yields in the different regions after the fit. The data yield in the signal region is 307, compared with 132 background events predicted by the best-fit result. The normalisations of the WW and the DY background are constrained with the help of the control regions and are scaled by $1.21_{-0.23}^{+0.19}$ (tot.) and $1.16_{-0.12}^{+0.10}$ (tot.), respectively.

By fitting the data and background event yields in the signal and control regions, the background-only hypothesis is rejected with a significance of 8.4 standard deviations, assuming that the systematic uncertainties are Gaussian-distributed up to large values. A signal strength of $1.33_{-0.14}^{+0.14}$ (stat.) $_{-0.17}^{+0.22}$ (syst.) is measured relative to the yield of elastic $\gamma\gamma \rightarrow WW$ events predicted by HERWIG7 scaled by the signal modelling correction to account for all photon-induced production mechanisms in a phase space with no tracks associated with the interaction vertex. These results constitute the observation of photon-induced WW production in pp collisions, a process for which only evidence with significances of 3.0σ [4] and 3.6σ [6] was previously reported.

Figure 5 shows two $p_T^{e\mu}$ distributions: on the left for events with $1 \leq n_{\text{trk}} \leq 4$ associated with the interaction vertex, and, on the right, for events with the exclusivity requirement of no tracks. The boundary between low- and high- $p_T^{e\mu}$ control and signal regions is at 30 GeV. The distributions in Figure 5 include the fitted normalisations and nuisance parameters described above; the resulting predictions are in good agreement with the data. Figure 6 shows the distribution of the number of reconstructed tracks for $p_T^{e\mu} > 30 \text{ GeV}$.

The fiducial phase space used for the cross-section measurement is defined to be close to the acceptance of the detector. The leptons must at particle level satisfy the pseudorapidity requirement $|\eta| < 2.5$. One of the leptons is required to have a transverse momentum of at least 27 GeV, whilst the other must have $p_T > 20 \text{ GeV}$. They are required to be prompt leptons from W decays. Photons in a cone of $\Delta R = 0.1$ around a lepton and not originating from the decays of hadrons are added to the four-momentum of the lepton. Events with exactly two leptons are selected with opposite-sign and different-flavour final states.

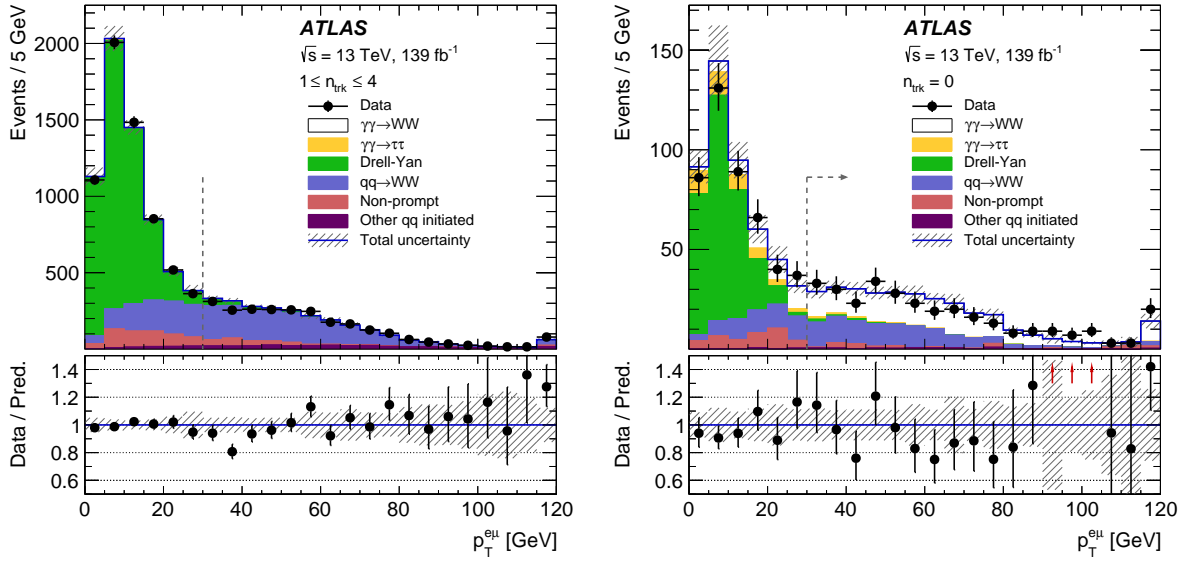


Figure 5: The distributions of $p_T^{e\mu}$ for $1 \leq n_{\text{trk}} \leq 4$ (left) and $n_{\text{trk}} = 0$ (right) are shown. The fitted normalisation factors and nuisance parameters have been used. The yields for the likelihood fit are given by the integrals of the distributions split at $p_T^{e\mu} = 30$ GeV, as indicated by the vertical dashed lines. The $\gamma\gamma \rightarrow WW$ signal region requires a selection of $p_T^{e\mu} > 30$ GeV with $n_{\text{trk}} = 0$, as indicated by the arrow. The $qq \rightarrow WW$ component also contains a small contribution from gluon-induced WW and electroweak $WWjj$ production. Similarly, ‘other qq initiated’ includes contributions not only from WZ and ZZ diboson production but also from top-quark production and other gluon-induced processes. The total uncertainties are shown as hatched bands. The lower panels show the ratio of the data to the prediction, with the total uncertainty displayed as a hatched band. The last bin in both distributions includes the overflow.

Decays of either W boson into a τ -lepton and neutrino are excluded. The invariant mass of the dilepton system is required to be $m_{\ell\ell} > 20$ GeV and its transverse momentum must be $p_T^{e\mu} > 30$ GeV. The number of charged particles, n_{ch} , with $p_T > 500$ MeV and within $|\eta| < 2.5$, excluding the selected leptons, is required to be zero.

Without requirements on the number of reconstructed tracks, the selection efficiency after reconstruction is 75% for elastic $\gamma\gamma \rightarrow WW$ events in the fiducial region. The full selection efficiency after applying $n_{\text{trk}} = 0$ is 39%. The predicted number of signal events includes a 5% contribution of non-prompt leptons from $W \rightarrow \tau\nu_\tau$, $\tau \rightarrow \ell\nu_\ell\nu_\tau$, which are removed from the measured fiducial cross section using this fractional contribution.

The observed signal strength translates into a fiducial cross section of

$$\sigma_{\text{meas}} = 3.13 \pm 0.31 (\text{stat.}) \pm 0.28 (\text{syst.}) \text{ fb}$$

for $pp(\gamma\gamma) \rightarrow p^{(*)}W^+W^-p^{(*)}$ production with $W^+W^- \rightarrow e^\pm\nu\mu^\mp\nu$. The uncertainties correspond to the statistical and systematic uncertainties, respectively. Table 2 gives an overview of the sources of systematic uncertainties which are discussed in Section 7 and presents their effect on the measured cross section. To evaluate the impact of one source of systematic uncertainty, the fit is performed with the corresponding nuisance parameter fixed one standard deviation up or down from the value obtained in the nominal fit, then these high and low variations are symmetrised.

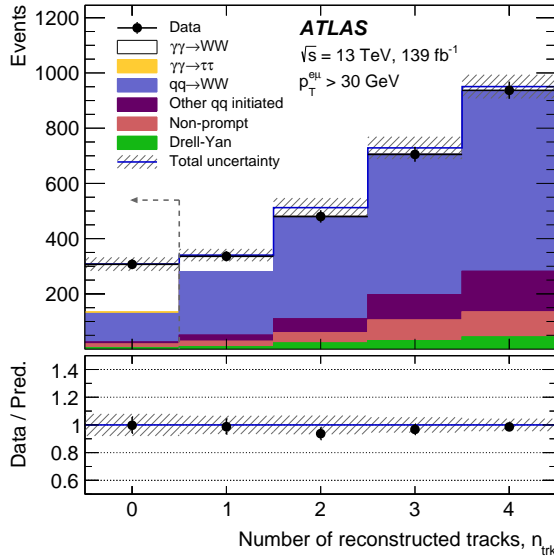


Figure 6: The distribution of the number of tracks associated with the interaction vertex is shown. The fitted normalisation factors and nuisance parameters have been used. The $\gamma\gamma \rightarrow WW$ signal region requires a selection of $n_{\text{trk}} = 0$, as indicated by the arrow. The $qq \rightarrow WW$ component also contains a small contribution from gluon-induced WW and electroweak $WWjj$ production. Similarly, ‘other qq initiated’ includes contributions not only from WZ and ZZ diboson production but also from top-quark production and other gluon-induced processes. The total uncertainties are shown as hatched bands. The lower panel shows the ratio of the data to the prediction, with the total uncertainty displayed as a hatched band.

The data measurement can be compared with two types of predictions. The first, used in the definition of the signal strength and the calculation of the expected significance, is based on the **HERWIG7** prediction for elastic $\gamma\gamma \rightarrow WW$ events scaled by the data-driven signal modelling correction to include the dissociative processes and rescattering effects as described in Section 5.3. It is found to be

$$\sigma_{\text{theo}} \times 3.59 \pm 0.15 \text{ (exp.)} \pm 0.39 \text{ (trans.)} = 2.34 \pm 0.27 \text{ fb ,}$$

where the uncertainty contains all experimental uncertainties and receives an additional component due to the transfer from the $\gamma\gamma \rightarrow \ell\ell$ to the $\gamma\gamma \rightarrow WW$ process described above. The uncertainties in the theory prediction are negligible as the scale uncertainty on the calculation of elastic production based on a photon-flux is small and partially cancels with the signal correction that is calculated with respect to the same photon-flux compared to the data. A stand-alone theory prediction for the fiducial cross section is computed with **MG5_AMC@NLO+PYTHIA8** using the appropriate MMHT2015qed PDF sets [82] for each of the contributions by applying the fiducial requirements to all photon-induced contributions, which yields $4.3 \pm 1.0 \text{ (scale)} \pm 0.12 \text{ (PDF)} \text{ fb}$. The scale uncertainty is determined by varying the factorisation scale by factors of 2 and 0.5 and symmetrising the effect. The contributions to this cross-section prediction from elastic and single-dissociative production are 16% and 81%, respectively. Double-dissociative production contributes only 3%. Using CT14qed [28] as the central PDF set yields a prediction which is 26% smaller and amounts to 3.2 fb.

The **MG5_AMC@NLO+PYTHIA8** prediction does not include rescattering effects that are expected to decrease the fiducial cross section. For elastic $\gamma\gamma \rightarrow WW$ production, a survival factor of 0.65 was estimated in Ref. [83]. In Ref. [84] a survival factor of 0.82 was calculated in a two-channel

Table 2: The impact of different components of systematic uncertainty on the measured fiducial cross section, without taking into account correlations. The impact of each source of systematic uncertainty is computed by first performing the fit with the corresponding nuisance parameter fixed to one standard deviation up or down from the value obtained in the nominal fit, then these high and low variations are symmetrised. The impacts of several sources of systematic uncertainty are added in quadrature for each component.

Source of uncertainty	Impact [%]
Experimental	
Track reconstruction	1.1
Electron energy scale and resolution, and efficiency	0.4
Muon momentum scale and resolution, and efficiency	0.5
Misidentified leptons	1.5
Background, statistical	6.7
Modelling	
Pile-up modelling	1.1
Underlying-event modelling	1.4
Signal modelling	2.1
WW modelling	4.0
Other backgrounds	1.7
Luminosity	1.7
Total	8.9

eikonal model also accounting for the helicity structure of the hard scattering process.³ Multiplying the MG5_AMC@NLO+PYTHIA8 prediction by these survival factors results in theoretical predictions of 2.8 ± 0.8 fb and 3.5 ± 1.0 fb, respectively, with the total uncertainties calculated as the quadratic sum of scale and PDF uncertainties. These predictions are in agreement with the measurement.

9 Conclusion

The photon-induced production process, $\gamma\gamma \rightarrow WW$, was studied in proton–proton collisions at $\sqrt{s} = 13$ TeV recorded with the ATLAS detector at the LHC corresponding to an integrated luminosity of 139 fb^{-1} . Events with leptonic W boson decays into $e^\pm\nu\mu^\mp\nu$ final states were selected by requiring that no tracks except those of the two charged leptons are associated with the production vertex. The background-only hypothesis is rejected with a significance of 8.4 standard deviations whereas 6.7 was expected. This measurement constitutes the observation of photon-induced WW production in pp collisions, a process for which only evidence was previously reported. The signal strength and the cross section for the sum of elastic and dissociative production mechanisms are measured. The cross section for the $pp(\gamma\gamma) \rightarrow p^{(*)}W^+W^-p^{(*)}$ process in the decay channel $W^+W^- \rightarrow e^\pm\nu\mu^\mp\nu$ in a fiducial phase space close to the experimental acceptance is measured to be $3.13 \pm 0.31 \text{ (stat.)} \pm 0.28 \text{ (syst.) fb}$. This result is in agreement with the theoretical predictions and may serve as input into EFT interpretations.

³ More recent calculations predict slightly lower absorption values for the dissociative processes [85].

Acknowledgements

We thank CERN for the very successful operation of the LHC, as well as the support staff from our institutions without whom ATLAS could not be operated efficiently.

We acknowledge the support of ANPCyT, Argentina; YerPhI, Armenia; ARC, Australia; BMWFW and FWF, Austria; ANAS, Azerbaijan; SSTC, Belarus; CNPq and FAPESP, Brazil; NSERC, NRC and CFI, Canada; CERN; ANID, Chile; CAS, MOST and NSFC, China; COLCIENCIAS, Colombia; MSMT CR, MPO CR and VSC CR, Czech Republic; DNRF and DNSRC, Denmark; IN2P3-CNRS and CEA-DRF/IRFU, France; SRNSFG, Georgia; BMBF, HGF and MPG, Germany; GSRT, Greece; RGC and Hong Kong SAR, China; ISF and Benoziyo Center, Israel; INFN, Italy; MEXT and JSPS, Japan; CNRST, Morocco; NWO, Netherlands; RCN, Norway; MNiSW and NCN, Poland; FCT, Portugal; MNE/IFA, Romania; MES of Russia and NRC KI, Russia Federation; JINR; MESTD, Serbia; MSSR, Slovakia; ARRS and MIZŠ, Slovenia; DST/NRF, South Africa; MICINN, Spain; SRC and Wallenberg Foundation, Sweden; SERI, SNSF and Cantons of Bern and Geneva, Switzerland; MOST, Taiwan; TAEK, Turkey; STFC, United Kingdom; DOE and NSF, United States of America. In addition, individual groups and members have received support from BCKDF, CANARIE, Compute Canada and CRC, Canada; ERC, ERDF, Horizon 2020, Marie Skłodowska-Curie Actions and COST, European Union; Investissements d’Avenir Labex, Investissements d’Avenir Idex and ANR, France; DFG and AvH Foundation, Germany; Herakleitos, Thales and Aristeia programmes co-financed by EU-ESF and the Greek NSRF, Greece; BSF-NSF and GIF, Israel; La Caixa Banking Foundation, CERCA Programme Generalitat de Catalunya and PROMETEO and GenT Programmes Generalitat Valenciana, Spain; Göran Gustafssons Stiftelse, Sweden; The Royal Society and Leverhulme Trust, United Kingdom.

The crucial computing support from all WLCG partners is acknowledged gratefully, in particular from CERN, the ATLAS Tier-1 facilities at TRIUMF (Canada), NDGF (Denmark, Norway, Sweden), CC-IN2P3 (France), KIT/GridKA (Germany), INFN-CNAF (Italy), NL-T1 (Netherlands), PIC (Spain), ASGC (Taiwan), RAL (UK) and BNL (USA), the Tier-2 facilities worldwide and large non-WLCG resource providers. Major contributors of computing resources are listed in Ref. [86].

References

- [1] E. Chapon, C. Royon and O. Kepka, *Anomalous quartic $WW\gamma\gamma$, $ZZ\gamma\gamma$, and trilinear $WW\gamma$ couplings in two-photon processes at high luminosity at the LHC*, *Phys. Rev. D* **81** (2010) 074003, arXiv: [0912.5161 \[hep-ph\]](#).
- [2] B. Grzadkowski, M. Iskrzyński, M. Misiak and J. Rosiek, *Dimension-six terms in the Standard Model Lagrangian*, *JHEP* **10** (2010) 085, arXiv: [1008.4884 \[hep-ph\]](#).
- [3] O. J. P. Éboli, M. C. Gonzalez-García, S. M. Lietti and S. F. Novaes, *Anomalous quartic gauge boson couplings at hadron colliders*, *Phys. Rev. D* **63** (2001) 075008, arXiv: [hep-ph/0009262](#).
- [4] ATLAS Collaboration, *Measurement of exclusive $\gamma\gamma \rightarrow W^+W^-$ production and search for exclusive Higgs boson production in pp collisions at $\sqrt{s} = 8$ TeV using the ATLAS detector*, *Phys. Rev. D* **94** (2016) 032011, arXiv: [1607.03745 \[hep-ex\]](#).
- [5] CMS Collaboration, *Study of exclusive two-photon production of W^+W^- in pp collisions at $\sqrt{s} = 7$ TeV and constraints on anomalous quartic gauge couplings*, *JHEP* **07** (2013) 116, arXiv: [1305.5596 \[hep-ex\]](#).
- [6] CMS Collaboration, *Evidence for exclusive $\gamma\gamma \rightarrow W^+W^-$ production and constraints on anomalous quartic gauge couplings in pp collisions at $\sqrt{s} = 7$ and 8 TeV*, *JHEP* **08** (2016) 119, arXiv: [1604.04464 \[hep-ex\]](#).
- [7] ATLAS Collaboration, *The ATLAS Experiment at the CERN Large Hadron Collider*, *JINST* **3** (2008) S08003.
- [8] ATLAS Collaboration, *ATLAS Insertable B-Layer Technical Design Report*, ATLAS-TDR-19; CERN-LHCC-2010-013, 2010, URL: <https://cds.cern.ch/record/1291633>.
- [9] B. Abbott et al., *Production and integration of the ATLAS Insertable B-Layer*, *JINST* **13** (2018) T05008, arXiv: [1803.00844 \[physics.ins-det\]](#).
- [10] ATLAS Collaboration, *Track Reconstruction Performance of the ATLAS Inner Detector at $\sqrt{s} = 13$ TeV*, ATL-PHYS-PUB-2015-018, 2015, URL: <https://cds.cern.ch/record/2037683>.
- [11] ATLAS Collaboration, *Performance of the ATLAS trigger system in 2015*, *Eur. Phys. J. C* **77** (2017) 317, arXiv: [1611.09661 \[hep-ex\]](#).
- [12] ATLAS Collaboration, *Luminosity determination in pp collisions at $\sqrt{s} = 13$ TeV using the ATLAS detector at the LHC*, ATLAS-CONF-2019-021, 2019, URL: <https://cds.cern.ch/record/2677054>.
- [13] ATLAS Collaboration, *Characterization of Interaction-Point Beam Parameters Using the pp Event-Vertex Distribution Reconstructed in the ATLAS Detector at the LHC*, ATLAS-CONF-2010-027, 2010, URL: <https://cds.cern.ch/record/1277659>.
- [14] ATLAS Collaboration, *ATLAS data quality operations and performance for 2015–2018 data-taking*, *JINST* **15** (2020) P04003, arXiv: [1911.04632 \[physics.ins-det\]](#).
- [15] G. Avoni et al., *The new LUCID-2 detector for luminosity measurement and monitoring in ATLAS*, *JINST* **13** (2018) P07017.
- [16] ATLAS Collaboration, *The ATLAS Simulation Infrastructure*, *Eur. Phys. J. C* **70** (2010) 823, arXiv: [1005.4568 \[physics.ins-det\]](#).
- [17] S. Agostinelli et al., *GEANT4 – a simulation toolkit*, *Nucl. Instrum. Meth. A* **506** (2003) 250.

- [18] ATLAS Collaboration, *The simulation principle and performance of the ATLAS fast calorimeter simulation FastCaloSim*, ATL-PHYS-PUB-2010-013, 2010, URL: <https://cds.cern.ch/record/1300517>.
- [19] T. Sjöstrand et al., *An introduction to PYTHIA 8.2*, *Comput. Phys. Commun.* **191** (2015) 159, arXiv: [1410.3012 \[hep-ph\]](https://arxiv.org/abs/1410.3012).
- [20] ATLAS Collaboration, *The Pythia 8 A3 tune description of ATLAS minimum bias and inelastic measurements incorporating the Donnachie–Landshoff diffractive model*, ATL-PHYS-PUB-2016-017, 2016, URL: <https://cds.cern.ch/record/2206965>.
- [21] R. D. Ball et al., *Parton distributions with LHC data*, *Nucl. Phys. B* **867** (2013) 244, arXiv: [1207.1303 \[hep-ph\]](https://arxiv.org/abs/1207.1303).
- [22] D. J. Lange, *The EvtGen particle decay simulation package*, *Nucl. Instrum. Meth. A* **462** (2001) 152.
- [23] M. Bahr et al., *Herwig++ physics and manual*, *Eur. Phys. J. C* **58** (2008) 639, arXiv: [0803.0883 \[hep-ph\]](https://arxiv.org/abs/0803.0883).
- [24] J. Bellm et al., *Herwig 7.0/Herwig++ 3.0 release note*, *Eur. Phys. J. C* **76** (2016) 196, arXiv: [1512.01178 \[hep-ph\]](https://arxiv.org/abs/1512.01178).
- [25] V. M. Budnev, I. F. Ginzburg, G. V. Meledin and V. G. Serbo, *The two-photon particle production mechanism. Physical problems. Applications. Equivalent photon approximation*, *Phys. Rept.* **15** (1975) 181.
- [26] L. Lönnblad, ‘THEPEG: Toolkit for High Energy Physics event generation’, *Proceedings, HERA and the LHC Workshop Series on the implications of HERA for LHC physics: 2006-2008*, DESY, 2009 733, arXiv: [0903.3861 \[hep-ph\]](https://arxiv.org/abs/0903.3861).
- [27] J. Alwall et al., *The automated computation of tree-level and next-to-leading order differential cross sections, and their matching to parton shower simulations*, *JHEP* **07** (2014) 079, arXiv: [1405.0301 \[hep-ph\]](https://arxiv.org/abs/1405.0301).
- [28] C. Schmidt, J. Pumplin, D. Stump and C.-P. Yuan, *CT14QED parton distribution functions from isolated photon production in deep inelastic scattering*, *Phys. Rev. D* **93** (2016) 114015, arXiv: [1509.02905 \[hep-ph\]](https://arxiv.org/abs/1509.02905).
- [29] J. A. M. Vermaasen, *Two-photon processes at very high energies*, *Nucl. Phys. B* **229** (1983) 347.
- [30] V. Bertone, S. Carrazza, N. Hartland and J. Rojo, *Illuminating the photon content of the proton within a global PDF analysis*, *SciPost Physics* **5** (2018), arXiv: [1712.07053 \[hep-ph\]](https://arxiv.org/abs/1712.07053).
- [31] P. Nason, *A new method for combining NLO QCD with shower Monte Carlo algorithms*, *JHEP* **11** (2004) 040, arXiv: [hep-ph/0409146](https://arxiv.org/abs/hep-ph/0409146).
- [32] S. Frixione, P. Nason and C. Oleari, *Matching NLO QCD computations with parton shower simulations: the POWHEG method*, *JHEP* **11** (2007) 070, arXiv: [0709.2092 \[hep-ph\]](https://arxiv.org/abs/0709.2092).
- [33] S. Alioli, P. Nason, C. Oleari and E. Re, *A general framework for implementing NLO calculations in shower Monte Carlo programs: the POWHEG BOX*, *JHEP* **06** (2010) 043, arXiv: [1002.2581 \[hep-ph\]](https://arxiv.org/abs/1002.2581).
- [34] T. Melia, P. Nason, R. Röntsch and G. Zanderighi, *W^+W^- , WZ and ZZ production in the POWHEG BOX*, *JHEP* **11** (2011) 078, arXiv: [1107.5051 \[hep-ph\]](https://arxiv.org/abs/1107.5051).
- [35] P. Nason and G. Zanderighi, *W^+W^- , WZ and ZZ production in the POWHEG-BOX-V2*, *Eur. Phys. J. C* **74** (2014) 2702, arXiv: [1311.1365 \[hep-ph\]](https://arxiv.org/abs/1311.1365).

- [36] H.-L. Lai et al., *New parton distributions for collider physics*, Phys. Rev. D **82** (2010) 074024, arXiv: [1007.2241 \[hep-ph\]](#).
- [37] ATLAS Collaboration, *Measurement of the Z/γ^* boson transverse momentum distribution in pp collisions at $\sqrt{s} = 7$ TeV with the ATLAS detector*, JHEP **09** (2014) 145, arXiv: [1406.3660 \[hep-ex\]](#).
- [38] J. Pumplin et al., *New Generation of Parton Distributions with Uncertainties from Global QCD Analysis*, JHEP **07** (2002) 012, arXiv: [hep-ph/0201195](#).
- [39] L. A. Harland-Lang, A. D. Martin, P. Motylinski and R. S. Thorne, *Parton distributions in the LHC era: MMHT 2014 PDFs*, Eur. Phys. J. C **75** (2015), arXiv: [1412.3989 \[hep-ph\]](#).
- [40] S. Höche, F. Krauss, S. Schumann and F. Siegert, *QCD matrix elements and truncated showers*, JHEP **05** (2009) 053, arXiv: [0903.1219 \[hep-ph\]](#).
- [41] E. Bothmann et al., *Event Generation with Sherpa 2.2*, SciPost Phys. **7** (2019) 034, arXiv: [1905.09127 \[hep-ph\]](#).
- [42] T. Gleisberg and S. Höche, *Comix, a new matrix element generator*, JHEP **12** (2008) 039, arXiv: [0808.3674 \[hep-ph\]](#).
- [43] S. Schumann and F. Krauss, *A parton shower algorithm based on Catani–Seymour dipole factorisation*, JHEP **03** (2008) 038, arXiv: [0709.1027 \[hep-ph\]](#).
- [44] S. Höche, F. Krauss, M. Schönher and F. Siegert, *A critical appraisal of NLO+PS matching methods*, JHEP **09** (2012) 049, arXiv: [1111.1220 \[hep-ph\]](#).
- [45] S. Höche, F. Krauss, M. Schönher and F. Siegert, *QCD matrix elements + parton showers. The NLO case*, JHEP **04** (2013) 027, arXiv: [1207.5030 \[hep-ph\]](#).
- [46] S. Catani, F. Krauss, R. Kuhn and B. R. Webber, *QCD Matrix Elements + Parton Showers*, JHEP **11** (2001) 063, arXiv: [hep-ph/0109231](#).
- [47] F. Buccioni et al., *OpenLoops 2*, Eur. Phys. J. C **79** (2019) 866, arXiv: [1907.13071 \[hep-ph\]](#).
- [48] F. Cascioli, P. Maierhöfer and S. Pozzorini, *Scattering Amplitudes with Open Loops*, Phys. Rev. Lett. **108** (2012) 111601, arXiv: [1111.5206 \[hep-ph\]](#).
- [49] A. Denner, S. Dittmaier and L. Hofer, *Collier: A fortran-based complex one-loop library in extended regularizations*, Comput. Phys. Commun. **212** (2017) 220, arXiv: [1604.06792 \[hep-ph\]](#).
- [50] R. D. Ball et al., *Parton distributions for the LHC run II*, JHEP **04** (2015) 040, arXiv: [1410.8849 \[hep-ph\]](#).
- [51] S. Frixione, P. Nason and G. Ridolfi, *A positive-weight next-to-leading-order Monte Carlo for heavy flavour hadroproduction*, JHEP **09** (2007) 126, arXiv: [0707.3088 \[hep-ph\]](#).
- [52] E. Re, *Single-top Wt-channel production matched with parton showers using the POWHEG method*, Eur. Phys. J. C **71** (2011) 1547, arXiv: [1009.2450 \[hep-ph\]](#).
- [53] ATLAS Collaboration, *ATLAS Pythia 8 tunes to 7 TeV data*, ATL-PHYS-PUB-2014-021, 2014, URL: <https://cds.cern.ch/record/1966419>.
- [54] S. Frixione, E. Laenen, P. Motylinski, C. D. White and B. R. Webber, *Single-top hadroproduction in association with a W boson*, JHEP **07** (2008) 029, arXiv: [0805.3067 \[hep-ph\]](#).
- [55] ATLAS Collaboration, *The Optimization of ATLAS Track Reconstruction in Dense Environments*, ATL-PHYS-PUB-2015-006, 2015, URL: <https://cds.cern.ch/record/2002609>.

- [56] ATLAS Collaboration, *Early Inner Detector Tracking Performance in the 2015 Data at $\sqrt{s} = 13$ TeV*, ATL-PHYS-PUB-2015-051, 2015, URL: <https://cds.cern.ch/record/2110140>.
- [57] R. Frühwirth, *Application of Kalman filtering to track and vertex fitting*, Nucl. Instrum. Meth. A **262** (1987) 444.
- [58] ATLAS Collaboration, *Electron reconstruction and identification in the ATLAS experiment using the 2015 and 2016 LHC proton–proton collision data at $\sqrt{s} = 13$ TeV*, Eur. Phys. J. C **79** (2019) 639, arXiv: [1902.04655 \[hep-ex\]](https://arxiv.org/abs/1902.04655).
- [59] ATLAS Collaboration, *Electron and photon performance measurements with the ATLAS detector using the 2015–2017 LHC proton–proton collision data*, JINST **14** (2019) P12006, arXiv: [1908.00005 \[hep-ex\]](https://arxiv.org/abs/1908.00005).
- [60] ATLAS Collaboration, *Muon reconstruction performance of the ATLAS detector in proton–proton collision data at $\sqrt{s} = 13$ TeV*, Eur. Phys. J. C **76** (2016) 292, arXiv: [1603.05598 \[hep-ex\]](https://arxiv.org/abs/1603.05598).
- [61] ATLAS Collaboration, *Performance of electron and photon triggers in ATLAS during LHC Run 2*, Eur. Phys. J. C **80** (2020) 47, arXiv: [1909.00761 \[hep-ex\]](https://arxiv.org/abs/1909.00761).
- [62] ATLAS Collaboration, *Performance of the ATLAS muon triggers in Run 2*, (2020), arXiv: [2004.13447 \[hep-ex\]](https://arxiv.org/abs/2004.13447).
- [63] ATLAS Collaboration, *Vertex Reconstruction Performance of the ATLAS Detector at $\sqrt{s} = 13$ TeV*, ATL-PHYS-PUB-2015-026, 2015, URL: <https://cds.cern.ch/record/2037717>.
- [64] S. Kallweit, E. Re, L. Rottoli and M. Wiesemann, *Accurate single- and double-differential resummation of colour-singlet processes with MATRIX+RadISH: W^+W^- production at the LHC*, (2020), arXiv: [2004.07720 \[hep-ph\]](https://arxiv.org/abs/2004.07720).
- [65] M. Grazzini, S. Kallweit and M. Wiesemann, *Fully differential NNLO computations with MATRIX*, Eur. Phys. J. C **78** (2018) 537, arXiv: [1711.06631 \[hep-ph\]](https://arxiv.org/abs/1711.06631).
- [66] M. Grazzini, S. Kallweit, S. Pozzorini, D. Rathlev and M. Wiesemann, *W^+W^- production at the LHC: fiducial cross sections and distributions in NNLO QCD*, JHEP **08** (2016) 140, arXiv: [1605.02716 \[hep-ph\]](https://arxiv.org/abs/1605.02716).
- [67] T. Gehrmann et al., *W^+W^- Production at Hadron Colliders in Next to Next to Leading Order QCD*, Phys. Rev. Lett. **113** (2014) 212001, arXiv: [1408.5243 \[hep-ph\]](https://arxiv.org/abs/1408.5243).
- [68] W. Bizon, P. F. Monni, E. Re, L. Rottoli and P. Torrielli, *Momentum-space resummation for transverse observables and the Higgs p_\perp at $N^3LL+NNLO$* , JHEP **02** (2018) 108, arXiv: [1705.09127 \[hep-ph\]](https://arxiv.org/abs/1705.09127).
- [69] P. F. Monni, E. Re and P. Torrielli, *Higgs Transverse-Momentum Resummation in Direct Space*, Phys. Rev. Lett. **116** (2016) 242001, arXiv: [1604.02191 \[hep-ph\]](https://arxiv.org/abs/1604.02191).
- [70] T. Gehrmann, A. von Manteuffel and L. Tancredi, *The two-loop helicity amplitudes for $q\bar{q}' \rightarrow V_1 V_2 \rightarrow 4$ leptons*, JHEP **09** (2015) 128, arXiv: [1503.04812 \[hep-ph\]](https://arxiv.org/abs/1503.04812).
- [71] S. Catani and M. Grazzini, *An NNLO subtraction formalism in hadron collisions and its application to Higgs boson production at the LHC*, Phys. Rev. Lett. **98** (2007) 222002, arXiv: [hep-ph/0703012 \[hep-ph\]](https://arxiv.org/abs/hep-ph/0703012).
- [72] S. Catani, L. Cieri, D. de Florian, G. Ferrera and M. Grazzini, *Vector boson production at hadron colliders: hard-collinear coefficients at the NNLO*, Eur. Phys. J. C **72** (2012) 2195, arXiv: [1209.0158 \[hep-ph\]](https://arxiv.org/abs/1209.0158).

- [73] ATLAS Collaboration, *Measurement of distributions sensitive to the underlying event in inclusive Z boson production in pp collisions at $\sqrt{s} = 13$ TeV with the ATLAS detector*, *Eur. Phys. J. C* **79** (2019) 666, arXiv: [1905.09752 \[hep-ex\]](#).
- [74] ATLAS Collaboration, *Measurement of charged-particle distributions sensitive to the underlying event in $\sqrt{s} = 13$ TeV proton–proton collisions with the ATLAS detector at the LHC*, *JHEP* **03** (2017) 157, arXiv: [1701.05390 \[hep-ex\]](#).
- [75] ATLAS Collaboration, *Measurement of event-shape observables in $Z \rightarrow \ell^+ \ell^-$ events in pp collisions at $\sqrt{s} = 7$ TeV with the ATLAS detector at the LHC*, *Eur. Phys. J. C* **76** (2016) 375, arXiv: [1602.08980 \[hep-ex\]](#).
- [76] ATLAS Collaboration, *Measurement of distributions sensitive to the underlying event in inclusive Z-boson production in pp collisions at $\sqrt{s} = 7$ TeV with the ATLAS detector*, *Eur. Phys. J. C* **74** (2014) 3195, arXiv: [1409.3433 \[hep-ex\]](#).
- [77] ATLAS Collaboration, *Measurement of the exclusive $\gamma\gamma \rightarrow \mu^+ \mu^-$ process in proton–proton collisions at $\sqrt{s} = 13$ TeV with the ATLAS detector*, *Phys. Lett. B* **777** (2018) 303, arXiv: [1708.04053 \[hep-ex\]](#).
- [78] G. D’Agostini, *A multidimensional unfolding method based on Bayes’ theorem*, *Nucl. Instrum. Meth. A* **362** (1995) 487, ISSN: 0168-9002.
- [79] G. D’Agostini, *Improved iterative Bayesian unfolding*, (2010), arXiv: [1010.0632 \[physics.data-an\]](#).
- [80] ATLAS Collaboration, *Charged-particle distributions in $\sqrt{s} = 13$ TeV pp interactions measured with the ATLAS detector at the LHC*, *Phys. Lett. B* **758** (2016) 67, arXiv: [1602.01633 \[hep-ex\]](#).
- [81] K. Cranmer, G. Lewis, L. Moneta, A. Shibata and W. Verkerke, *HistFactory: A tool for creating statistical models for use with RooFit and RooStats*, CERN-OPEN-2012-016, 2012, URL: <https://cds.cern.ch/record/1456844>.
- [82] L. Harland-Lang, A. Martin, R. Nathvani and R. Thorne, *Ad Lucem: QED Parton Distribution Functions in the MMHT Framework*, *Eur. Phys. J. C* **79** (2019) 811, arXiv: [1907.02750 \[hep-ph\]](#).
- [83] M. Dyndal and L. Schoeffel, *The role of finite-size effects on the spectrum of equivalent photons in proton–proton collisions at the LHC*, *Phys. Lett. B* **741** (2015) 66, arXiv: [1410.2983 \[hep-ph\]](#).
- [84] L. Harland-Lang, V. Khoze and M. Ryskin, *Exclusive physics at the LHC with SuperChic 2*, *Eur. Phys. J. C* **76** (2016) 9, arXiv: [1508.02718 \[hep-ph\]](#).
- [85] L. Harland-Lang, V. Khoze and M. Ryskin, *The photon PDF in events with rapidity gaps*, *Eur. Phys. J. C* **76** (2016) 255, arXiv: [1601.03772 \[hep-ph\]](#).
- [86] ATLAS Collaboration, *ATLAS Computing Acknowledgements*, ATL-SOFT-PUB-2020-001, URL: <https://cds.cern.ch/record/2717821>.

The ATLAS Collaboration

G. Aad¹⁰², B. Abbott¹²⁸, D.C. Abbott¹⁰³, A. Abed Abud³⁶, K. Abeling⁵³, D.K. Abhayasinghe⁹⁴, S.H. Abidi¹⁶⁶, O.S. AbouZeid⁴⁰, N.L. Abraham¹⁵⁵, H. Abramowicz¹⁶⁰, H. Abreu¹⁵⁹, Y. Abulaiti⁶, B.S. Acharya^{67a,67b,o}, B. Achkar⁵³, L. Adam¹⁰⁰, C. Adam Bourdarios⁵, L. Adamczyk^{84a}, L. Adamek¹⁶⁶, J. Adelman¹²¹, A. Adiguzel^{12c}, S. Adorni⁵⁴, T. Adye¹⁴³, A.A. Affolder¹⁴⁵, Y. Afik¹⁵⁹, C. Agapopoulou⁶⁵, M.N. Agaras³⁸, A. Aggarwal¹¹⁹, C. Agheorghiesei^{27c}, J.A. Aguilar-Saavedra^{139f,139a,ac}, A. Ahmad³⁶, F. Ahmadov⁸⁰, W.S. Ahmed¹⁰⁴, X. Ai¹⁸, G. Aielli^{74a,74b}, S. Akatsuka⁸⁶, M. Akbiyik¹⁰⁰, T.P.A. Åkesson⁹⁷, E. Akilli⁵⁴, A.V. Akimov¹¹¹, K. Al Khoury⁶⁵, G.L. Alberghi^{23b,23a}, J. Albert¹⁷⁵, M.J. Alconada Verzini¹⁶⁰, S. Alderweireldt³⁶, M. Aleksa³⁶, I.N. Aleksandrov⁸⁰, C. Alexa^{27b}, T. Alexopoulos¹⁰, A. Alfonsi¹²⁰, F. Alfonsi^{23b,23a}, M. Alhroob¹²⁸, B. Ali¹⁴¹, S. Ali¹⁵⁷, M. Aliev¹⁶⁵, G. Alimonti^{69a}, C. Allaire³⁶, B.M.M. Allbrooke¹⁵⁵, B.W. Allen¹³¹, P.P. Allport²¹, A. Aloisio^{70a,70b}, F. Alonso⁸⁹, C. Alpigiani¹⁴⁷, E. Alunno Camelia^{74a,74b}, M. Alvarez Estevez⁹⁹, M.G. Alvaggi^{70a,70b}, Y. Amaral Coutinho^{81b}, A. Ambler¹⁰⁴, L. Ambroz¹³⁴, C. Amelung³⁶, D. Amidei¹⁰⁶, S.P. Amor Dos Santos^{139a}, S. Amoroso⁴⁶, C.S. Amrouche⁵⁴, F. An⁷⁹, C. Anastopoulos¹⁴⁸, N. Andari¹⁴⁴, T. Andeen¹¹, J.K. Anders²⁰, S.Y. Andrean^{45a,45b}, A. Andreazza^{69a,69b}, V. Andrei^{61a}, C.R. Anelli¹⁷⁵, S. Angelidakis⁹, A. Angerami³⁹, A.V. Anisenkov^{122b,122a}, A. Annovi^{72a}, C. Antel⁵⁴, M.T. Anthony¹⁴⁸, E. Antipov¹²⁹, M. Antonelli⁵¹, D.J.A. Antrim¹⁸, F. Anulli^{73a}, M. Aoki⁸², J.A. Aparisi Pozo¹⁷³, M.A. Aparo¹⁵⁵, L. Aperio Bella⁴⁶, N. Aranzabal³⁶, V. Araujo Ferraz^{81a}, R. Araujo Pereira^{81b}, C. Arcangeletti⁵¹, A.T.H. Arce⁴⁹, J-F. Arguin¹¹⁰, S. Argyropoulos⁵², J.-H. Arling⁴⁶, A.J. Armbruster³⁶, A. Armstrong¹⁷⁰, O. Arnaez¹⁶⁶, H. Arnold¹²⁰, Z.P. Arrubarrena Tame¹¹⁴, G. Artoni¹³⁴, H. Asada¹¹⁷, K. Asai¹²⁶, S. Asai¹⁶², T. Asawatavonvanich¹⁶⁴, N. Asbah⁵⁹, E.M. Asimakopoulou¹⁷¹, L. Asquith¹⁵⁵, J. Assahsah^{35d}, K. Assamagan²⁹, R. Astalos^{28a}, R.J. Atkin^{33a}, M. Atkinson¹⁷², N.B. Atlay¹⁹, H. Atmani⁶⁵, P.A. Atmasiddha¹⁰⁶, K. Augsten¹⁴¹, V.A. Astrup¹⁸¹, G. Avolio³⁶, M.K. Ayoub^{15a}, G. Azuelos^{110,aj}, D. Babal^{28a}, H. Bachacou¹⁴⁴, K. Bachas¹⁶¹, F. Backman^{45a,45b}, P. Bagnaia^{73a,73b}, M. Bahmani⁸⁵, H. Bahrasemani¹⁵¹, A.J. Bailey¹⁷³, V.R. Bailey¹⁷², J.T. Baines¹⁴³, C. Bakalis¹⁰, O.K. Baker¹⁸², P.J. Bakker¹²⁰, E. Bakos¹⁶, D. Bakshi Gupta⁸, S. Balaji¹⁵⁶, R. Balasubramanian¹²⁰, E.M. Baldin^{122b,122a}, P. Balek¹⁷⁹, F. Balli¹⁴⁴, W.K. Balunas¹³⁴, J. Balz¹⁰⁰, E. Banas⁸⁵, M. Bandieramonte¹³⁸, A. Bandyopadhyay¹⁹, Sw. Banerjee^{180j}, L. Barak¹⁶⁰, W.M. Barbe³⁸, E.L. Barberio¹⁰⁵, D. Barberis^{55b,55a}, M. Barbero¹⁰², G. Barbour⁹⁵, T. Barillari¹¹⁵, M-S. Barisits³⁶, J. Barkeloo¹³¹, T. Barklow¹⁵², R. Barnea¹⁵⁹, B.M. Barnett¹⁴³, R.M. Barnett¹⁸, Z. Barnovska-Blenessy^{60a}, A. Baroncelli^{60a}, G. Barone²⁹, A.J. Barr¹³⁴, L. Barranco Navarro^{45a,45b}, F. Barreiro⁹⁹, J. Barreiro Guimarães da Costa^{15a}, U. Barron¹⁶⁰, S. Barsov¹³⁷, F. Bartels^{61a}, R. Bartoldus¹⁵², G. Bartolini¹⁰², A.E. Barton⁹⁰, P. Bartos^{28a}, A. Basalaev⁴⁶, A. Basan¹⁰⁰, A. Bassalat^{65,ag}, M.J. Basso¹⁶⁶, R.L. Bates⁵⁷, S. Batlamous^{35e}, J.R. Batley³², B. Batool¹⁵⁰, M. Battaglia¹⁴⁵, M. Bauce^{73a,73b}, F. Bauer¹⁴⁴, P. Bauer²⁴, H.S. Bawa³¹, A. Bayirli^{12c}, J.B. Beacham⁴⁹, T. Beau¹³⁵, P.H. Beauchemin¹⁶⁹, F. Becherer⁵², P. Bechtle²⁴, H.C. Beck⁵³, H.P. Beck^{20,q}, K. Becker¹⁷⁷, C. Becot⁴⁶, A. Beddall^{12d}, A.J. Beddall^{12a}, V.A. Bednyakov⁸⁰, M. Bedognetti¹²⁰, C.P. Bee¹⁵⁴, T.A. Beermann¹⁸¹, M. Begalli^{81b}, M. Begel²⁹, A. Behera¹⁵⁴, J.K. Behr⁴⁶, F. Beisiegel²⁴, M. Belfkir⁵, A.S. Bell⁹⁵, G. Bella¹⁶⁰, L. Bellagamba^{23b}, A. Bellerive³⁴, P. Bellos⁹, K. Beloborodov^{122b,122a}, K. Belotskiy¹¹², N.L. Belyaev¹¹², D. Benchekroun^{35a}, N. Benekos¹⁰, Y. Benhammou¹⁶⁰, D.P. Benjamin⁶, M. Benoit²⁹, J.R. Bensinger²⁶, S. Bentvelsen¹²⁰, L. Beresford¹³⁴, M. Beretta⁵¹, D. Berge¹⁹, E. Bergeaas Kuutmann¹⁷¹, N. Berger⁵, B. Bergmann¹⁴¹, L.J. Bergsten²⁶, J. Beringer¹⁸, S. Berlendis⁷, G. Bernardi¹³⁵, C. Bernius¹⁵², F.U. Bernlochner²⁴, T. Berry⁹⁴, P. Berta¹⁰⁰, A. Berthold⁴⁸, I.A. Bertram⁹⁰, O. Bessidskaia Bylund¹⁸¹, N. Besson¹⁴⁴, S. Bethke¹¹⁵, A. Betti⁴², A.J. Bevan⁹³, J. Beyer¹¹⁵, S. Bhattacharya¹⁷⁶, P. Bhattarai²⁶, V.S. Bhopatkar⁶, R. Bi¹³⁸, R.M. Bianchi¹³⁸, O. Biebel¹¹⁴, D. Biedermann¹⁹, R. Bielski³⁶, K. Bierwagen¹⁰⁰, N.V. Biesuz^{72a,72b}, M. Biglietti^{75a}, T.R.V. Billoud¹⁴¹, M. Bindi⁵³, A. Bingul^{12d},

C. Bini^{73a,73b}, S. Biondi^{23b,23a}, C.J. Birch-sykes¹⁰¹, M. Birman¹⁷⁹, T. Bisanz³⁶, J.P. Biswal³,
 D. Biswas^{180,j}, A. Bitadze¹⁰¹, C. Bittrich⁴⁸, K. Bjørke¹³³, T. Blazek^{28a}, I. Bloch⁴⁶, C. Blocker²⁶, A. Blue⁵⁷,
 U. Blumenschein⁹³, G.J. Bobbink¹²⁰, V.S. Bobrovnikov^{122b,122a}, S.S. Bocchetta⁹⁷, D. Bogavac¹⁴,
 A.G. Bogdanchikov^{122b,122a}, C. Bohm^{45a}, V. Boisvert⁹⁴, P. Bokan^{171,171,53}, T. Bold^{84a}, A.E. Bolz^{61b},
 M. Bomben¹³⁵, M. Bona⁹³, J.S. Bonilla¹³¹, M. Boonekamp¹⁴⁴, C.D. Booth⁹⁴, A.G. Borbély⁵⁷,
 H.M. Borecka-Bielska⁹¹, L.S. Borgna⁹⁵, A. Borisov¹²³, G. Borissov⁹⁰, D. Bortoletto¹³⁴, D. Boscherini^{23b},
 M. Bosman¹⁴, J.D. Bossio Sola¹⁰⁴, K. Bouaouda^{35a}, J. Boudreau¹³⁸, E.V. Bouhova-Thacker⁹⁰,
 D. Boumediene³⁸, A. Boveia¹²⁷, J. Boyd³⁶, D. Boye^{33c}, I.R. Boyko⁸⁰, A.J. Bozson⁹⁴, J. Bracinik²¹,
 N. Brahimi^{60d}, G. Brandt¹⁸¹, O. Brandt³², F. Braren⁴⁶, B. Brau¹⁰³, J.E. Brau¹³¹, W.D. Breaden Madden⁵⁷,
 K. Brendlinger⁴⁶, R. Brener¹⁵⁹, L. Brenner³⁶, R. Brenner¹⁷¹, S. Bressler¹⁷⁹, B. Brickwedde¹⁰⁰,
 D.L. Briglin²¹, D. Britton⁵⁷, D. Britzger¹¹⁵, I. Brock²⁴, R. Brock¹⁰⁷, G. Brooijmans³⁹, W.K. Brooks^{146d},
 E. Brost²⁹, P.A. Bruckman de Renstrom⁸⁵, B. Brüers⁴⁶, D. Bruncko^{28b}, A. Bruni^{23b}, G. Brunni^{23b},
 M. Bruschi^{23b}, N. Bruscino^{73a,73b}, L. Bryngemark¹⁵², T. Buanes¹⁷, Q. Buat¹⁵⁴, P. Buchholz¹⁵⁰,
 A.G. Buckley⁵⁷, I.A. Budagov⁸⁰, M.K. Bugge¹³³, O. Bulekov¹¹², B.A. Bullard⁵⁹, T.J. Burch¹²¹,
 S. Burdin⁹¹, C.D. Burgard¹²⁰, A.M. Burger¹²⁹, B. Burghgrave⁸, J.T.P. Burr⁴⁶, C.D. Burton¹¹,
 J.C. Burzynski¹⁰³, V. Büscher¹⁰⁰, E. Buschmann⁵³, P.J. Bussey⁵⁷, J.M. Butler²⁵, C.M. Buttar⁵⁷,
 J.M. Butterworth⁹⁵, P. Butti³⁶, W. Buttinger¹⁴³, C.J. Buxo Vazquez¹⁰⁷, A. Buzatu¹⁵⁷,
 A.R. Buzykaev^{122b,122a}, G. Cabras^{23b,23a}, S. Cabrera Urbán¹⁷³, D. Caforio⁵⁶, H. Cai¹³⁸, V.M.M. Cairo¹⁵²,
 O. Cakir^{4a}, N. Calace³⁶, P. Calafiura¹⁸, G. Calderini¹³⁵, P. Calfayan⁶⁶, G. Callea⁵⁷, L.P. Caloba^{81b},
 A. Caltabiano^{74a,74b}, S. Calvente Lopez⁹⁹, D. Calvet³⁸, S. Calvet³⁸, T.P. Calvet¹⁰², M. Calvetti^{72a,72b},
 R. Camacho Toro¹³⁵, S. Camarda³⁶, D. Camarero Munoz⁹⁹, P. Camarri^{74a,74b}, M.T. Camerlingo^{75a,75b},
 D. Cameron¹³³, C. Camincher³⁶, S. Campana³⁶, M. Campanelli⁹⁵, A. Camplani⁴⁰, V. Canale^{70a,70b},
 A. Canesse¹⁰⁴, M. Cano Bret⁷⁸, J. Cantero¹²⁹, T. Cao¹⁶⁰, Y. Cao¹⁷², M. Capua^{41b,41a}, R. Cardarelli^{74a},
 F. Cardillo¹⁷³, G. Carducci^{41b,41a}, I. Carli¹⁴², T. Carli³⁶, G. Carlino^{70a}, B.T. Carlson¹³⁸,
 E.M. Carlson^{175,167a}, L. Carminati^{69a,69b}, R.M.D. Carney¹⁵², S. Caron¹¹⁹, E. Carquin^{146d}, S. Carrá⁴⁶,
 G. Carratta^{23b,23a}, J.W.S. Carter¹⁶⁶, T.M. Carter⁵⁰, M.P. Casado^{14,g}, A.F. Casha¹⁶⁶, E.G. Castiglia¹⁸²,
 F.L. Castillo¹⁷³, L. Castillo Garcia¹⁴, V. Castillo Gimenez¹⁷³, N.F. Castro^{139a,139e}, A. Catinaccio³⁶,
 J.R. Catmore¹³³, A. Cattai³⁶, V. Cavalieri²⁹, V. Cavasinni^{72a,72b}, E. Celebi^{12b}, F. Celli¹³⁴, K. Cerny¹³⁰,
 A.S. Cerqueira^{81a}, A. Cerri¹⁵⁵, L. Cerrito^{74a,74b}, F. Cerutti¹⁸, A. Cervelli^{23b,23a}, S.A. Cetin^{12b}, Z. Chadi^{35a},
 D. Chakraborty¹²¹, J. Chan¹⁸⁰, W.S. Chan¹²⁰, W.Y. Chan⁹¹, J.D. Chapman³², B. Chargeishvili^{158b},
 D.G. Charlton²¹, T.P. Charman⁹³, M. Chatterjee²⁰, C.C. Chau³⁴, S. Che¹²⁷, S. Chekanov⁶,
 S.V. Chekulaev^{167a}, G.A. Chelkov^{80,ae}, B. Chen⁷⁹, C. Chen^{60a}, C.H. Chen⁷⁹, H. Chen^{15c}, H. Chen²⁹,
 J. Chen^{60a}, J. Chen³⁹, J. Chen²⁶, S. Chen¹³⁶, S.J. Chen^{15c}, X. Chen^{15b}, Y. Chen^{60a}, Y-H. Chen⁴⁶,
 H.C. Cheng^{63a}, H.J. Cheng^{15a}, A. Cheplakov⁸⁰, E. Cheremushkina¹²³, R. Cherkaoui El Moursli^{35e},
 E. Cheu⁷, K. Cheung⁶⁴, T.J.A. Chevaléries¹⁴⁴, L. Chevalier¹⁴⁴, V. Chiarella⁵¹, G. Chiarella^{72a},
 G. Chiodini^{68a}, A.S. Chisholm²¹, A. Chitan^{27b}, I. Chiu¹⁶², Y.H. Chiu¹⁷⁵, M.V. Chizhov⁸⁰, K. Choi¹¹,
 A.R. Chomont^{73a,73b}, Y. Chou¹⁰³, Y.S. Chow¹²⁰, L.D. Christopher^{33e}, M.C. Chu^{63a}, X. Chu^{15a,15d},
 J. Chudoba¹⁴⁰, J.J. Chwastowski⁸⁵, L. Chytka¹³⁰, D. Cieri¹¹⁵, K.M. Ciesla⁸⁵, V. Cindro⁹², I.A. Cioară^{27b},
 A. Ciocio¹⁸, F. Cirotto^{70a,70b}, Z.H. Citron^{179,k}, M. Citterio^{69a}, D.A. Ciubotaru^{27b}, B.M. Ciungu¹⁶⁶,
 A. Clark⁵⁴, P.J. Clark⁵⁰, S.E. Clawson¹⁰¹, C. Clement^{45a,45b}, L. Clissa^{23b,23a}, Y. Coadou¹⁰²,
 M. Cobal^{67a,67c}, A. Coccaro^{55b}, J. Cochran⁷⁹, R. Coelho Lopes De Sa¹⁰³, H. Cohen¹⁶⁰, A.E.C. Coimbra³⁶,
 B. Cole³⁹, A.P. Colijn¹²⁰, J. Collot⁵⁸, P. Conde Muiño^{139a,139h}, S.H. Connell^{33c}, I.A. Connolly⁵⁷,
 S. Constantinescu^{27b}, F. Conventi^{70a,ak}, A.M. Cooper-Sarkar¹³⁴, F. Cormier¹⁷⁴, K.J.R. Cormier¹⁶⁶,
 L.D. Corpe⁹⁵, M. Corradi^{73a,73b}, E.E. Corrigan⁹⁷, F. Corriveau^{104,aa}, M.J. Costa¹⁷³, F. Costanza⁵,
 D. Costanzo¹⁴⁸, G. Cowan⁹⁴, J.W. Cowley³², J. Crane¹⁰¹, K. Cranmer¹²⁵, R.A. Creager¹³⁶,
 S. Crépé-Renaudin⁵⁸, F. Crescioli¹³⁵, M. Cristinziani²⁴, V. Croft¹⁶⁹, G. Crosetti^{41b,41a}, A. Cueto⁵,
 T. Cuhadar Donszelmann¹⁷⁰, H. Cui^{15a,15d}, A.R. Cukierman¹⁵², W.R. Cunningham⁵⁷, S. Czekierda⁸⁵,

P. Czodrowski³⁶, M.M. Czurylo^{61b}, M.J. Da Cunha Sargedas De Sousa^{60b}, J.V. Da Fonseca Pinto^{81b},
 C. Da Via¹⁰¹, W. Dabrowski^{84a}, F. Dachs³⁶, T. Dado⁴⁷, S. Dahbi^{33e}, T. Dai¹⁰⁶, C. Dallapiccola¹⁰³,
 M. Dam⁴⁰, G. D'amen²⁹, V. D'Amico^{75a,75b}, J. Damp¹⁰⁰, J.R. Dandoy¹³⁶, M.F. Daneri³⁰, M. Danninger¹⁵¹,
 V. Dao³⁶, G. Darbo^{55b}, O. Dartsi⁵, A. Dattagupta¹³¹, T. Daubney⁴⁶, S. D'Auria^{69a,69b}, C. David^{167b},
 T. Davidek¹⁴², D.R. Davis⁴⁹, I. Dawson¹⁴⁸, K. De⁸, R. De Asmundis^{70a}, M. De Beurs¹²⁰,
 S. De Castro^{23b,23a}, N. De Groot¹¹⁹, P. de Jong¹²⁰, H. De la Torre¹⁰⁷, A. De Maria^{15c}, D. De Pedis^{73a},
 A. De Salvo^{73a}, U. De Sanctis^{74a,74b}, M. De Santis^{74a,74b}, A. De Santo¹⁵⁵, J.B. De Vivie De Regie⁶⁵,
 D.V. Dedovich⁸⁰, A.M. Deiana⁴², J. Del Peso⁹⁹, Y. Delabat Diaz⁴⁶, D. Delgove⁶⁵, F. Deliot¹⁴⁴,
 C.M. Delitzsch⁷, M. Della Pietra^{70a,70b}, D. Della Volpe⁵⁴, A. Dell'Acqua³⁶, L. Dell'Asta^{74a,74b},
 M. Delmastro⁵, C. Delporte⁶⁵, P.A. Delsart⁵⁸, S. Demers¹⁸², M. Demichev⁸⁰, G. Demontigny¹¹⁰,
 S.P. Denisov¹²³, L. D'Eramo¹²¹, D. Derendarz⁸⁵, J.E. Derkaoui^{35d}, F. Derue¹³⁵, P. Dervan⁹¹, K. Desch²⁴,
 K. Dette¹⁶⁶, C. Deutsch²⁴, M.R. Devesa³⁰, P.O. Deviveiros³⁶, F.A. Di Bello^{73a,73b}, A. Di Ciaccio^{74a,74b},
 L. Di Ciaccio⁵, W.K. Di Clemente¹³⁶, C. Di Donato^{70a,70b}, A. Di Girolamo³⁶, G. Di Gregorio^{72a,72b},
 A. Di Luca^{76a,76b}, B. Di Micco^{75a,75b}, R. Di Nardo^{75a,75b}, K.F. Di Petrillo⁵⁹, R. Di Sipio¹⁶⁶, C. Diaconu¹⁰²,
 F.A. Dias¹²⁰, T. Dias Do Vale^{139a}, M.A. Diaz^{146a}, F.G. Diaz Capriles²⁴, J. Dickinson¹⁸, M. Didenko¹⁶⁵,
 E.B. Diehl¹⁰⁶, J. Dietrich¹⁹, S. Díez Cornell⁴⁶, C. Diez Pardos¹⁵⁰, A. Dimitrievska¹⁸, W. Ding^{15b},
 J. Dingfelder²⁴, S.J. Dittmeier^{61b}, F. Dittus³⁶, F. Djama¹⁰², T. Djobava^{158b}, J.I. Djuvslund¹⁷,
 M.A.B. Do Vale^{81c}, M. Dobre^{27b}, D. Dodsworth²⁶, C. Doglioni⁹⁷, J. Dolejsi¹⁴², Z. Dolezal¹⁴²,
 M. Donadelli^{81d}, B. Dong^{60c}, J. Donini³⁸, A. D'onofrio^{15c}, M. D'Onofrio⁹¹, J. Dopke¹⁴³, A. Doria^{70a},
 M.T. Dova⁸⁹, A.T. Doyle⁵⁷, E. Drechsler¹⁵¹, E. Dreyer¹⁵¹, T. Dreyer⁵³, A.S. Drobac¹⁶⁹, D. Du^{60b},
 T.A. du Pree¹²⁰, Y. Duan^{60d}, F. Dubinin¹¹¹, M. Dubovsky^{28a}, A. Dubreuil⁵⁴, E. Duchovni¹⁷⁹,
 G. Duckeck¹¹⁴, O.A. Ducu³⁶, D. Duda¹¹⁵, A. Dudarev³⁶, A.C. Dudder¹⁰⁰, E.M. Duffield¹⁸, M. D'uffizi¹⁰¹,
 L. Duflot⁶⁵, M. Dührssen³⁶, C. Dülsen¹⁸¹, M. Dumancic¹⁷⁹, A.E. Dumitriu^{27b}, M. Dunford^{61a}, S. Dungs⁴⁷,
 A. Duperrin¹⁰², H. Duran Yildiz^{4a}, M. Düren⁵⁶, A. Durglishvili^{158b}, D. Duschinger⁴⁸, B. Dutta⁴⁶,
 D. Duvnjak¹, G.I. Dyckes¹³⁶, M. Dyndal³⁶, S. Dysch¹⁰¹, B.S. Dziedzic⁸⁵, M.G. Eggleston⁴⁹, T. Eifert⁸,
 G. Eigen¹⁷, K. Einsweiler¹⁸, T. Ekelof¹⁷¹, H. El Jarrari^{35e}, V. Ellajosyula¹⁷¹, M. Ellert¹⁷¹, F. Ellinghaus¹⁸¹,
 A.A. Elliot⁹³, N. Ellis³⁶, J. Elmsheuser²⁹, M. Elsing³⁶, D. Emelianov¹⁴³, A. Emerman³⁹, Y. Enari¹⁶²,
 M.B. Epland⁴⁹, J. Erdmann⁴⁷, A. Ereditato²⁰, P.A. Erland⁸⁵, M. Errenst¹⁸¹, M. Escalier⁶⁵, C. Escobar¹⁷³,
 O. Estrada Pastor¹⁷³, E. Etzion¹⁶⁰, G.E. Evans^{139a}, H. Evans⁶⁶, M.O. Evans¹⁵⁵, A. Ezhilov¹³⁷, F. Fabbri⁵⁷,
 L. Fabbri^{23b,23a}, V. Fabiani¹¹⁹, G. Facini¹⁷⁷, R.M. Fakhrutdinov¹²³, S. Falciano^{73a}, P.J. Falke²⁴, S. Falke³⁶,
 J. Faltova¹⁴², Y. Fang^{15a}, Y. Fang^{15a}, G. Fanourakis⁴⁴, M. Fanti^{69a,69b}, M. Faraj^{67a,67c}, A. Farbin⁸,
 A. Farilla^{75a}, E.M. Farina^{71a,71b}, T. Farooque¹⁰⁷, S.M. Farrington⁵⁰, P. Farthouat³⁶, F. Fassi^{35e},
 P. Fassnacht³⁶, D. Fassouliotis⁹, M. Faucci Giannelli⁵⁰, W.J. Fawcett³², L. Fayard⁶⁵, O.L. Fedin^{137,p},
 W. Fedorko¹⁷⁴, A. Fehr²⁰, M. Feickert¹⁷², L. Feligioni¹⁰², A. Fell¹⁴⁸, C. Feng^{60b}, M. Feng⁴⁹,
 M.J. Fenton¹⁷⁰, A.B. Fenyuk¹²³, S.W. Ferguson⁴³, J. Ferrando⁴⁶, A. Ferrari¹⁷¹, P. Ferrari¹²⁰, R. Ferrari^{71a},
 D.E. Ferreira de Lima^{61b}, A. Ferrer¹⁷³, D. Ferrere⁵⁴, C. Ferretti¹⁰⁶, F. Fiedler¹⁰⁰, A. Filipčič⁹²,
 F. Filthaut¹¹⁹, K.D. Finelli²⁵, M.C.N. Fiolhais^{139a,139c,a}, L. Fiorini¹⁷³, F. Fischer¹¹⁴, J. Fischer¹⁰⁰,
 W.C. Fisher¹⁰⁷, T. Fitschen²¹, I. Fleck¹⁵⁰, P. Fleischmann¹⁰⁶, T. Flick¹⁸¹, B.M. Flierl¹¹⁴, L. Flores¹³⁶,
 L.R. Flores Castillo^{63a}, F.M. Follega^{76a,76b}, N. Fomin¹⁷, J.H. Foo¹⁶⁶, G.T. Forcolin^{76a,76b}, B.C. Forland⁶⁶,
 A. Formica¹⁴⁴, F.A. Förster¹⁴, A.C. Forti¹⁰¹, E. Fortin¹⁰², M.G. Foti¹³⁴, D. Fournier⁶⁵, H. Fox⁹⁰,
 P. Francavilla^{72a,72b}, S. Francescato^{73a,73b}, M. Franchini^{23b,23a}, S. Franchino^{61a}, D. Francis³⁶, L. Franco⁵,
 L. Franconi²⁰, M. Franklin⁵⁹, G. Frattari^{73a,73b}, A.N. Fray⁹³, P.M. Freeman²¹, B. Freund¹¹⁰,
 W.S. Freund^{81b}, E.M. Freundlich⁴⁷, D.C. Frizzell¹²⁸, D. Froidevaux³⁶, J.A. Frost¹³⁴, M. Fujimoto¹²⁶,
 C. Fukunaga¹⁶³, E. Fullana Torregrosa¹⁷³, T. Fusayasu¹¹⁶, J. Fuster¹⁷³, A. Gabrielli^{23b,23a}, A. Gabrielli³⁶,
 S. Gadatsch⁵⁴, P. Gadow¹¹⁵, G. Gagliardi^{55b,55a}, L.G. Gagnon¹¹⁰, G.E. Gallardo¹³⁴, E.J. Gallas¹³⁴,
 B.J. Gallop¹⁴³, R. Gamboa Goni⁹³, K.K. Gan¹²⁷, S. Ganguly¹⁷⁹, J. Gao^{60a}, Y. Gao⁵⁰, Y.S. Gao^{31,m},
 F.M. Garay Walls^{146a}, C. García¹⁷³, J.E. García Navarro¹⁷³, J.A. García Pascual^{15a}, C. Garcia-Argos⁵²,

M. Garcia-Sciveres¹⁸, R.W. Gardner³⁷, N. Garelli¹⁵², S. Gargiulo⁵², C.A. Garner¹⁶⁶, V. Garonne¹³³,
 S.J. Gasiorowski¹⁴⁷, P. Gaspar^{81b}, A. Gaudiello^{55b,55a}, G. Gaudio^{71a}, P. Gauzzi^{73a,73b}, I.L. Gavrilenko¹¹¹,
 A. Gavrilyuk¹²⁴, C. Gay¹⁷⁴, G. Gaycken⁴⁶, E.N. Gazis¹⁰, A.A. Geanta^{27b}, C.M. Gee¹⁴⁵, C.N.P. Gee¹⁴³,
 J. Geisen⁹⁷, M. Geisen¹⁰⁰, C. Gemme^{55b}, M.H. Genest⁵⁸, C. Geng¹⁰⁶, S. Gentile^{73a,73b}, S. George⁹⁴,
 T. Geralis⁴⁴, L.O. Gerlach⁵³, P. Gessinger-Befurt¹⁰⁰, G. Gessner⁴⁷, M. Ghasemi Bostanabad¹⁷⁵,
 M. Ghneimat¹⁵⁰, A. Ghosh⁶⁵, A. Ghosh⁷⁸, B. Giacobbe^{23b}, S. Giagu^{73a,73b}, N. Giangiocomi¹⁶⁶,
 P. Giannetti^{72a}, A. Giannini^{70a,70b}, G. Giannini¹⁴, S.M. Gibson⁹⁴, M. Gignac¹⁴⁵, D.T. Gil^{84b}, B.J. Gilbert³⁹,
 D. Gillberg³⁴, G. Gilles¹⁸¹, N.E.K. Gillwald⁴⁶, D.M. Gingrich^{3,aj}, M.P. Giordani^{67a,67c}, P.F. Giraud¹⁴⁴,
 G. Giugliarelli^{67a,67c}, D. Giugni^{69a}, F. Giuli^{74a,74b}, S. Gkaitatzis¹⁶¹, I. Gkialas^{9,h}, E.L. Gkougkousis¹⁴,
 P. Gkountoumis¹⁰, L.K. Gladilin¹¹³, C. Glasman⁹⁹, J. Glatzer¹⁴, P.C.F. Glaysher⁴⁶, A. Glazov⁴⁶,
 G.R. Gledhill¹³¹, I. Gnesi^{41b,c}, M. Goblirsch-Kolb²⁶, D. Godin¹¹⁰, S. Goldfarb¹⁰⁵, T. Golling⁵⁴,
 D. Golubkov¹²³, A. Gomes^{139a,139b}, R. Goncalves Gama⁵³, R. Gonçalo^{139a,139c}, G. Gonella¹³¹,
 L. Gonella²¹, A. Gongadze⁸⁰, F. Gonnella²¹, J.L. Gonski³⁹, S. González de la Hoz¹⁷³,
 S. Gonzalez Fernandez¹⁴, R. Gonzalez Lopez⁹¹, C. Gonzalez Renteria¹⁸, R. Gonzalez Suarez¹⁷¹,
 S. Gonzalez-Sevilla⁵⁴, G.R. Gonzalvo Rodriguez¹⁷³, L. Goossens³⁶, N.A. Gorasia²¹, P.A. Gorbounov¹²⁴,
 H.A. Gordon²⁹, B. Gorini³⁶, E. Gorini^{68a,68b}, A. Gorišek⁹², A.T. Goshaw⁴⁹, M.I. Gostkin⁸⁰,
 C.A. Gottardo¹¹⁹, M. Gouighri^{35b}, A.G. Goussiou¹⁴⁷, N. Govender^{33c}, C. Goy⁵, I. Grabowska-Bold^{84a},
 E.C. Graham⁹¹, J. Gramling¹⁷⁰, E. Gramstad¹³³, S. Grancagnolo¹⁹, M. Grandi¹⁵⁵, V. Gratchev¹³⁷,
 P.M. Gravila^{27f}, F.G. Gravili^{68a,68b}, C. Gray⁵⁷, H.M. Gray¹⁸, C. Grefe²⁴, K. Gregersen⁹⁷, I.M. Gregor⁴⁶,
 P. Grenier¹⁵², K. Grevtsov⁴⁶, C. Grieco¹⁴, N.A. Grieser¹²⁸, A.A. Grillo¹⁴⁵, K. Grimm^{31,l}, S. Grinstein^{14,w},
 J.-F. Grivaz⁶⁵, S. Groh¹⁰⁰, E. Gross¹⁷⁹, J. Grosse-Knetter⁵³, Z.J. Grout⁹⁵, C. Grud¹⁰⁶, A. Grummer¹¹⁸,
 J.C. Grundy¹³⁴, L. Guan¹⁰⁶, W. Guan¹⁸⁰, C. Gubbels¹⁷⁴, J. Guenther⁷⁷, A. Guerguichon⁶⁵,
 J.G.R. Guerrero Rojas¹⁷³, F. Guescini¹¹⁵, D. Guest⁷⁷, R. Gugel¹⁰⁰, A. Guida⁴⁶, T. Guillemin⁵,
 S. Guindon³⁶, J. Guo^{60c}, W. Guo¹⁰⁶, Y. Guo^{60a}, Z. Guo¹⁰², R. Gupta⁴⁶, S. Gurbuz^{12c}, G. Gustavino¹²⁸,
 M. Guth⁵², P. Gutierrez¹²⁸, C. Gutschow⁹⁵, C. Guyot¹⁴⁴, C. Gwenlan¹³⁴, C.B. Gwilliam⁹¹,
 E.S. Haaland¹³³, A. Haas¹²⁵, C. Haber¹⁸, H.K. Hadavand⁸, A. Hadef¹⁰⁰, M. Haleem¹⁷⁶, J. Haley¹²⁹,
 J.J. Hall¹⁴⁸, G. Halladjian¹⁰⁷, G.D. Hallewell¹⁰², K. Hamano¹⁷⁵, H. Hamdaoui^{35e}, M. Hamer²⁴,
 G.N. Hamity⁵⁰, K. Han^{60a}, L. Han^{15c}, L. Han^{60a}, S. Han¹⁸, Y.F. Han¹⁶⁶, K. Hanagaki^{82,u}, M. Hance¹⁴⁵,
 D.M. Handl¹¹⁴, M.D. Hank³⁷, R. Hankache¹³⁵, E. Hansen⁹⁷, J.B. Hansen⁴⁰, J.D. Hansen⁴⁰,
 M.C. Hansen²⁴, P.H. Hansen⁴⁰, E.C. Hanson¹⁰¹, K. Hara¹⁶⁸, T. Harenberg¹⁸¹, S. Harkusha¹⁰⁸,
 P.F. Harrison¹⁷⁷, N.M. Hartman¹⁵², N.M. Hartmann¹¹⁴, Y. Hasegawa¹⁴⁹, A. Hasib⁵⁰, S. Hassani¹⁴⁴,
 S. Haug²⁰, R. Hauser¹⁰⁷, M. Havranek¹⁴¹, C.M. Hawkes²¹, R.J. Hawkings³⁶, S. Hayashida¹¹⁷,
 D. Hayden¹⁰⁷, C. Hayes¹⁰⁶, R.L. Hayes¹⁷⁴, C.P. Hays¹³⁴, J.M. Hays⁹³, H.S. Hayward⁹¹, S.J. Haywood¹⁴³,
 F. He^{60a}, Y. He¹⁶⁴, M.P. Heath⁵⁰, V. Hedberg⁹⁷, A.L. Heggelund¹³³, N.D. Hehir⁹³, C. Heidegger⁵²,
 K.K. Heidegger⁵², W.D. Heidorn⁷⁹, J. Heilman³⁴, S. Heim⁴⁶, T. Heim¹⁸, B. Heinemann^{46,ah},
 J.G. Heinlein¹³⁶, J.J. Heinrich¹³¹, L. Heinrich³⁶, J. Hejbal¹⁴⁰, L. Helary⁴⁶, A. Held¹²⁵, S. Hellesund¹³³,
 C.M. Helling¹⁴⁵, S. Hellman^{45a,45b}, C. Helsens³⁶, R.C.W. Henderson⁹⁰, L. Henkelmann³²,
 A.M. Henriques Correia³⁶, H. Herde²⁶, Y. Hernández Jiménez^{33e}, H. Herr¹⁰⁰, M.G. Herrmann¹¹⁴,
 T. Herrmann⁴⁸, G. Herten⁵², R. Hertenberger¹¹⁴, L. Hervas³⁶, G.G. Hesketh⁹⁵, N.P. Hessey^{167a}, H. Hibi⁸³,
 S. Higashino⁸², E. Higón-Rodriguez¹⁷³, K. Hildebrand³⁷, J.C. Hill³², K.K. Hill²⁹, K.H. Hiller⁴⁶,
 S.J. Hillier²¹, M. Hils⁴⁸, I. Hincliffe¹⁸, F. Hinterkeuser²⁴, M. Hirose¹³², S. Hirose¹⁶⁸, D. Hirschbuehl¹⁸¹,
 B. Hiti⁹², O. Hladik¹⁴⁰, J. Hobbs¹⁵⁴, R. Hobincu^{27e}, N. Hod¹⁷⁹, M.C. Hodgkinson¹⁴⁸, A. Hoecker³⁶,
 D. Hohn⁵², D. Hohov⁶⁵, T. Holm²⁴, T.R. Holmes³⁷, M. Holzbock¹¹⁵, L.B.A.H. Hommels³², T.M. Hong¹³⁸,
 J.C. Honig⁵², A. Hönle¹¹⁵, B.H. Hooberman¹⁷², W.H. Hopkins⁶, Y. Horii¹¹⁷, P. Horn⁴⁸, L.A. Horyn³⁷,
 S. Hou¹⁵⁷, A. Hoummada^{35a}, J. Howarth⁵⁷, J. Hoya⁸⁹, M. Hrabovsky¹³⁰, J. Hrvnac⁶⁵, A. Hrynevich¹⁰⁹,
 T. Hryn'ova⁵, P.J. Hsu⁶⁴, S.-C. Hsu¹⁴⁷, Q. Hu³⁹, S. Hu^{60c}, Y.F. Hu^{15a,15d,al}, D.P. Huang⁹⁵, X. Huang^{15c},
 Y. Huang^{60a}, Y. Huang^{15a}, Z. Hubacek¹⁴¹, F. Hubaut¹⁰², M. Huebner²⁴, F. Huegging²⁴, T.B. Huffman¹³⁴,

M. Huhtinen³⁶, R. Hulskens⁵⁸, R.F.H. Hunter³⁴, N. Huseynov^{80,ab}, J. Huston¹⁰⁷, J. Huth⁵⁹, R. Hyneman¹⁵², S. Hyrych^{28a}, G. Iacobucci⁵⁴, G. Iakovidis²⁹, I. Ibragimov¹⁵⁰, L. Iconomou-Fayard⁶⁵, P. Iengo³⁶, R. Ignazzi⁴⁰, R. Iguchi¹⁶², T. Iizawa⁵⁴, Y. Ikegami⁸², M. Ikeno⁸², N. Ilie^{119,166,aa}, F. Iltzsche⁴⁸, H. Imam^{35a}, G. Introzzi^{71a,71b}, M. Iodice^{75a}, K. Iordanidou^{167a}, V. Ippolito^{73a,73b}, M.F. Isacson¹⁷¹, M. Ishino¹⁶², W. Islam¹²⁹, C. Issever^{19,46}, S. Istiin¹⁵⁹, J.M. Iturbe Ponce^{63a}, R. Iuppa^{76a,76b}, A. Ivina¹⁷⁹, J.M. Izen⁴³, V. Izzo^{70a}, P. Jacka¹⁴⁰, P. Jackson¹, R.M. Jacobs⁴⁶, B.P. Jaeger¹⁵¹, V. Jain², G. Jäkel¹⁸¹, K.B. Jakobi¹⁰⁰, K. Jakobs⁵², T. Jakoubek¹⁷⁹, J. Jamieson⁵⁷, K.W. Janas^{84a}, R. Jansky⁵⁴, M. Janus⁵³, P.A. Janus^{84a}, G. Jarlskog⁹⁷, A.E. Jaspan⁹¹, N. Javadov^{80,ab}, T. Javůrek³⁶, M. Javurkova¹⁰³, F. Jeanneau¹⁴⁴, L. Jeanty¹³¹, J. Jejelava^{158a}, P. Jenni^{52,d}, N. Jeong⁴⁶, S. Jézéquel⁵, J. Jia¹⁵⁴, Z. Jia^{15c}, H. Jiang⁷⁹, Y. Jiang^{60a}, Z. Jiang¹⁵², S. Jiggins⁵², F.A. Jimenez Morales³⁸, J. Jimenez Pena¹¹⁵, S. Jin^{15c}, A. Jinaru^{27b}, O. Jinnouchi¹⁶⁴, H. Jivan^{33e}, P. Johansson¹⁴⁸, K.A. Johns⁷, C.A. Johnson⁶⁶, E. Jones¹⁷⁷, R.W.L. Jones⁹⁰, S.D. Jones¹⁵⁵, T.J. Jones⁹¹, J. Jovicevic³⁶, X. Ju¹⁸, J.J. Junggeburth¹¹⁵, A. Juste Rozas^{14,w}, A. Kaczmarska⁸⁵, M. Kado^{73a,73b}, H. Kagan¹²⁷, M. Kagan¹⁵², A. Kahn³⁹, C. Kahra¹⁰⁰, T. Kaji¹⁷⁸, E. Kajomovitz¹⁵⁹, C.W. Kalderon²⁹, A. Kaluza¹⁰⁰, A. Kamenshchikov¹²³, M. Kaneda¹⁶², N.J. Kang¹⁴⁵, S. Kang⁷⁹, Y. Kano¹¹⁷, J. Kanzaki⁸², L.S. Kaplan¹⁸⁰, D. Kar^{33e}, K. Karava¹³⁴, M.J. Kareem^{167b}, I. Karkanias¹⁶¹, S.N. Karpov⁸⁰, Z.M. Karpova⁸⁰, V. Kartvelishvili⁹⁰, A.N. Karyukhin¹²³, E. Kasimi¹⁶¹, A. Kastanas^{45a,45b}, C. Kato^{60d}, J. Katzy⁴⁶, K. Kawade¹⁴⁹, K. Kawagoe⁸⁸, T. Kawaguchi¹¹⁷, T. Kawamoto¹⁴⁴, G. Kawamura⁵³, E.F. Kay¹⁷⁵, F.I. Kaya¹⁶⁹, S. Kazakos¹⁴, V.F. Kazanin^{122b,122a}, J.M. Keaveney^{33a}, R. Keeler¹⁷⁵, J.S. Keller³⁴, E. Kellermann⁹⁷, D. Kelsey¹⁵⁵, J.J. Kempster²¹, J. Kendrick²¹, K.E. Kennedy³⁹, O. Kepka¹⁴⁰, S. Kersten¹⁸¹, B.P. Kerševan⁹², S. Ketabchi Haghighe¹⁶⁶, F. Khalil-Zada¹³, M. Khandoga¹⁴⁴, A. Khanov¹²⁹, A.G. Kharlamov^{122b,122a}, T. Kharlamova^{122b,122a}, E.E. Khoda¹⁷⁴, T.J. Khoo⁷⁷, G. Khoriauli¹⁷⁶, E. Khramov⁸⁰, J. Khubua^{158b}, S. Kido⁸³, M. Kiehn³⁶, E. Kim¹⁶⁴, Y.K. Kim³⁷, N. Kimura⁹⁵, A. Kirchhoff⁵³, D. Kirchmeier⁴⁸, J. Kirk¹⁴³, A.E. Kiryunin¹¹⁵, T. Kishimoto¹⁶², D.P. Kisliuk¹⁶⁶, V. Kitali⁴⁶, C. Kitsaki¹⁰, O. Kivernyk²⁴, T. Klapdor-Kleingrothaus⁵², M. Klassen^{61a}, C. Klein³⁴, M.H. Klein¹⁰⁶, M. Klein⁹¹, U. Klein⁹¹, K. Kleinknecht¹⁰⁰, P. Klimek³⁶, A. Klimentov²⁹, F. Klimpel³⁶, T. Klingl²⁴, T. Klioutchnikova³⁶, F.F. Klitzner¹¹⁴, P. Kluit¹²⁰, S. Kluth¹¹⁵, E. Kneringer⁷⁷, E.B.F.G. Knoops¹⁰², A. Knue⁵², D. Kobayashi⁸⁸, M. Kobel⁴⁸, M. Kocian¹⁵², T. Kodama¹⁶², P. Kodys¹⁴², D.M. Koeck¹⁵⁵, P.T. Koenig²⁴, T. Koffas³⁴, N.M. Köhler³⁶, M. Kolb¹⁴⁴, I. Koletsou⁵, T. Komarek¹³⁰, T. Kondo⁸², K. Köneke⁵², A.X.Y. Kong¹, A.C. König¹¹⁹, T. Kono¹²⁶, V. Konstantinides⁹⁵, N. Konstantinidis⁹⁵, B. Konya⁹⁷, R. Kopeliansky⁶⁶, S. Koperny^{84a}, K. Korcyl⁸⁵, K. Kordas¹⁶¹, G. Koren¹⁶⁰, A. Korn⁹⁵, I. Korolkov¹⁴, E.V. Korolkova¹⁴⁸, N. Korotkova¹¹³, O. Kortner¹¹⁵, S. Kortner¹¹⁵, V.V. Kostyukhin^{148,165}, A. Kotsokechagia⁶⁵, A. Kotwal⁴⁹, A. Koulouris¹⁰, A. Kourkoumeli-Charalampidi^{71a,71b}, C. Kourkoumelis⁹, E. Kourlitis⁶, V. Kouskoura²⁹, R. Kowalewski¹⁷⁵, W. Kozanecki¹⁰¹, A.S. Kozhin¹²³, V.A. Kramarenko¹¹³, G. Kramberger⁹², D. Krasnopevtsev^{60a}, M.W. Krasny¹³⁵, A. Krasznahorkay³⁶, D. Krauss¹¹⁵, J.A. Kremer¹⁰⁰, J. Kretzschmar⁹¹, K. Kreul¹⁹, P. Krieger¹⁶⁶, F. Krieter¹¹⁴, S. Krishnamurthy¹⁰³, A. Krishnan^{61b}, M. Krivos¹⁴², K. Krizka¹⁸, K. Kroeninger⁴⁷, H. Kroha¹¹⁵, J. Kroll¹⁴⁰, J. Kroll¹³⁶, K.S. Krowpman¹⁰⁷, U. Kruchonak⁸⁰, H. Krüger²⁴, N. Krumnack⁷⁹, M.C. Kruse⁴⁹, J.A. Krzysiak⁸⁵, A. Kubota¹⁶⁴, O. Kuchinskaia¹⁶⁵, S. Kuday^{4b}, D. Kuechler⁴⁶, J.T. Kuechler⁴⁶, S. Kuehn³⁶, T. Kuhl⁴⁶, V. Kukhtin⁸⁰, Y. Kulchitsky^{108,ad}, S. Kuleshov^{146b}, Y.P. Kulinich¹⁷², M. Kuna⁵⁸, A. Kupco¹⁴⁰, T. Kupfer⁴⁷, O. Kuprash⁵², H. Kurashige⁸³, L.I. Kurchaninov^{167a}, Y.A. Kurochkin¹⁰⁸, A. Kurova¹¹², M.G. Kurth^{15a,15d}, E.S. Kuwertz³⁶, M. Kuze¹⁶⁴, A.K. Kvam¹⁴⁷, J. Kvita¹³⁰, T. Kwan¹⁰⁴, C. Lacasta¹⁷³, F. Lacava^{73a,73b}, D.P.J. Lack¹⁰¹, H. Lacker¹⁹, D. Lacour¹³⁵, E. Ladygin⁸⁰, R. Lafaye⁵, B. Laforge¹³⁵, T. Lagouri^{146c}, S. Lai⁵³, I.K. Lakomiec^{84a}, J.E. Lambert¹²⁸, S. Lammers⁶⁶, W. Lampl⁷, C. Lampoudis¹⁶¹, E. Lançon²⁹, U. Landgraf⁵², M.P.J. Landon⁹³, V.S. Lang⁵², J.C. Lange⁵³, R.J. Langenberg¹⁰³, A.J. Lankford¹⁷⁰, F. Lanni²⁹, K. Lantzsch²⁴, A. Lanza^{71a}, A. Lapertosa^{55b,55a}, J.F. Laporte¹⁴⁴, T. Lari^{69a}, F. Lasagni Manghi^{23b,23a}, M. Lassnig³⁶, V. Latonova¹⁴⁰, T.S. Lau^{63a}, A. Laudrain¹⁰⁰, A. Laurier³⁴, M. Lavorgna^{70a,70b},

S.D. Lawlor⁹⁴, M. Lazzaroni^{69a,69b}, B. Le¹⁰¹, E. Le Guirriec¹⁰², A. Lebedev⁷⁹, M. LeBlanc⁷,
 T. LeCompte⁶, F. Ledroit-Guillon⁵⁸, A.C.A. Lee⁹⁵, C.A. Lee²⁹, G.R. Lee¹⁷, L. Lee⁵⁹, S.C. Lee¹⁵⁷,
 S. Lee⁷⁹, B. Lefebvre^{167a}, H.P. Lefebvre⁹⁴, M. Lefebvre¹⁷⁵, C. Leggett¹⁸, K. Lehmann¹⁵¹, N. Lehmann²⁰,
 G. Lehmann Miotto³⁶, W.A. Leight⁴⁶, A. Leisos^{161,v}, M.A.L. Leite^{81d}, C.E. Leitgeb¹¹⁴, R. Leitner¹⁴²,
 K.J.C. Leney⁴², T. Lenz²⁴, S. Leone^{72a}, C. Leonidopoulos⁵⁰, A. Leopold¹³⁵, C. Leroy¹¹⁰, R. Les¹⁰⁷,
 C.G. Lester³², M. Levchenko¹³⁷, J. Levêque⁵, D. Levin¹⁰⁶, L.J. Levinson¹⁷⁹, D.J. Lewis²¹, B. Li^{15b},
 B. Li¹⁰⁶, C.-Q. Li^{60c,60d}, F. Li^{60c}, H. Li^{60a}, H. Li^{60b}, J. Li^{60c}, K. Li¹⁴⁷, L. Li^{60c}, M. Li^{15a,15d}, Q.Y. Li^{60a},
 S. Li^{60d,60c,b}, X. Li⁴⁶, Y. Li⁴⁶, Z. Li^{60b}, Z. Li¹³⁴, Z. Li¹⁰⁴, Z. Li⁹¹, Z. Liang^{15a}, M. Liberatore⁴⁶,
 B. Liberti^{74a}, K. Lie^{63c}, S. Lim²⁹, C.Y. Lin³², K. Lin¹⁰⁷, R.A. Linck⁶⁶, R.E. Lindley⁷, J.H. Lindon²¹,
 A. Linss⁴⁶, A.L. Lionti⁵⁴, E. Lipeles¹³⁶, A. Lipniacka¹⁷, T.M. Liss^{172,ai}, A. Lister¹⁷⁴, J.D. Little⁸, B. Liu⁷⁹,
 B.L. Liu¹⁵¹, H.B. Liu²⁹, J.B. Liu^{60a}, J.K.K. Liu³⁷, K. Liu^{60d}, M. Liu^{60a}, M.Y. Liu^{60a}, P. Liu^{15a}, X. Liu^{60a},
 Y. Liu⁴⁶, Y. Liu^{15a,15d}, Y.L. Liu¹⁰⁶, Y.W. Liu^{60a}, M. Livan^{71a,71b}, A. Lleres⁵⁸, J. Llorente Merino¹⁵¹,
 S.L. Lloyd⁹³, C.Y. Lo^{63b}, E.M. Lobodzinska⁴⁶, P. Loch⁷, S. Loffredo^{74a,74b}, T. Lohse¹⁹, K. Lohwasser¹⁴⁸,
 M. Lokajicek¹⁴⁰, J.D. Long¹⁷², R.E. Long⁹⁰, I. Longarini^{73a,73b}, L. Longo³⁶, I. Lopez Paz¹⁰¹,
 A. Lopez Solis¹⁴⁸, J. Lorenz¹¹⁴, N. Lorenzo Martinez⁵, A.M. Lory¹¹⁴, A. Lösle⁵², X. Lou^{45a,45b},
 X. Lou^{15a}, A. Lounis⁶⁵, J. Love⁶, P.A. Love⁹⁰, J.J. Lozano Bahilo¹⁷³, M. Lu^{60a}, Y.J. Lu⁶⁴, H.J. Lubatti¹⁴⁷,
 C. Luci^{73a,73b}, F.L. Lucio Alves^{15c}, A. Lucotte⁵⁸, F. Luehring⁶⁶, I. Luise¹⁵⁴, L. Luminari^{73a},
 B. Lund-Jensen¹⁵³, N.A. Luongo¹³¹, M.S. Lutz¹⁶⁰, D. Lynn²⁹, H. Lyons⁹¹, R. Lysak¹⁴⁰, E. Lytken⁹⁷,
 F. Lyu^{15a}, V. Lyubushkin⁸⁰, T. Lyubushkina⁸⁰, H. Ma²⁹, L.L. Ma^{60b}, Y. Ma⁹⁵, D.M. Mac Donell¹⁷⁵,
 G. Maccarrone⁵¹, C.M. Macdonald¹⁴⁸, J.C. MacDonald¹⁴⁸, J. Machado Miguens¹³⁶, R. Madar³⁸,
 W.F. Mader⁴⁸, M. Madugoda Ralalage Don¹²⁹, N. Madysa⁴⁸, J. Maeda⁸³, T. Maeno²⁹, M. Maerker⁴⁸,
 V. Magerl⁵², N. Magini⁷⁹, J. Magro^{67a,67c,r}, D.J. Mahon³⁹, C. Maidantchik^{81b}, A. Maio^{139a,139b,139d},
 K. Maj^{84a}, O. Majersky^{28a}, S. Majewski¹³¹, Y. Makida⁸², N. Makovec⁶⁵, B. Malaescu¹³⁵, Pa. Malecki⁸⁵,
 V.P. Maleev¹³⁷, F. Malek⁵⁸, D. Malito^{41b,41a}, U. Mallik⁷⁸, C. Malone³², S. Maltezos¹⁰, S. Malyukov⁸⁰,
 J. Mamuzic¹⁷³, G. Mancini⁵¹, J.P. Mandalia⁹³, I. Mandić⁹², L. Manhaes de Andrade Filho^{81a},
 I.M. Maniatis¹⁶¹, J. Manjarres Ramos⁴⁸, K.H. Mankinen⁹⁷, A. Mann¹¹⁴, A. Manousos⁷⁷, B. Mansoulie¹⁴⁴,
 I. Manthos¹⁶¹, S. Manzoni¹²⁰, A. Marantis¹⁶¹, G. Marceca³⁰, L. Marchese¹³⁴, G. Marchiori¹³⁵,
 M. Marcisovsky¹⁴⁰, L. Marcoccia^{74a,74b}, C. Marcon⁹⁷, M. Marjanovic¹²⁸, Z. Marshall¹⁸,
 M.U.F. Martensson¹⁷¹, S. Marti-Garcia¹⁷³, C.B. Martin¹²⁷, T.A. Martin¹⁷⁷, V.J. Martin⁵⁰,
 B. Martin dit Latour¹⁷, L. Martinelli^{75a,75b}, M. Martinez^{14,w}, P. Martinez Agullo¹⁷³,
 VI. Martinez Outschoorn¹⁰³, S. Martin-Haugh¹⁴³, V.S. Martoiu^{27b}, A.C. Martyniuk⁹⁵, A. Marzin³⁶,
 S.R. Maschek¹¹⁵, L. Masetti¹⁰⁰, T. Mashimo¹⁶², R. Mashinistov¹¹¹, J. Masik¹⁰¹, A.L. Maslennikov^{122b,122a},
 L. Massa^{23b,23a}, P. Massarotti^{70a,70b}, P. Mastrandrea^{72a,72b}, A. Mastroberardino^{41b,41a}, T. Masubuchi¹⁶²,
 D. Matakias²⁹, A. Matic¹¹⁴, N. Matsuzawa¹⁶², P. Mättig²⁴, J. Maurer^{27b}, B. Maček⁹²,
 D.A. Maximov^{122b,122a}, R. Mazini¹⁵⁷, I. Maznas¹⁶¹, S.M. Mazza¹⁴⁵, J.P. Mc Gowan¹⁰⁴, S.P. Mc Kee¹⁰⁶,
 T.G. McCarthy¹¹⁵, W.P. McCormack¹⁸, E.F. McDonald¹⁰⁵, A.E. McDougall¹²⁰, J.A. McFayden¹⁸,
 G. Mchedlidze^{158b}, M.A. McKay⁴², K.D. McLean¹⁷⁵, S.J. McMahon¹⁴³, P.C. McNamara¹⁰⁵,
 C.J. McNicol¹⁷⁷, R.A. McPherson^{175,aa}, J.E. Mdhluli^{33e}, Z.A. Meadows¹⁰³, S. Meehan³⁶, T. Megy³⁸,
 S. Mehlhase¹¹⁴, A. Mehta⁹¹, B. Meirose⁴³, D. Melini¹⁵⁹, B.R. Mellado Garcia^{33e}, J.D. Mellenthin⁵³,
 M. Melo^{28a}, F. Meloni⁴⁶, A. Melzer²⁴, E.D. Mendes Gouveia^{139a,139e}, A.M. Mendes Jacques Da Costa²¹,
 H.Y. Meng¹⁶⁶, L. Meng³⁶, X.T. Meng¹⁰⁶, S. Menke¹¹⁵, E. Meoni^{41b,41a}, S. Mergelmeyer¹⁹,
 S.A.M. Merkt¹³⁸, C. Merlassino¹³⁴, P. Mermod⁵⁴, L. Merola^{70a,70b}, C. Meroni^{69a}, G. Merz¹⁰⁶,
 O. Meshkov^{113,111}, J.K.R. Meshreki¹⁵⁰, J. Metcalfe⁶, A.S. Mete⁶, C. Meyer⁶⁶, J.-P. Meyer¹⁴⁴,
 M. Michetti¹⁹, R.P. Middleton¹⁴³, L. Mijović⁵⁰, G. Mikenberg¹⁷⁹, M. Mikestikova¹⁴⁰, M. Mikuž⁹²,
 H. Mildner¹⁴⁸, A. Milic¹⁶⁶, C.D. Milke⁴², D.W. Miller³⁷, L.S. Miller³⁴, A. Milov¹⁷⁹, D.A. Milstead^{45a,45b},
 A.A. Minaenko¹²³, I.A. Minashvili^{158b}, L. Mince⁵⁷, A.I. Mincer¹²⁵, B. Mindur^{84a}, M. Mineev⁸⁰,
 Y. Minegishi¹⁶², Y. Mino⁸⁶, L.M. Mir¹⁴, M. Mironova¹³⁴, T. Mitani¹⁷⁸, J. Mitrevski¹¹⁴, V.A. Mitsou¹⁷³,

M. Mittal^{60c}, O. Miu¹⁶⁶, A. Miucci²⁰, P.S. Miyagawa⁹³, A. Mizukami⁸², J.U. Mjörnmark⁹⁷,
 T. Mkrtchyan^{61a}, M. Mlynarikova¹²¹, T. Moa^{45a,45b}, S. Mobius⁵³, K. Mochizuki¹¹⁰, P. Moder⁴⁶,
 P. Mogg¹¹⁴, S. Mohapatra³⁹, R. Moles-Valls²⁴, K. Mönig⁴⁶, E. Monnier¹⁰², A. Montalbano¹⁵¹,
 J. Montejo Berlingen³⁶, M. Montella⁹⁵, F. Monticelli⁸⁹, S. Monzani^{69a}, N. Morange⁶⁵,
 A.L. Moreira De Carvalho^{139a}, D. Moreno^{22a}, M. Moreno Llácer¹⁷³, C. Moreno Martinez¹⁴,
 P. Morettini^{55b}, M. Morgenstern¹⁵⁹, S. Morgenstern⁴⁸, D. Mori¹⁵¹, M. Morii⁵⁹, M. Morinaga¹⁷⁸,
 V. Morisbak¹³³, A.K. Morley³⁶, G. Mornacchi³⁶, A.P. Morris⁹⁵, L. Morvaj³⁶, P. Moschovakos³⁶,
 B. Moser¹²⁰, M. Mosidze^{158b}, T. Moskalets¹⁴⁴, P. Moskvitina¹¹⁹, J. Moss^{31,n}, E.J.W. Moyse¹⁰³,
 S. Muanza¹⁰², J. Mueller¹³⁸, R.S.P. Mueller¹¹⁴, D. Muenstermann⁹⁰, G.A. Mullier⁹⁷, D.P. Mungo^{69a,69b},
 J.L. Munoz Martinez¹⁴, F.J. Munoz Sanchez¹⁰¹, P. Murin^{28b}, W.J. Murray^{177,143}, A. Murrone^{69a,69b},
 J.M. Muse¹²⁸, M. Muškinja¹⁸, C. Mwewa^{33a}, A.G. Myagkov^{123,ae}, A.A. Myers¹³⁸, G. Myers⁶⁶, J. Myers¹³¹,
 M. Myska¹⁴¹, B.P. Nachman¹⁸, O. Nackenhorst⁴⁷, A.Nag Nag⁴⁸, K. Nagai¹³⁴, K. Nagano⁸², Y. Nagasaka⁶²,
 J.L. Nagle²⁹, E. Nagy¹⁰², A.M. Nairz³⁶, Y. Nakahama¹¹⁷, K. Nakamura⁸², T. Nakamura¹⁶², H. Nanjo¹³²,
 F. Napolitano^{61a}, R.F. Naranjo Garcia⁴⁶, R. Narayan⁴², I. Naryshkin¹³⁷, M. Naseri³⁴, T. Naumann⁴⁶,
 G. Navarro^{22a}, P.Y. Nechaeva¹¹¹, F. Nechansky⁴⁶, T.J. Neep²¹, A. Negri^{71a,71b}, M. Negrini^{23b}, C. Nellist¹¹⁹,
 C. Nelson¹⁰⁴, M.E. Nelson^{45a,45b}, S. Nemecek¹⁴⁰, M. Nessi^{36,f}, M.S. Neubauer¹⁷², F. Neuhaus¹⁰⁰,
 M. Neumann¹⁸¹, R. Newhouse¹⁷⁴, P.R. Newman²¹, C.W. Ng¹³⁸, Y.S. Ng¹⁹, Y.W.Y. Ng¹⁷⁰, B. Ngair^{35e},
 H.D.N. Nguyen¹⁰², T. Nguyen Manh¹¹⁰, E. Nibigira³⁸, R.B. Nickerson¹³⁴, R. Nicolaïdou¹⁴⁴,
 D.S. Nielsen⁴⁰, J. Nielsen¹⁴⁵, M. Niemeyer⁵³, N. Nikiforou¹¹, V. Nikolaenko^{123,ae}, I. Nikolic-Audit¹³⁵,
 K. Nikolopoulos²¹, P. Nilsson²⁹, H.R. Nindhito⁵⁴, A. Nisati^{73a}, N. Nishu^{60c}, R. Nisius¹¹⁵, I. Nitsche⁴⁷,
 T. Nitta¹⁷⁸, T. Nobe¹⁶², D.L. Noel³², Y. Noguchi⁸⁶, I. Nomidis¹³⁵, M.A. Nomura²⁹, M. Nordberg³⁶,
 J. Novak⁹², T. Novak⁹², O. Novgorodova⁴⁸, R. Novotny¹¹⁸, L. Nozka¹³⁰, K. Ntekas¹⁷⁰, E. Nurse⁹⁵,
 F.G. Oakham^{34,aj}, J. Ocariz¹³⁵, A. Ochi⁸³, I. Ochoa^{139a}, J.P. Ochoa-Ricoux^{146a}, K. O'Connor²⁶, S. Oda⁸⁸,
 S. Odaka⁸², S. Oerdekk⁵³, A. Ogrodnik^{84a}, A. Oh¹⁰¹, C.C. Ohm¹⁵³, H. Oide¹⁶⁴, R. Oishi¹⁶², M.L. Ojeda¹⁶⁶,
 H. Okawa¹⁶⁸, Y. Okazaki⁸⁶, M.W. O'Keeffe⁹¹, Y. Okumura¹⁶², A. Olariu^{27b}, L.F. Oleiro Seabra^{139a},
 S.A. Olivares Pino^{146a}, D. Oliveira Damazio²⁹, J.L. Oliver¹, M.J.R. Olsson¹⁷⁰, A. Olszewski⁸⁵,
 J. Olszowska⁸⁵, Ö.O. Öncel²⁴, D.C. O'Neil¹⁵¹, A.P. O'neill¹³⁴, A. Onofre^{139a,139e}, P.U.E. Onyisi¹¹,
 H. Oppen¹³³, R.G. Oreamuno Madriz¹²¹, M.J. Oreglia³⁷, G.E. Orellana⁸⁹, D. Orestano^{75a,75b},
 N. Orlando¹⁴, R.S. Orr¹⁶⁶, V. O'Shea⁵⁷, R. Ospanov^{60a}, G. Otero y Garzon³⁰, H. Otono⁸⁸, P.S. Ott^{61a},
 G.J. Ottino¹⁸, M. Ouchrif^{35d}, J. Ouellette²⁹, F. Ould-Saada¹³³, A. Ouraou¹⁴⁴, Q. Ouyang^{15a}, M. Owen⁵⁷,
 R.E. Owen¹⁴³, V.E. Ozcan^{12c}, N. Ozturk⁸, J. Pacalt¹³⁰, H.A. Pacey³², K. Pachal⁴⁹, A. Pacheco Pages¹⁴,
 C. Padilla Aranda¹⁴, S. Pagan Griso¹⁸, G. Palacino⁶⁶, S. Palazzo⁵⁰, S. Palestini³⁶, M. Palka^{84b}, P. Palni^{84a},
 C.E. Pandini⁵⁴, J.G. Panduro Vazquez⁹⁴, P. Pani⁴⁶, G. Panizzo^{67a,67c}, L. Paolozzi⁵⁴, C. Papadatos¹¹⁰,
 K. Papageorgiou^{9,h}, S. Parajuli⁴², A. Paramonov⁶, C. Paraskevopoulos¹⁰, D. Paredes Hernandez^{63b},
 S.R. Paredes Saenz¹³⁴, B. Parida¹⁷⁹, T.H. Park¹⁶⁶, A.J. Parker³¹, M.A. Parker³², F. Parodi^{55b,55a},
 E.W. Parrish¹²¹, J.A. Parsons³⁹, U. Parzefall⁵², L. Pascual Dominguez¹³⁵, V.R. Pascuzzi¹⁸,
 J.M.P. Pasner¹⁴⁵, F. Pasquali¹²⁰, E. Pasqualucci^{73a}, S. Passaggio^{55b}, F. Pastore⁹⁴, P. Pasuwan^{45a,45b},
 S. Pataria¹⁰⁰, J.R. Pater¹⁰¹, A. Pathak^{180,j}, J. Patton⁹¹, T. Pauly³⁶, J. Pearkes¹⁵², M. Pedersen¹³³,
 L. Pedraza Diaz¹¹⁹, R. Pedro^{139a}, T. Peiffer⁵³, S.V. Peleganchuk^{122b,122a}, O. Penc¹⁴⁰, C. Peng^{63b},
 H. Peng^{60a}, B.S. Peralva^{81a}, M.M. Perego⁶⁵, A.P. Pereira Peixoto^{139a}, L. Pereira Sanchez^{45a,45b},
 D.V. Perepelitsa²⁹, E. Perez Codina^{167a}, L. Perini^{69a,69b}, H. Pernegger³⁶, S. Perrella³⁶, A. Perrevoort¹²⁰,
 K. Peters⁴⁶, R.F.Y. Peters¹⁰¹, B.A. Petersen³⁶, T.C. Petersen⁴⁰, E. Petit¹⁰², V. Petousis¹⁴¹, C. Petridou¹⁶¹,
 F. Petrucci^{75a,75b}, M. Pettee¹⁸², N.E. Pettersson¹⁰³, K. Petukhova¹⁴², A. Peyaud¹⁴⁴, R. Pezoa^{146d},
 L. Pezzotti^{71a,71b}, T. Pham¹⁰⁵, P.W. Phillips¹⁴³, M.W. Phipps¹⁷², G. Piacquadio¹⁵⁴, E. Pianori¹⁸,
 A. Picazio¹⁰³, R.H. Pickles¹⁰¹, R. Piegaia³⁰, D. Pietreanu^{27b}, J.E. Pilcher³⁷, A.D. Pilkington¹⁰¹,
 M. Pinamonti^{67a,67c}, J.L. Pinfold³, C. Pitman Donaldson⁹⁵, M. Pitt¹⁶⁰, L. Pizzimento^{74a,74b}, A. Pizzini¹²⁰,
 M.-A. Pleier²⁹, V. Plesanovs⁵², V. Pleskot¹⁴², E. Plotnikova⁸⁰, P. Podbereko^{122b,122a}, R. Poettgen⁹⁷,

R. Poggi⁵⁴, L. Poggioli¹³⁵, I. Pogrebnyak¹⁰⁷, D. Pohl²⁴, I. Pokharel⁵³, G. Polesello^{71a}, A. Poley^{151,167a},
 A. Policicchio^{73a,73b}, R. Polifka¹⁴², A. Polini^{23b}, C.S. Pollard⁴⁶, V. Polychronakos²⁹, D. Ponomarenko¹¹²,
 L. Pontecorvo³⁶, S. Popa^{27a}, G.A. Popeneciu^{27d}, L. Portales⁵, D.M. Portillo Quintero⁵⁸, S. Pospisil¹⁴¹,
 K. Potamianos⁴⁶, I.N. Potrap⁸⁰, C.J. Potter³², H. Potti¹¹, T. Poulsen⁹⁷, J. Poveda¹⁷³, T.D. Powell¹⁴⁸,
 G. Pownall⁴⁶, M.E. Pozo Astigarraga³⁶, A. Prades Ibanez¹⁷³, P. Pralavorio¹⁰², M.M. Prapa⁴⁴, S. Prell⁷⁹,
 D. Price¹⁰¹, M. Primavera^{68a}, M.L. Proffitt¹⁴⁷, N. Proklova¹¹², K. Prokofiev^{63c}, F. Prokoshin⁸⁰,
 S. Protopopescu²⁹, J. Proudfoot⁶, M. Przybycien^{84a}, D. Pudzha¹³⁷, A. Puri¹⁷², P. Puzo⁶⁵,
 D. Pyatiizbyantseva¹¹², J. Qian¹⁰⁶, Y. Qin¹⁰¹, A. Quadt⁵³, M. Queitsch-Maitland³⁶, G. Rabanal Bolanos⁵⁹,
 M. Racko^{28a}, F. Ragusa^{69a,69b}, G. Rahal⁹⁸, J.A. Raine⁵⁴, S. Rajagopalan²⁹, A. Ramirez Morales⁹³,
 K. Ran^{15a,15d}, D.F. Rassloff^{61a}, D.M. Rauch⁴⁶, F. Rauscher¹¹⁴, S. Rave¹⁰⁰, B. Ravina⁵⁷, I. Ravinovich¹⁷⁹,
 J.H. Rawling¹⁰¹, M. Raymond³⁶, A.L. Read¹³³, N.P. Readioff¹⁴⁸, M. Reale^{68a,68b}, D.M. Rebuzzi^{71a,71b},
 G. Redlinger²⁹, K. Reeves⁴³, D. Reikher¹⁶⁰, A. Reiss¹⁰⁰, A. Rej¹⁵⁰, C. Rembser³⁶, A. Renardi⁴⁶,
 M. Renda^{27b}, M.B. Rendel¹¹⁵, A.G. Rennie⁵⁷, S. Resconi^{69a}, E.D. Ressegue¹⁸, S. Rettie⁹⁵, B. Reynolds¹²⁷,
 E. Reynolds²¹, O.L. Rezanova^{122b,122a}, P. Reznicek¹⁴², E. Ricci^{76a,76b}, R. Richter¹¹⁵, S. Richter⁴⁶,
 E. Richter-Was^{84b}, M. Ridel¹³⁵, P. Rieck¹¹⁵, O. Rifki⁴⁶, M. Rijssenbeek¹⁵⁴, A. Rimoldi^{71a,71b},
 M. Rimoldi⁴⁶, L. Rinaldi^{23b}, T.T. Rinn¹⁷², G. Ripellino¹⁵³, I. Riu¹⁴, P. Rivadeneira⁴⁶,
 J.C. Rivera Vergara¹⁷⁵, F. Rizatdinova¹²⁹, E. Rizvi⁹³, C. Rizzi³⁶, S.H. Robertson^{104,aa}, M. Robin⁴⁶,
 D. Robinson³², C.M. Robles Gajardo^{146d}, M. Robles Manzano¹⁰⁰, A. Robson⁵⁷, A. Rocchi^{74a,74b},
 C. Roda^{72a,72b}, S. Rodriguez Bosca¹⁷³, A. Rodriguez Rodriguez⁵², A.M. Rodríguez Vera^{167b}, S. Roe³⁶,
 J. Roggel¹⁸¹, O. Røhne¹³³, R. Röhrig¹¹⁵, R.A. Rojas^{146d}, B. Roland⁵², C.P.A. Roland⁶⁶, J. Roloff²⁹,
 A. Romaniouk¹¹², M. Romano^{23b,23a}, N. Rompotis⁹¹, M. Ronzani¹²⁵, L. Roos¹³⁵, S. Rosati^{73a}, G. Rosin¹⁰³,
 B.J. Rosser¹³⁶, E. Rossi⁴⁶, E. Rossi^{75a,75b}, E. Rossi^{70a,70b}, L.P. Rossi^{55b}, L. Rossini⁴⁶, R. Rosten¹⁴,
 M. Rotaru^{27b}, B. Rottler⁵², D. Rousseau⁶⁵, G. Rovelli^{71a,71b}, A. Roy¹¹, D. Roy^{33e}, A. Rozanov¹⁰²,
 Y. Rozen¹⁵⁹, X. Ruan^{33e}, T.A. Ruggeri¹, F. Rühr⁵², A. Ruiz-Martinez¹⁷³, A. Rummler³⁶, Z. Rurikova⁵²,
 N.A. Rusakovich⁸⁰, H.L. Russell¹⁰⁴, L. Rustige^{38,47}, J.P. Rutherford⁷, E.M. Rüttinger¹⁴⁸, M. Rybar¹⁴²,
 G. Rybkin⁶⁵, E.B. Rye¹³³, A. Ryzhov¹²³, J.A. Sabater Iglesias⁴⁶, P. Sabatini¹⁷³, L. Sabetta^{73a,73b},
 S. Sacerdoti⁶⁵, H.F-W. Sadrozinski¹⁴⁵, R. Sadykov⁸⁰, F. Safai Tehrani^{73a}, B. Safarzadeh Samani¹⁵⁵,
 M. Safdari¹⁵², P. Saha¹²¹, S. Saha¹⁰⁴, M. Sahinsoy¹¹⁵, A. Sahu¹⁸¹, M. Saimpert³⁶, M. Saito¹⁶², T. Saito¹⁶²,
 H. Sakamoto¹⁶², D. Salamani⁵⁴, G. Salamanna^{75a,75b}, A. Salnikov¹⁵², J. Salt¹⁷³, A. Salvador Salas¹⁴,
 D. Salvatore^{41b,41a}, F. Salvatore¹⁵⁵, A. Salvucci^{63a}, A. Salzburger³⁶, J. Samarati³⁶, D. Sammel⁵²,
 D. Sampsonidis¹⁶¹, D. Sampsonidou^{60d,60c}, J. Sánchez¹⁷³, A. Sanchez Pineda^{67a,36,67c}, H. Sandaker¹³³,
 C.O. Sander⁴⁶, I.G. Sanderswood⁹⁰, M. Sandhoff¹⁸¹, C. Sandoval^{22b}, D.P.C. Sankey¹⁴³, M. Sannino^{55b,55a},
 Y. Sano¹¹⁷, A. Sansoni⁵¹, C. Santoni³⁸, H. Santos^{139a,139b}, S.N. Santpur¹⁸, A. Santra¹⁷³, K.A. Saoucha¹⁴⁸,
 A. Sapronov⁸⁰, J.G. Saraiva^{139a,139d}, O. Sasaki⁸², K. Sato¹⁶⁸, F. Sauerburger⁵², E. Sauvan⁵, P. Savard^{166,aj},
 R. Sawada¹⁶², C. Sawyer¹⁴³, L. Sawyer⁹⁶, I. Sayago Galvan¹⁷³, C. Sbarra^{23b}, A. Sbrizzi^{67a,67c},
 T. Scanlon⁹⁵, J. Schaarschmidt¹⁴⁷, P. Schacht¹¹⁵, D. Schaefer³⁷, L. Schaefer¹³⁶, U. Schäfer¹⁰⁰,
 A.C. Schaffer⁶⁵, D. Schaile¹¹⁴, R.D. Schamberger¹⁵⁴, E. Schanet¹¹⁴, C. Scharf¹⁹, N. Scharmberg¹⁰¹,
 V.A. Schegelsky¹³⁷, D. Scheirich¹⁴², F. Schenck¹⁹, M. Schernau¹⁷⁰, C. Schiavi^{55b,55a}, L.K. Schildgen²⁴,
 Z.M. Schillaci²⁶, E.J. Schioppa^{68a,68b}, M. Schioppa^{41b,41a}, K.E. Schleicher⁵², S. Schlenker³⁶,
 K.R. Schmidt-Sommerfeld¹¹⁵, K. Schmieden¹⁰⁰, C. Schmitt¹⁰⁰, S. Schmitt⁴⁶, L. Schoeffel¹⁴⁴,
 A. Schoening^{61b}, P.G. Scholer⁵², E. Schopf¹³⁴, M. Schott¹⁰⁰, J.F.P. Schouwenberg¹¹⁹, J. Schovancova³⁶,
 S. Schramm⁵⁴, F. Schroeder¹⁸¹, A. Schulte¹⁰⁰, H-C. Schultz-Coulon^{61a}, M. Schumacher⁵²,
 B.A. Schumm¹⁴⁵, Ph. Schune¹⁴⁴, A. Schwartzman¹⁵², T.A. Schwarz¹⁰⁶, Ph. Schwemling¹⁴⁴,
 R. Schwienhorst¹⁰⁷, A. Sciandra¹⁴⁵, G. Sciolla²⁶, F. Scuri^{72a}, F. Scutti¹⁰⁵, L.M. Scyboz¹¹⁵,
 C.D. Sebastiani⁹¹, K. Sedlaczek⁴⁷, P. Seema¹⁹, S.C. Seidel¹¹⁸, A. Seiden¹⁴⁵, B.D. Seidlitz²⁹, T. Seiss³⁷,
 C. Seitz⁴⁶, J.M. Seixas^{81b}, G. Sekhniaidze^{70a}, S.J. Sekula⁴², N. Semprini-Cesari^{23b,23a}, S. Sen⁴⁹,
 C. Serfon²⁹, L. Serin⁶⁵, L. Serkin^{67a,67b}, M. Sessa^{60a}, H. Severini¹²⁸, S. Sevova¹⁵², F. Sforza^{55b,55a}

A. Sfyrla⁵⁴, E. Shabalina⁵³, J.D. Shahinian¹³⁶, N.W. Shaikh^{45a,45b}, D. Shaked Renous¹⁷⁹, L.Y. Shan^{15a}, M. Shapiro¹⁸, A. Sharma³⁶, A.S. Sharma¹, P.B. Shatalov¹²⁴, K. Shaw¹⁵⁵, S.M. Shaw¹⁰¹, M. Shehade¹⁷⁹, Y. Shen¹²⁸, A.D. Sherman²⁵, P. Sherwood⁹⁵, L. Shi⁹⁵, C.O. Shimmin¹⁸², Y. Shimogama¹⁷⁸, M. Shimojima¹¹⁶, J.D. Shinner⁹⁴, I.P.J. Shipsey¹³⁴, S. Shirabe¹⁶⁴, M. Shiyakova^{80,y}, J. Shlomi¹⁷⁹, A. Shmeleva¹¹¹, M.J. Shochet³⁷, J. Shojaei¹⁰⁵, D.R. Shope¹⁵³, S. Shrestha¹²⁷, E.M. Shrif^{33e}, M.J. Shroff¹⁷⁵, E. Shulga¹⁷⁹, P. Sicho¹⁴⁰, A.M. Sickles¹⁷², E. Sideras Haddad^{33e}, O. Sidiropoulou³⁶, A. Sidoti^{23b,23a}, F. Siegert⁴⁸, Dj. Sijacki¹⁶, M.Jr. Silva¹⁸⁰, M.V. Silva Oliveira³⁶, S.B. Silverstein^{45a}, S. Simion⁶⁵, R. Simonello¹⁰⁰, C.J. Simpson-allsop²¹, S. Simsek^{12b}, P. Sinervo¹⁶⁶, V. Sinetckii¹¹³, S. Singh¹⁵¹, S. Sinha^{33e}, M. Sioli^{23b,23a}, I. Siral¹³¹, S.Yu. Sivoklokov¹¹³, J. Sjölin^{45a,45b}, A. Skaf⁵³, E. Skorda⁹⁷, P. Skubic¹²⁸, M. Slawinska⁸⁵, K. Sliwa¹⁶⁹, V. Smakhtin¹⁷⁹, B.H. Smart¹⁴³, J. Smiesko^{28b}, N. Smirnov¹¹², S.Yu. Smirnov¹¹², Y. Smirnov¹¹², L.N. Smirnova^{113,s}, O. Smirnova⁹⁷, E.A. Smith³⁷, H.A. Smith¹³⁴, M. Smizanska⁹⁰, K. Smolek¹⁴¹, A. Smykiewicz⁸⁵, A.A. Snesarev¹¹¹, H.L. Snoek¹²⁰, I.M. Snyder¹³¹, S. Snyder²⁹, R. Sobie^{175,aa}, A. Soffer¹⁶⁰, A. Søgaard⁵⁰, F. Sohns⁵³, C.A. Solans Sanchez³⁶, E.Yu. Soldatov¹¹², U. Soldevila¹⁷³, A.A. Solodkov¹²³, A. Soloshenko⁸⁰, O.V. Solovyev¹²³, V. Solovyev¹³⁷, P. Sommer¹⁴⁸, H. Son¹⁶⁹, A. Sonay¹⁴, W. Song¹⁴³, W.Y. Song^{167b}, A. Sopczak¹⁴¹, A.L. Sopio⁹⁵, F. Sopkova^{28b}, S. Sottocornola^{71a,71b}, R. Soualah^{67a,67c}, A.M. Soukharev^{122b,122a}, D. South⁴⁶, S. Spagnolo^{68a,68b}, M. Spalla¹¹⁵, M. Spangenberg¹⁷⁷, F. Spanò⁹⁴, D. Sperlich⁵², T.M. Spieker^{61a}, G. Spigo³⁶, M. Spina¹⁵⁵, D.P. Spiteri⁵⁷, M. Spousta¹⁴², A. Stabile^{69a,69b}, B.L. Stamas¹²¹, R. Stamen^{61a}, M. Stamenkovic¹²⁰, A. Stampeki²¹, E. Stanecka⁸⁵, B. Stanislaus¹³⁴, M.M. Stanitzki⁴⁶, M. Stankaityte¹³⁴, B. Stapf¹²⁰, E.A. Starchenko¹²³, G.H. Stark¹⁴⁵, J. Stark⁵⁸, P. Staroba¹⁴⁰, P. Starovoitov^{61a}, S. Stärz¹⁰⁴, R. Staszewski⁸⁵, G. Stavropoulos⁴⁴, M. Stegler⁴⁶, P. Steinberg²⁹, A.L. Steinhebel¹³¹, B. Stelzer^{151,167a}, H.J. Stelzer¹³⁸, O. Stelzer-Chilton^{167a}, H. Stenzel⁵⁶, T.J. Stevenson¹⁵⁵, G.A. Stewart³⁶, M.C. Stockton³⁶, G. Stoica^{27b}, M. Stolarski^{139a}, S. Stonjek¹¹⁵, A. Straessner⁴⁸, J. Strandberg¹⁵³, S. Strandberg^{45a,45b}, M. Strauss¹²⁸, T. Strebler¹⁰², P. Strizenec^{28b}, R. Ströhmer¹⁷⁶, D.M. Strom¹³¹, R. Stroynowski⁴², A. Strubig^{45a,45b}, S.A. Stucci²⁹, B. Stugu¹⁷, J. Stupak¹²⁸, N.A. Styles⁴⁶, D. Su¹⁵², W. Su^{60d,147,60c}, X. Su^{60a}, N.B. Suarez¹³⁸, V.V. Sulin¹¹¹, M.J. Sullivan⁹¹, D.M.S. Sultan⁵⁴, S. Sultansoy^{4c}, T. Sumida⁸⁶, S. Sun¹⁰⁶, X. Sun¹⁰¹, C.J.E. Suster¹⁵⁶, M.R. Sutton¹⁵⁵, S. Suzuki⁸², M. Svatos¹⁴⁰, M. Swiatlowski^{167a}, S.P. Swift², T. Swirski¹⁷⁶, A. Sydorenko¹⁰⁰, I. Sykora^{28a}, M. Sykora¹⁴², T. Sykora¹⁴², D. Ta¹⁰⁰, K. Tackmann^{46,x}, J. Taenzer¹⁶⁰, A. Taffard¹⁷⁰, R. Tafirout^{167a}, E. Tagiev¹²³, R.H.M. Taibah¹³⁵, R. Takashima⁸⁷, K. Takeda⁸³, T. Takeshita¹⁴⁹, E.P. Takeva⁵⁰, Y. Takubo⁸², M. Talby¹⁰², A.A. Talyshев^{122b,122a}, K.C. Tam^{63b}, N.M. Tamir¹⁶⁰, J. Tanaka¹⁶², R. Tanaka⁶⁵, S. Tapia Araya¹⁷², S. Tapprogge¹⁰⁰, A. Tarek Abouelfadl Mohamed¹⁰⁷, S. Tarem¹⁵⁹, K. Tariq^{60b}, G. Tarna^{27b,e}, G.F. Tartarelli^{69a}, P. Tas¹⁴², M. Tasevsky¹⁴⁰, E. Tassi^{41b,41a}, G. Tateno¹⁶², A. Tavares Delgado^{139a}, Y. Tayalati^{35e}, A.J. Taylor⁵⁰, G.N. Taylor¹⁰⁵, W. Taylor^{167b}, H. Teagle⁹¹, A.S. Tee⁹⁰, R. Teixeira De Lima¹⁵², P. Teixeira-Dias⁹⁴, H. Ten Kate³⁶, J.J. Teoh¹²⁰, K. Terashi¹⁶², J. Terron⁹⁹, S. Terzo¹⁴, M. Testa⁵¹, R.J. Teuscher^{166,aa}, N. Themistokleous⁵⁰, T. Theveneaux-Pelzer¹⁹, D.W. Thomas⁹⁴, J.P. Thomas²¹, E.A. Thompson⁴⁶, P.D. Thompson²¹, E. Thomson¹³⁶, E.J. Thorpe⁹³, V.O. Tikhomirov^{111,af}, Yu.A. Tikhonov^{122b,122a}, S. Timoshenko¹¹², P. Tipton¹⁸², S. Tisserant¹⁰², K. Todome^{23b,23a}, S. Todorova-Nova¹⁴², S. Todt⁴⁸, J. Tojo⁸⁸, S. Tokár^{28a}, K. Tokushuku⁸², E. Tolley¹²⁷, R. Tombs³², K.G. Tomiwa^{33e}, M. Tomoto^{82,117}, L. Tompkins¹⁵², P. Tornambe¹⁰³, E. Torrence¹³¹, H. Torres⁴⁸, E. Torró Pastor¹⁷³, M. Toscani³⁰, C. Tosciri¹³⁴, J. Toth^{102,z}, D.R. Tovey¹⁴⁸, A. Traeet¹⁷, C.J. Treado¹²⁵, T. Trefzger¹⁷⁶, F. Tresoldi¹⁵⁵, A. Tricoli²⁹, I.M. Trigger^{167a}, S. Trincaz-Duvold¹³⁵, D.A. Trischuk¹⁷⁴, W. Trischuk¹⁶⁶, B. Trocmé⁵⁸, A. Trofymov⁶⁵, C. Troncon^{69a}, F. Trovato¹⁵⁵, L. Truong^{33c}, M. Trzebinski⁸⁵, A. Trzupek⁸⁵, F. Tsai⁴⁶, P.V. Tsiareshka^{108,ad}, A. Tsirigotis^{161,v}, V. Tsiskaridze¹⁵⁴, E.G. Tskhadadze^{158a}, M. Tsopoulou¹⁶¹, I.I. Tsukerman¹²⁴, V. Tsulaia¹⁸, S. Tsuno⁸², D. Tsbychev¹⁵⁴, Y. Tu^{63b}, A. Tudorache^{27b}, V. Tudorache^{27b}, A.N. Tuna³⁶, S. Turchikhin⁸⁰, D. Turgeman¹⁷⁹, I. Turk Cakir^{4b,t}, R.J. Turner²¹, R. Turra^{69a}, P.M. Tuts³⁹, S. Tzamarias¹⁶¹, E. Tzovara¹⁰⁰, K. Uchida¹⁶², F. Ukegawa¹⁶⁸, G. Unal³⁶,

M. Unal¹¹, A. Undrus²⁹, G. Unel¹⁷⁰, F.C. Ungaro¹⁰⁵, Y. Unno⁸², K. Uno¹⁶², J. Urban^{28b}, P. Urquijo¹⁰⁵,
 G. Usai⁸, Z. Uysal^{12d}, V. Vacek¹⁴¹, B. Vachon¹⁰⁴, K.O.H. Vadla¹³³, T. Vafeiadis³⁶, A. Vaidya⁹⁵,
 C. Valderanis¹¹⁴, E. Valdes Santurio^{45a,45b}, M. Valente^{167a}, S. Valentineti^{23b,23a}, A. Valero¹⁷³, L. Valéry⁴⁶,
 R.A. Vallance²¹, A. Vallier³⁶, J.A. Valls Ferrer¹⁷³, T.R. Van Daalen¹⁴, P. Van Gemmeren⁶, S. Van Stroud⁹⁵,
 I. Van Vulpen¹²⁰, M. Vanadia^{74a,74b}, W. Vandelli³⁶, M. Vandenbroucke¹⁴⁴, E.R. Vandewall¹²⁹,
 D. Vannicola^{73a,73b}, R. Vari^{73a}, E.W. Varnes⁷, C. Varni^{55b,55a}, T. Varol¹⁵⁷, D. Varouchas⁶⁵, K.E. Varvell¹⁵⁶,
 M.E. Vasile^{27b}, G.A. Vasquez¹⁷⁵, F. Vazeille³⁸, D. Vazquez Furelos¹⁴, T. Vazquez Schroeder³⁶, J. Veatch⁵³,
 V. Vecchio¹⁰¹, M.J. Veen¹²⁰, L.M. Veloce¹⁶⁶, F. Veloso^{139a,139c}, S. Veneziano^{73a}, A. Ventura^{68a,68b},
 A. Verbytskyi¹¹⁵, V. Vercesi^{71a}, M. Verducci^{72a,72b}, C.M. Vergel Infante⁷⁹, C. Vergis²⁴, W. Verkerke¹²⁰,
 A.T. Vermeulen¹²⁰, J.C. Vermeulen¹²⁰, C. Vernieri¹⁵², P.J. Verschuuren⁹⁴, M.C. Vetterli^{151,aj},
 N. Viaux Maira^{146d}, T. Vickey¹⁴⁸, O.E. Vickey Boeriu¹⁴⁸, G.H.A. Viehhauser¹³⁴, L. Vigani^{61b},
 M. Villa^{23b,23a}, M. Villaplana Perez¹⁷³, E.M. Villhauer⁵⁰, E. Vilucchi⁵¹, M.G. Vinctor³⁴, G.S. Virdee²¹,
 A. Vishwakarma⁵⁰, C. Vittori^{23b,23a}, I. Vivarelli¹⁵⁵, M. Vogel¹⁸¹, P. Vokac¹⁴¹, J. Von Ahnen⁴⁶,
 S.E. von Buddenbrock^{33e}, E. Von Toerne²⁴, V. Vorobel¹⁴², K. Vorobev¹¹², M. Vos¹⁷³, J.H. Vossebeld⁹¹,
 M. Vozak¹⁰¹, N. Vranjes¹⁶, M. Vranjes Milosavljevic¹⁶, V. Vrba¹⁴¹, M. Vreeswijk¹²⁰, N.K. Vu¹⁰²,
 R. Vuillermet³⁶, I. Vukotic³⁷, S. Wada¹⁶⁸, P. Wagner²⁴, W. Wagner¹⁸¹, J. Wagner-Kuhr¹¹⁴, S. Wahdan¹⁸¹,
 H. Wahlberg⁸⁹, R. Wakasa¹⁶⁸, V.M. Walbrecht¹¹⁵, J. Walder¹⁴³, R. Walker¹¹⁴, S.D. Walker⁹⁴,
 W. Walkowiak¹⁵⁰, V. Wallangen^{45a,45b}, A.M. Wang⁵⁹, A.Z. Wang¹⁸⁰, C. Wang^{60a}, C. Wang^{60c}, H. Wang¹⁸,
 H. Wang³, J. Wang^{63a}, P. Wang⁴², Q. Wang¹²⁸, R.-J. Wang¹⁰⁰, R. Wang^{60a}, R. Wang⁶, S.M. Wang¹⁵⁷,
 W.T. Wang^{60a}, W. Wang^{15c}, W.X. Wang^{60a}, Y. Wang^{60a}, Z. Wang¹⁰⁶, C. Wanotayaroj⁴⁶, A. Warburton¹⁰⁴,
 C.P. Ward³², R.J. Ward²¹, N. Warrack⁵⁷, A.T. Watson²¹, M.F. Watson²¹, G. Watts¹⁴⁷, B.M. Waugh⁹⁵,
 A.F. Webb¹¹, C. Weber²⁹, M.S. Weber²⁰, S.A. Weber³⁴, S.M. Weber^{61a}, Y. Wei¹³⁴, A.R. Weidberg¹³⁴,
 J. Weingarten⁴⁷, M. Weirich¹⁰⁰, C. Weiser⁵², P.S. Wells³⁶, T. Wenaus²⁹, B. Wendland⁴⁷, T. Wengler³⁶,
 S. Wenig³⁶, N. Wermes²⁴, M. Wessels^{61a}, T.D. Weston²⁰, K. Whalen¹³¹, A.M. Wharton⁹⁰, A.S. White¹⁰⁶,
 A. White⁸, M.J. White¹, D. Whiteson¹⁷⁰, B.W. Whitmore⁹⁰, W. Wiedenmann¹⁸⁰, C. Wiel⁴⁸, M. Wielaers¹⁴³,
 N. Wieseotte¹⁰⁰, C. Wiglesworth⁴⁰, L.A.M. Wiik-Fuchs⁵², H.G. Wilkens³⁶, L.J. Wilkins⁹⁴,
 D.M. Williams³⁹, H.H. Williams¹³⁶, S. Williams³², S. Willocq¹⁰³, P.J. Windischhofer¹³⁴,
 I. Wingerter-Seez⁵, E. Winkels¹⁵⁵, F. Winklmeier¹³¹, B.T. Winter⁵², M. Wittgen¹⁵², M. Wobisch⁹⁶,
 A. Wolf¹⁰⁰, R. Wölker¹³⁴, J. Wollrath⁵², M.W. Wolter⁸⁵, H. Wolters^{139a,139c}, V.W.S. Wong¹⁷⁴,
 A.F. Wongel⁴⁶, N.L. Woods¹⁴⁵, S.D. Worm⁴⁶, B.K. Wosiek⁸⁵, K.W. Woźniak⁸⁵, K. Wraight⁵⁷, S.L. Wu¹⁸⁰,
 X. Wu⁵⁴, Y. Wu^{60a}, J. Wuerzinger¹³⁴, T.R. Wyatt¹⁰¹, B.M. Wynne⁵⁰, S. Xella⁴⁰, L. Xia¹⁷⁷, J. Xiang^{63c},
 X. Xiao¹⁰⁶, X. Xie^{60a}, I. Xiotidis¹⁵⁵, D. Xu^{15a}, H. Xu^{60a}, H. Xu^{60a}, L. Xu²⁹, R. Xu¹³⁶, T. Xu¹⁴⁴, W. Xu¹⁰⁶,
 Y. Xu^{15b}, Z. Xu^{60b}, Z. Xu¹⁵², B. Yabsley¹⁵⁶, S. Yacoob^{33a}, D.P. Yallup⁹⁵, N. Yamaguchi⁸⁸,
 Y. Yamaguchi¹⁶⁴, A. Yamamoto⁸², M. Yamatani¹⁶², T. Yamazaki¹⁶², Y. Yamazaki⁸³, J. Yan^{60c}, Z. Yan²⁵,
 H.J. Yang^{60c,60d}, H.T. Yang¹⁸, S. Yang^{60a}, T. Yang^{63c}, X. Yang^{60a}, X. Yang^{60b,58}, Y. Yang¹⁶², Z. Yang^{60a},
 W-M. Yao¹⁸, Y.C. Yap⁴⁶, H. Ye^{15c}, J. Ye⁴², S. Ye²⁹, I. Yeletskikh⁸⁰, M.R. Yexley⁹⁰, E. Yigitbasi²⁵,
 P. Yin³⁹, K. Yorita¹⁷⁸, K. Yoshihara⁷⁹, C.J.S. Young³⁶, C. Young¹⁵², J. Yu⁷⁹, R. Yuan^{60b,i}, X. Yue^{61a},
 M. Zaazoua^{35e}, B. Zabinski⁸⁵, G. Zacharis¹⁰, E. Zaffaroni⁵⁴, J. Zahreddine¹³⁵, A.M. Zaitsev^{123,ae},
 T. Zakareishvili^{158b}, N. Zakharchuk³⁴, S. Zambito³⁶, D. Zanzi³⁶, S.V. Zeißner⁴⁷, C. Zeitnitz¹⁸¹,
 G. Zemaityte¹³⁴, J.C. Zeng¹⁷², O. Zenin¹²³, T. Ženīš^{28a}, D. Zerwas⁶⁵, M. Zgubič¹³⁴, B. Zhang^{15c},
 D.F. Zhang^{15b}, G. Zhang^{15b}, J. Zhang⁶, Kaili. Zhang^{15a}, L. Zhang^{15c}, L. Zhang^{60a}, M. Zhang¹⁷²,
 R. Zhang¹⁸⁰, S. Zhang¹⁰⁶, X. Zhang^{60c}, X. Zhang^{60b}, Y. Zhang^{15a,15d}, Z. Zhang^{63a}, Z. Zhang⁶⁵, P. Zhao⁴⁹,
 Y. Zhao¹⁴⁵, Z. Zhao^{60a}, A. Zhemchugov⁸⁰, Z. Zheng¹⁰⁶, D. Zhong¹⁷², B. Zhou¹⁰⁶, C. Zhou¹⁸⁰, H. Zhou⁷,
 M. Zhou¹⁵⁴, N. Zhou^{60c}, Y. Zhou⁷, C.G. Zhu^{60b}, C. Zhu^{15a,15d}, H.L. Zhu^{60a}, H. Zhu^{15a}, J. Zhu¹⁰⁶,
 Y. Zhu^{60a}, X. Zhuang^{15a}, K. Zhukov¹¹¹, V. Zhulanov^{122b,122a}, D. Zieminska⁶⁶, N.I. Zimine⁸⁰,
 S. Zimmermann⁵², Z. Zinonos¹¹⁵, M. Ziolkowski¹⁵⁰, L. Živković¹⁶, G. Zobernig¹⁸⁰, A. Zoccoli^{23b,23a},
 K. Zoch⁵³, T.G. Zorbas¹⁴⁸, R. Zou³⁷, L. Zwalinski³⁶.

- ¹Department of Physics, University of Adelaide, Adelaide; Australia.
- ²Physics Department, SUNY Albany, Albany NY; United States of America.
- ³Department of Physics, University of Alberta, Edmonton AB; Canada.
- ^{4(a)}Department of Physics, Ankara University, Ankara; ^(b)Istanbul Aydin University, Application and Research Center for Advanced Studies, Istanbul; ^(c)Division of Physics, TOBB University of Economics and Technology, Ankara; Turkey.
- ⁵LAPP, Université Grenoble Alpes, Université Savoie Mont Blanc, CNRS/IN2P3, Annecy; France.
- ⁶High Energy Physics Division, Argonne National Laboratory, Argonne IL; United States of America.
- ⁷Department of Physics, University of Arizona, Tucson AZ; United States of America.
- ⁸Department of Physics, University of Texas at Arlington, Arlington TX; United States of America.
- ⁹Physics Department, National and Kapodistrian University of Athens, Athens; Greece.
- ¹⁰Physics Department, National Technical University of Athens, Zografou; Greece.
- ¹¹Department of Physics, University of Texas at Austin, Austin TX; United States of America.
- ^{12(a)}Bahcesehir University, Faculty of Engineering and Natural Sciences, Istanbul; ^(b)Istanbul Bilgi University, Faculty of Engineering and Natural Sciences, Istanbul; ^(c)Department of Physics, Bogazici University, Istanbul; ^(d)Department of Physics Engineering, Gaziantep University, Gaziantep; Turkey.
- ¹³Institute of Physics, Azerbaijan Academy of Sciences, Baku; Azerbaijan.
- ¹⁴Institut de Física d'Altes Energies (IFAE), Barcelona Institute of Science and Technology, Barcelona; Spain.
- ^{15(a)}Institute of High Energy Physics, Chinese Academy of Sciences, Beijing; ^(b)Physics Department, Tsinghua University, Beijing; ^(c)Department of Physics, Nanjing University, Nanjing; ^(d)University of Chinese Academy of Science (UCAS), Beijing, China.
- ¹⁶Institute of Physics, University of Belgrade, Belgrade; Serbia.
- ¹⁷Department for Physics and Technology, University of Bergen, Bergen; Norway.
- ¹⁸Physics Division, Lawrence Berkeley National Laboratory and University of California, Berkeley CA; United States of America.
- ¹⁹Institut für Physik, Humboldt Universität zu Berlin, Berlin; Germany.
- ²⁰Albert Einstein Center for Fundamental Physics and Laboratory for High Energy Physics, University of Bern, Bern; Switzerland.
- ²¹School of Physics and Astronomy, University of Birmingham, Birmingham; United Kingdom.
- ^{22(a)}Facultad de Ciencias y Centro de Investigaciones, Universidad Antonio Nariño, Bogotá; ^(b)Departamento de Física, Universidad Nacional de Colombia, Bogotá, Colombia; Colombia.
- ^{23(a)}INFN Bologna and Universita' di Bologna, Dipartimento di Fisica; ^(b)INFN Sezione di Bologna; Italy.
- ²⁴Physikalisches Institut, Universität Bonn, Bonn; Germany.
- ²⁵Department of Physics, Boston University, Boston MA; United States of America.
- ²⁶Department of Physics, Brandeis University, Waltham MA; United States of America.
- ^{27(a)}Transilvania University of Brasov, Brasov; ^(b)Horia Hulubei National Institute of Physics and Nuclear Engineering, Bucharest; ^(c)Department of Physics, Alexandru Ioan Cuza University of Iasi, Iasi; ^(d)National Institute for Research and Development of Isotopic and Molecular Technologies, Physics Department, Cluj-Napoca; ^(e)University Politehnica Bucharest, Bucharest; ^(f)West University in Timisoara, Timisoara; Romania.
- ^{28(a)}Faculty of Mathematics, Physics and Informatics, Comenius University, Bratislava; ^(b)Department of Subnuclear Physics, Institute of Experimental Physics of the Slovak Academy of Sciences, Kosice; Slovak Republic.
- ²⁹Physics Department, Brookhaven National Laboratory, Upton NY; United States of America.
- ³⁰Departamento de Física, Universidad de Buenos Aires, Buenos Aires; Argentina.
- ³¹California State University, CA; United States of America.

- ³²Cavendish Laboratory, University of Cambridge, Cambridge; United Kingdom.
- ³³^(a)Department of Physics, University of Cape Town, Cape Town;^(b)iThemba Labs, Western Cape;^(c)Department of Mechanical Engineering Science, University of Johannesburg, Johannesburg;^(d)University of South Africa, Department of Physics, Pretoria;^(e)School of Physics, University of the Witwatersrand, Johannesburg; South Africa.
- ³⁴Department of Physics, Carleton University, Ottawa ON; Canada.
- ³⁵^(a)Faculté des Sciences Ain Chock, Réseau Universitaire de Physique des Hautes Energies - Université Hassan II, Casablanca;^(b)Faculté des Sciences, Université Ibn-Tofail, Kénitra;^(c)Faculté des Sciences Semlalia, Université Cadi Ayyad, LPHEA-Marrakech;^(d)Faculté des Sciences, Université Mohamed Premier and LPTPM, Oujda;^(e)Faculté des sciences, Université Mohammed V, Rabat; Morocco.
- ³⁶CERN, Geneva; Switzerland.
- ³⁷Enrico Fermi Institute, University of Chicago, Chicago IL; United States of America.
- ³⁸LPC, Université Clermont Auvergne, CNRS/IN2P3, Clermont-Ferrand; France.
- ³⁹Nevis Laboratory, Columbia University, Irvington NY; United States of America.
- ⁴⁰Niels Bohr Institute, University of Copenhagen, Copenhagen; Denmark.
- ⁴¹^(a)Dipartimento di Fisica, Università della Calabria, Rende;^(b)INFN Gruppo Collegato di Cosenza, Laboratori Nazionali di Frascati; Italy.
- ⁴²Physics Department, Southern Methodist University, Dallas TX; United States of America.
- ⁴³Physics Department, University of Texas at Dallas, Richardson TX; United States of America.
- ⁴⁴National Centre for Scientific Research "Demokritos", Agia Paraskevi; Greece.
- ⁴⁵^(a)Department of Physics, Stockholm University;^(b)Oskar Klein Centre, Stockholm; Sweden.
- ⁴⁶Deutsches Elektronen-Synchrotron DESY, Hamburg and Zeuthen; Germany.
- ⁴⁷Lehrstuhl für Experimentelle Physik IV, Technische Universität Dortmund, Dortmund; Germany.
- ⁴⁸Institut für Kern- und Teilchenphysik, Technische Universität Dresden, Dresden; Germany.
- ⁴⁹Department of Physics, Duke University, Durham NC; United States of America.
- ⁵⁰SUPA - School of Physics and Astronomy, University of Edinburgh, Edinburgh; United Kingdom.
- ⁵¹INFN e Laboratori Nazionali di Frascati, Frascati; Italy.
- ⁵²Physikalisches Institut, Albert-Ludwigs-Universität Freiburg, Freiburg; Germany.
- ⁵³II. Physikalisches Institut, Georg-August-Universität Göttingen, Göttingen; Germany.
- ⁵⁴Département de Physique Nucléaire et Corpusculaire, Université de Genève, Genève; Switzerland.
- ⁵⁵^(a)Dipartimento di Fisica, Università di Genova, Genova;^(b)INFN Sezione di Genova; Italy.
- ⁵⁶II. Physikalisches Institut, Justus-Liebig-Universität Giessen, Giessen; Germany.
- ⁵⁷SUPA - School of Physics and Astronomy, University of Glasgow, Glasgow; United Kingdom.
- ⁵⁸LPSC, Université Grenoble Alpes, CNRS/IN2P3, Grenoble INP, Grenoble; France.
- ⁵⁹Laboratory for Particle Physics and Cosmology, Harvard University, Cambridge MA; United States of America.
- ⁶⁰^(a)Department of Modern Physics and State Key Laboratory of Particle Detection and Electronics, University of Science and Technology of China, Hefei;^(b)Institute of Frontier and Interdisciplinary Science and Key Laboratory of Particle Physics and Particle Irradiation (MOE), Shandong University, Qingdao;^(c)School of Physics and Astronomy, Shanghai Jiao Tong University, KLPPAC-MoE, SKLPPC, Shanghai;^(d)Tsung-Dao Lee Institute, Shanghai; China.
- ⁶¹^(a)Kirchhoff-Institut für Physik, Ruprecht-Karls-Universität Heidelberg, Heidelberg;^(b)Physikalisch Institut, Ruprecht-Karls-Universität Heidelberg, Heidelberg; Germany.
- ⁶²Faculty of Applied Information Science, Hiroshima Institute of Technology, Hiroshima; Japan.
- ⁶³^(a)Department of Physics, Chinese University of Hong Kong, Shatin, N.T., Hong Kong;^(b)Department of Physics, University of Hong Kong, Hong Kong;^(c)Department of Physics and Institute for Advanced Study, Hong Kong University of Science and Technology, Clear Water Bay, Kowloon, Hong Kong; China.

- ⁶⁴Department of Physics, National Tsing Hua University, Hsinchu; Taiwan.
- ⁶⁵IJCLab, Université Paris-Saclay, CNRS/IN2P3, 91405, Orsay; France.
- ⁶⁶Department of Physics, Indiana University, Bloomington IN; United States of America.
- ^{67(a)}INFN Gruppo Collegato di Udine, Sezione di Trieste, Udine;^(b)ICTP, Trieste;^(c)Dipartimento Politecnico di Ingegneria e Architettura, Università di Udine, Udine; Italy.
- ^{68(a)}INFN Sezione di Lecce;^(b)Dipartimento di Matematica e Fisica, Università del Salento, Lecce; Italy.
- ^{69(a)}INFN Sezione di Milano;^(b)Dipartimento di Fisica, Università di Milano, Milano; Italy.
- ^{70(a)}INFN Sezione di Napoli;^(b)Dipartimento di Fisica, Università di Napoli, Napoli; Italy.
- ^{71(a)}INFN Sezione di Pavia;^(b)Dipartimento di Fisica, Università di Pavia, Pavia; Italy.
- ^{72(a)}INFN Sezione di Pisa;^(b)Dipartimento di Fisica E. Fermi, Università di Pisa, Pisa; Italy.
- ^{73(a)}INFN Sezione di Roma;^(b)Dipartimento di Fisica, Sapienza Università di Roma, Roma; Italy.
- ^{74(a)}INFN Sezione di Roma Tor Vergata;^(b)Dipartimento di Fisica, Università di Roma Tor Vergata, Roma; Italy.
- ^{75(a)}INFN Sezione di Roma Tre;^(b)Dipartimento di Matematica e Fisica, Università Roma Tre, Roma; Italy.
- ^{76(a)}INFN-TIFPA;^(b)Università degli Studi di Trento, Trento; Italy.
- ⁷⁷Institut für Astro- und Teilchenphysik, Leopold-Franzens-Universität, Innsbruck; Austria.
- ⁷⁸University of Iowa, Iowa City IA; United States of America.
- ⁷⁹Department of Physics and Astronomy, Iowa State University, Ames IA; United States of America.
- ⁸⁰Joint Institute for Nuclear Research, Dubna; Russia.
- ^{81(a)}Departamento de Engenharia Elétrica, Universidade Federal de Juiz de Fora (UFJF), Juiz de Fora;^(b)Universidade Federal do Rio De Janeiro COPPE/EE/IF, Rio de Janeiro;^(c)Universidade Federal de São João del Rei (UFSJ), São João del Rei;^(d)Instituto de Física, Universidade de São Paulo, São Paulo; Brazil.
- ⁸²KEK, High Energy Accelerator Research Organization, Tsukuba; Japan.
- ⁸³Graduate School of Science, Kobe University, Kobe; Japan.
- ^{84(a)}AGH University of Science and Technology, Faculty of Physics and Applied Computer Science, Krakow;^(b)Marian Smoluchowski Institute of Physics, Jagiellonian University, Krakow; Poland.
- ⁸⁵Institute of Nuclear Physics Polish Academy of Sciences, Krakow; Poland.
- ⁸⁶Faculty of Science, Kyoto University, Kyoto; Japan.
- ⁸⁷Kyoto University of Education, Kyoto; Japan.
- ⁸⁸Research Center for Advanced Particle Physics and Department of Physics, Kyushu University, Fukuoka ; Japan.
- ⁸⁹Instituto de Física La Plata, Universidad Nacional de La Plata and CONICET, La Plata; Argentina.
- ⁹⁰Physics Department, Lancaster University, Lancaster; United Kingdom.
- ⁹¹Oliver Lodge Laboratory, University of Liverpool, Liverpool; United Kingdom.
- ⁹²Department of Experimental Particle Physics, Jožef Stefan Institute and Department of Physics, University of Ljubljana, Ljubljana; Slovenia.
- ⁹³School of Physics and Astronomy, Queen Mary University of London, London; United Kingdom.
- ⁹⁴Department of Physics, Royal Holloway University of London, Egham; United Kingdom.
- ⁹⁵Department of Physics and Astronomy, University College London, London; United Kingdom.
- ⁹⁶Louisiana Tech University, Ruston LA; United States of America.
- ⁹⁷Fysiska institutionen, Lunds universitet, Lund; Sweden.
- ⁹⁸Centre de Calcul de l’Institut National de Physique Nucléaire et de Physique des Particules (IN2P3), Villeurbanne; France.
- ⁹⁹Departamento de Física Teorica C-15 and CIAFF, Universidad Autónoma de Madrid, Madrid; Spain.
- ¹⁰⁰Institut für Physik, Universität Mainz, Mainz; Germany.

- ¹⁰¹School of Physics and Astronomy, University of Manchester, Manchester; United Kingdom.
- ¹⁰²CPPM, Aix-Marseille Université, CNRS/IN2P3, Marseille; France.
- ¹⁰³Department of Physics, University of Massachusetts, Amherst MA; United States of America.
- ¹⁰⁴Department of Physics, McGill University, Montreal QC; Canada.
- ¹⁰⁵School of Physics, University of Melbourne, Victoria; Australia.
- ¹⁰⁶Department of Physics, University of Michigan, Ann Arbor MI; United States of America.
- ¹⁰⁷Department of Physics and Astronomy, Michigan State University, East Lansing MI; United States of America.
- ¹⁰⁸B.I. Stepanov Institute of Physics, National Academy of Sciences of Belarus, Minsk; Belarus.
- ¹⁰⁹Research Institute for Nuclear Problems of Byelorussian State University, Minsk; Belarus.
- ¹¹⁰Group of Particle Physics, University of Montreal, Montreal QC; Canada.
- ¹¹¹P.N. Lebedev Physical Institute of the Russian Academy of Sciences, Moscow; Russia.
- ¹¹²National Research Nuclear University MEPhI, Moscow; Russia.
- ¹¹³D.V. Skobeltsyn Institute of Nuclear Physics, M.V. Lomonosov Moscow State University, Moscow; Russia.
- ¹¹⁴Fakultät für Physik, Ludwig-Maximilians-Universität München, München; Germany.
- ¹¹⁵Max-Planck-Institut für Physik (Werner-Heisenberg-Institut), München; Germany.
- ¹¹⁶Nagasaki Institute of Applied Science, Nagasaki; Japan.
- ¹¹⁷Graduate School of Science and Kobayashi-Maskawa Institute, Nagoya University, Nagoya; Japan.
- ¹¹⁸Department of Physics and Astronomy, University of New Mexico, Albuquerque NM; United States of America.
- ¹¹⁹Institute for Mathematics, Astrophysics and Particle Physics, Radboud University Nijmegen/Nikhef, Nijmegen; Netherlands.
- ¹²⁰Nikhef National Institute for Subatomic Physics and University of Amsterdam, Amsterdam; Netherlands.
- ¹²¹Department of Physics, Northern Illinois University, DeKalb IL; United States of America.
- ¹²²^(a)Budker Institute of Nuclear Physics and NSU, SB RAS, Novosibirsk; ^(b)Novosibirsk State University Novosibirsk; Russia.
- ¹²³Institute for High Energy Physics of the National Research Centre Kurchatov Institute, Protvino; Russia.
- ¹²⁴Institute for Theoretical and Experimental Physics named by A.I. Alikhanov of National Research Centre "Kurchatov Institute", Moscow; Russia.
- ¹²⁵Department of Physics, New York University, New York NY; United States of America.
- ¹²⁶Ochanomizu University, Otsuka, Bunkyo-ku, Tokyo; Japan.
- ¹²⁷Ohio State University, Columbus OH; United States of America.
- ¹²⁸Homer L. Dodge Department of Physics and Astronomy, University of Oklahoma, Norman OK; United States of America.
- ¹²⁹Department of Physics, Oklahoma State University, Stillwater OK; United States of America.
- ¹³⁰Palacký University, RCPTM, Joint Laboratory of Optics, Olomouc; Czech Republic.
- ¹³¹Institute for Fundamental Science, University of Oregon, Eugene, OR; United States of America.
- ¹³²Graduate School of Science, Osaka University, Osaka; Japan.
- ¹³³Department of Physics, University of Oslo, Oslo; Norway.
- ¹³⁴Department of Physics, Oxford University, Oxford; United Kingdom.
- ¹³⁵LPNHE, Sorbonne Université, Université de Paris, CNRS/IN2P3, Paris; France.
- ¹³⁶Department of Physics, University of Pennsylvania, Philadelphia PA; United States of America.
- ¹³⁷Konstantinov Nuclear Physics Institute of National Research Centre "Kurchatov Institute", PNPI, St. Petersburg; Russia.
- ¹³⁸Department of Physics and Astronomy, University of Pittsburgh, Pittsburgh PA; United States of

America.

¹³⁹(*a*) Laboratório de Instrumentação e Física Experimental de Partículas - LIP, Lisboa; ^(b)Departamento de Física, Faculdade de Ciências, Universidade de Lisboa, Lisboa; ^(c)Departamento de Física, Universidade de Coimbra, Coimbra; ^(d)Centro de Física Nuclear da Universidade de Lisboa, Lisboa; ^(e)Departamento de Física, Universidade do Minho, Braga; ^(f)Departamento de Física Teórica y del Cosmos, Universidad de Granada, Granada (Spain); ^(g)Dep Física and CEFITEC of Faculdade de Ciências e Tecnologia, Universidade Nova de Lisboa, Caparica; ^(h)Instituto Superior Técnico, Universidade de Lisboa, Lisboa; Portugal.

¹⁴⁰Institute of Physics of the Czech Academy of Sciences, Prague; Czech Republic.

¹⁴¹Czech Technical University in Prague, Prague; Czech Republic.

¹⁴²Charles University, Faculty of Mathematics and Physics, Prague; Czech Republic.

¹⁴³Particle Physics Department, Rutherford Appleton Laboratory, Didcot; United Kingdom.

¹⁴⁴IRFU, CEA, Université Paris-Saclay, Gif-sur-Yvette; France.

¹⁴⁵Santa Cruz Institute for Particle Physics, University of California Santa Cruz, Santa Cruz CA; United States of America.

¹⁴⁶(*a*) Departamento de Física, Pontificia Universidad Católica de Chile, Santiago; ^(b)Universidad Andres Bello, Department of Physics, Santiago; ^(c)Instituto de Alta Investigación, Universidad de Tarapacá; ^(d)Departamento de Física, Universidad Técnica Federico Santa María, Valparaíso; Chile.

¹⁴⁷Department of Physics, University of Washington, Seattle WA; United States of America.

¹⁴⁸Department of Physics and Astronomy, University of Sheffield, Sheffield; United Kingdom.

¹⁴⁹Department of Physics, Shinshu University, Nagano; Japan.

¹⁵⁰Department Physik, Universität Siegen, Siegen; Germany.

¹⁵¹Department of Physics, Simon Fraser University, Burnaby BC; Canada.

¹⁵²SLAC National Accelerator Laboratory, Stanford CA; United States of America.

¹⁵³Physics Department, Royal Institute of Technology, Stockholm; Sweden.

¹⁵⁴Departments of Physics and Astronomy, Stony Brook University, Stony Brook NY; United States of America.

¹⁵⁵Department of Physics and Astronomy, University of Sussex, Brighton; United Kingdom.

¹⁵⁶School of Physics, University of Sydney, Sydney; Australia.

¹⁵⁷Institute of Physics, Academia Sinica, Taipei; Taiwan.

¹⁵⁸(*a*) E. Andronikashvili Institute of Physics, Iv. Javakhishvili Tbilisi State University, Tbilisi; ^(b)High Energy Physics Institute, Tbilisi State University, Tbilisi; Georgia.

¹⁵⁹Department of Physics, Technion, Israel Institute of Technology, Haifa; Israel.

¹⁶⁰Raymond and Beverly Sackler School of Physics and Astronomy, Tel Aviv University, Tel Aviv; Israel.

¹⁶¹Department of Physics, Aristotle University of Thessaloniki, Thessaloniki; Greece.

¹⁶²International Center for Elementary Particle Physics and Department of Physics, University of Tokyo, Tokyo; Japan.

¹⁶³Graduate School of Science and Technology, Tokyo Metropolitan University, Tokyo; Japan.

¹⁶⁴Department of Physics, Tokyo Institute of Technology, Tokyo; Japan.

¹⁶⁵Tomsk State University, Tomsk; Russia.

¹⁶⁶Department of Physics, University of Toronto, Toronto ON; Canada.

¹⁶⁷(*a*) TRIUMF, Vancouver BC; ^(b)Department of Physics and Astronomy, York University, Toronto ON; Canada.

¹⁶⁸Division of Physics and Tomonaga Center for the History of the Universe, Faculty of Pure and Applied Sciences, University of Tsukuba, Tsukuba; Japan.

¹⁶⁹Department of Physics and Astronomy, Tufts University, Medford MA; United States of America.

¹⁷⁰Department of Physics and Astronomy, University of California Irvine, Irvine CA; United States of

America.

¹⁷¹Department of Physics and Astronomy, University of Uppsala, Uppsala; Sweden.

¹⁷²Department of Physics, University of Illinois, Urbana IL; United States of America.

¹⁷³Instituto de Física Corpuscular (IFIC), Centro Mixto Universidad de Valencia - CSIC, Valencia; Spain.

¹⁷⁴Department of Physics, University of British Columbia, Vancouver BC; Canada.

¹⁷⁵Department of Physics and Astronomy, University of Victoria, Victoria BC; Canada.

¹⁷⁶Fakultät für Physik und Astronomie, Julius-Maximilians-Universität Würzburg, Würzburg; Germany.

¹⁷⁷Department of Physics, University of Warwick, Coventry; United Kingdom.

¹⁷⁸Waseda University, Tokyo; Japan.

¹⁷⁹Department of Particle Physics and Astrophysics, Weizmann Institute of Science, Rehovot; Israel.

¹⁸⁰Department of Physics, University of Wisconsin, Madison WI; United States of America.

¹⁸¹Fakultät für Mathematik und Naturwissenschaften, Fachgruppe Physik, Bergische Universität Wuppertal, Wuppertal; Germany.

¹⁸²Department of Physics, Yale University, New Haven CT; United States of America.

^a Also at Borough of Manhattan Community College, City University of New York, New York NY; United States of America.

^b Also at Center for High Energy Physics, Peking University; China.

^c Also at Centro Studi e Ricerche Enrico Fermi; Italy.

^d Also at CERN, Geneva; Switzerland.

^e Also at CPPM, Aix-Marseille Université, CNRS/IN2P3, Marseille; France.

^f Also at Département de Physique Nucléaire et Corpusculaire, Université de Genève, Genève; Switzerland.

^g Also at Departament de Fisica de la Universitat Autonoma de Barcelona, Barcelona; Spain.

^h Also at Department of Financial and Management Engineering, University of the Aegean, Chios; Greece.

ⁱ Also at Department of Physics and Astronomy, Michigan State University, East Lansing MI; United States of America.

^j Also at Department of Physics and Astronomy, University of Louisville, Louisville, KY; United States of America.

^k Also at Department of Physics, Ben Gurion University of the Negev, Beer Sheva; Israel.

^l Also at Department of Physics, California State University, East Bay; United States of America.

^m Also at Department of Physics, California State University, Fresno; United States of America.

ⁿ Also at Department of Physics, California State University, Sacramento; United States of America.

^o Also at Department of Physics, King's College London, London; United Kingdom.

^p Also at Department of Physics, St. Petersburg State Polytechnical University, St. Petersburg; Russia.

^q Also at Department of Physics, University of Fribourg, Fribourg; Switzerland.

^r Also at Dipartimento di Matematica, Informatica e Fisica, Università di Udine, Udine; Italy.

^s Also at Faculty of Physics, M.V. Lomonosov Moscow State University, Moscow; Russia.

^t Also at Giresun University, Faculty of Engineering, Giresun; Turkey.

^u Also at Graduate School of Science, Osaka University, Osaka; Japan.

^v Also at Hellenic Open University, Patras; Greece.

^w Also at Institutio Catalana de Recerca i Estudis Avancats, ICREA, Barcelona; Spain.

^x Also at Institut für Experimentalphysik, Universität Hamburg, Hamburg; Germany.

^y Also at Institute for Nuclear Research and Nuclear Energy (INRNE) of the Bulgarian Academy of Sciences, Sofia; Bulgaria.

^z Also at Institute for Particle and Nuclear Physics, Wigner Research Centre for Physics, Budapest; Hungary.

^{aa} Also at Institute of Particle Physics (IPP); Canada.

ab Also at Institute of Physics, Azerbaijan Academy of Sciences, Baku; Azerbaijan.

ac Also at Instituto de Fisica Teorica, IFT-UAM/CSIC, Madrid; Spain.

ad Also at Joint Institute for Nuclear Research, Dubna; Russia.

ae Also at Moscow Institute of Physics and Technology State University, Dolgoprudny; Russia.

af Also at National Research Nuclear University MEPhI, Moscow; Russia.

ag Also at Physics Department, An-Najah National University, Nablus; Palestine.

ah Also at Physikalisches Institut, Albert-Ludwigs-Universität Freiburg, Freiburg; Germany.

ai Also at The City College of New York, New York NY; United States of America.

aj Also at TRIUMF, Vancouver BC; Canada.

ak Also at Universita di Napoli Parthenope, Napoli; Italy.

al Also at University of Chinese Academy of Sciences (UCAS), Beijing; China.

* Deceased